



TECHNICAL REPORT

ROBOCUP RESCUE HARDWARE SECTION

TABLE OF CONTENTS

1.0 Introduction	7
2.0 Aims & Objectives	8
2.1 Hardware Requirements	8
2.2 Victim identification Requirements	8
3.0 Specification	9
3.1 Dimensions	9
3.2 Robot Speed	11
3.3 BackPack Mobility	11
3.4 Battery Duration	11
3.5 Robot Weight	12
3.6 Specification Summary	13
4.0 Concept Designs	14
4.1 Literature Review	14
4.2 Competition research	14
4.3 Concept Chassis	16
4.4 Concept Robot Arm	17
5.0 Key Components	19
5.1 Caterpillar Tracks	19
5.2 Main Motors	20
5.2.1 Driving Power Requirements	20
5.2.2 Main Motor Specifications	21
5.2.3 Flipper Requirements	22
5.2.4 Flipper Motor Specification	23
5.2.1 Motor Control	23
5.3 Power Requirements	25
5.3.1 Capacity	25

5.3.2 Battery Chemistry Technologies.....	26
5.3.3 Cell cost and weight.....	27
5.3.4 Pack Design.....	28
5.3.5 Power Systems.....	28
5.3.6 Charge and Discharge Characteristics	29
5.3.7 Charging.....	29
5.4 Bearings and Seals.....	30
5.4.1 Roller Ball Bearings	30
5.4.2 Double Row Angular Contact Bearings.....	30
5.4.3 Spherical Thrust Roller Bearings.....	31
5.4.4 Needle Roller Bearings	31
5.4.5 Polymer Bearings.....	31
5.4.6 Bearing Comparison	32
6.0 Mechanical Design	33
6.1 Design Approach	33
6.1.1 Chassis construction	34
6.1.2 Fixings and Hardware	35
6.1.3 SolidWorks Design Aids	35
6.2 CAD Design Approach.....	36
6.3 Pulley Design	36
6.4 Rear Drive Train Design	38
6.4.1 Circlip Fixing Method.....	39
6.4.2 Motor Positioning.....	39
6.4.3 Gearbox	39
6.5 Flipper Drive Train Design	41
6.5.1 Flipper Motor and Shaft Drive Mechanism	42
6.5.2 Flipper Arm Exploded View	43

6.5.3 Belt Tensioning	44
6.6 Centre Chassis Section.....	45
6.6.1 Belt Tensioning	45
6.7 Sub-assemblies	46
6.8 Robot Arm	46
7.0 Manufacturing	49
7.1 Design for Manufacture	49
7.2 Part Manufacture	49
7.2.1 Pulley Machining.....	49
7.2.2 Flipper Shaft Machining.....	50
7.2.3 Plate Machining	51
7.3 Finishing.....	51
7.4 Manufactured Components	52
7.5 Re-design for Mass Production	54
7.5.1 Pulley Manufacture	54
7.5.2 Chassis Manufacture	54
8.0 Raw Materials	55
8.1 Aluminium vs polymer.....	55
8.2 Aluminium specifications	55
8.3 Polymer Specifications	55
9.0 Electronics.....	56
9.1 Power control pcb	56
9.1.1 MOSFET switching	56
9.1.2 Power Supplies	57
9.1.3 Emergency-Stop.....	58
9.1.4 Heat Sinks	59
9.1.5 connection to microcontroller pcb.....	59

9.2 Microcontroller pcb.....	59
9.2.1 Serial to USB Conversion	59
9.2.2 Programmable Interface Controller (PIC).....	60
9.3 PCB alterations	60
9.4 LED array Design.....	61
9.4.1 LED Luminosity.....	61
9.4.2 LED Circuit Design	63
9.5 Rotary Testing.....	64
9.6 Communications.....	66
9.7 Tests for Checking Circuit Works.....	66
9.8 Main Processor.....	68
9.9 What could go wrong?	68
9.10 Electronics conclusion	69
9.11 Sensors	70
9.11.1 Laser Scanner.....	70
9.11.2 Vision Cameras	70
9.11.3 Thermal Imaging Camera.....	71
9.11.4 Sonar Sensors	72
9.11.5 Digital Compass	73
9.11.6 6DoF Inertial Measurement Unit.....	73
10.0 Assembly	74
11.0 Conclusions	77
12.0 Recommendations	78
12.1 General Project Recommendations	78
12.2 Additional functionality with existing chassis	78
12.3 Electronics Recommendations	79
12.4 Redesign	79

13.0 Glossary.....	80
14.0 Bibliography and References	81
15.0 Appendices.....	83
15.1 CD of CAD Models	83
15.2 Gates Mectrol Polyurethane Belts Catalogue	84
15.3 Magmotor Specification Sheet	88
15.4 Annsman Battery Data Sheet	89
15.5 Aluminium Physical Properties.....	90
15.6 Nylon 66 Physical Properties.....	92
15.7 Electronics Appendix E	93

1.0 INTRODUCTION

This report contains the detailed Technical Background behind the RoboCup Rescue Robot Chassis, associated hardware and electronics introduced in the Main Group Report. The purpose of the chassis is to provide a mobile platform to move the sensor array about the competition environment. The hardware requirements are derived from the competition requirements. The first section of this report is to specify the minimum and maximum dimensions to allow design and specification of sensors and other components.

The Mechanical design section of the report describes the Chassis design, Drive Train and the Robot Arm. Initially Concept designs of the robot discussed, defined by the geometry of the competition environment. This is followed by a detailed analysis of the complete manufacturing process from CAD design to final assembly. The Electronics section of the report uses the sensor specification to design the power supplies, followed by the safety control electronics.

2.0 AIMS & OBJECTIVES

The project has a detailed list of aims in the main report where the following has the most relevance to the hardware section.

“Design and build a Robocup Rescue certified Robot”

In addition to this the project has several objectives related to achieving this goal;

- Develop a robot chassis capable of navigating the scenario terrain
- Design and build a test environment for the robot
- Produce a sensor array capable of mapping the environment
- Investigate the implementation of victim identification using thermal imaging, motion, sound and CO2 sensors

2.1 HARDWARE REQUIREMENTS

The relevant robot hardware requirements as specified by the competition are as follows:

- Capable of operating for 15 minutes in Preliminary rounds and 25 minutes in the Final rounds
- Negotiate through a random maze consisting of;
 - 1.2m wide hallways, defined by 1.2m square walls and corners
 - Non-flat flooring with increasing complexity, 10° and 15° slopes
 - Stepfield pallets (Orange: half-cubic, Red: full-cubic)
 - Confined spaces (ceiling blocks under elevated floors)
 - Stairs (40°, 20cm riser, 25cm tread depth, 5 in total)
 - Ramp with carpet for traction (inclined at 45° to test torque and center of gravity)
 - 20cm step/pipe combination to challenge robots reliant on the sharpness of step edges for traction
 - Acoustic tiles used for soundproofing; generally made from sound absorbing foam
 - Reflective surfaces present in most buildings in the form of glass, plastics etc
 - Excessively dark light absorptive materials such as felt

2.2 VICTIM IDENTIFICATION REQUIREMENTS

- Simulated victims will be placed in cardboard boxes with at least three signs of life:
 - Human form and Heat, Sound, motion, and/or CO2
- Multi-level box stacks provide searchable voids that may contain victims at various heights (45cm/18in boxes, up to three levels high)
- "Void" victims will be contained in box stacks with open box faces and tops
- "Entombed" victims will be contained in boxes with 15cm holes requiring sensor placement directly in front of the holes to identify sensory targets inside (eye charts and/or hazmat labels inside count as "form" points)
 - Variable illumination near the camera is required victim identification

3.0 SPECIFICATION

3.1 DIMENSIONS

For the purposes of search and rescue a robot should have high mobility and manoeuvrability in addition to being small and compact. By considering the terrain specifications and desired mobility, the robots maximum dimensions can be determined.

Mobility is vital to the robot achieving its goals in the fastest time possible, removing unnecessary positional turning and the need to go around 90° bends is a considerable factor. For the robot to take the diagonals through the arena, its maximum width is set to 0.85m. To ensure maximum manoeuvrability (ability to turn on the spot) the robots maximum turning circle can be no more than the defined width (any features that protrude will expand the turning circle), hence an upper design limit for the turning circle is defined as 0.85m (this takes precedence over the mobility dimensions).

Driving the robot through tele-operation limits the amount of visual feedback available to the operator which also limits the operator's ability to gauge their position in an arena. It is therefore necessary to add a buffer or *safety* zone on either side of the robot, allowing non-central on-the-spot rotation. The size of this buffer has been set to the maximum allowable (668mm), due to need to maintain maximum manoeuvrability whilst still allowing the robot to traverse stairs (see *figure 3*).

(*Figure 1 - Maze Dimensions, Figure 2 - Stair Climbing Dimensions and Figure 3 - Robot Dimensions*) showing the constraints of the map and the robot sizes derived from the requirements.

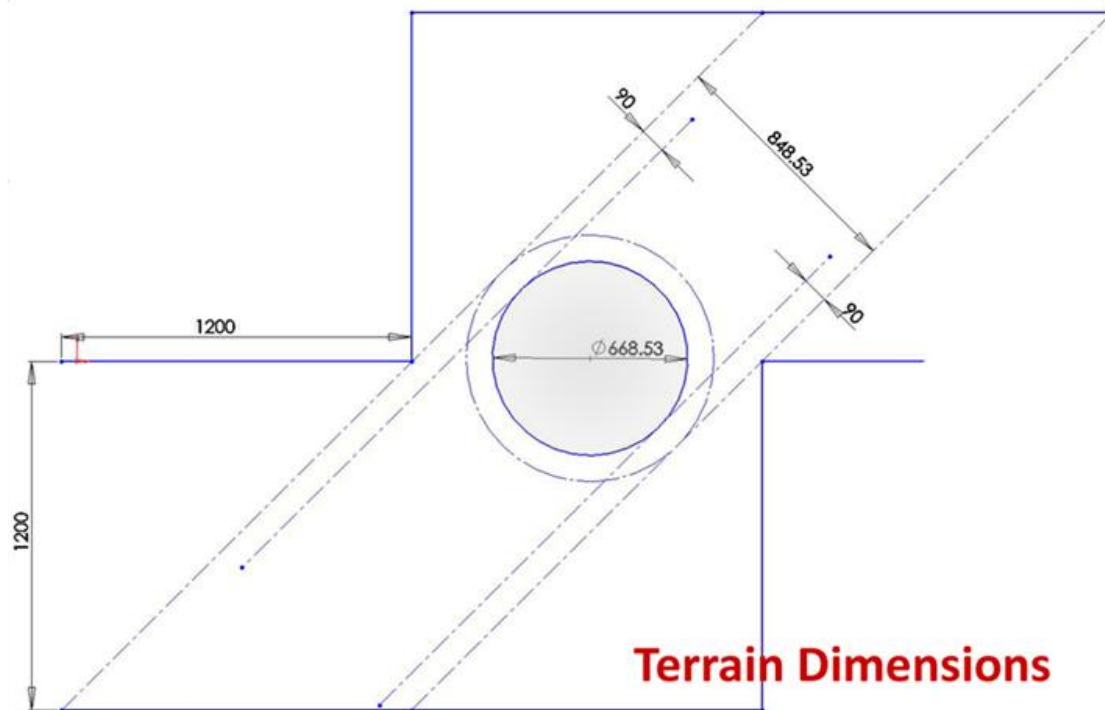


Figure 1 - Maze Dimensions

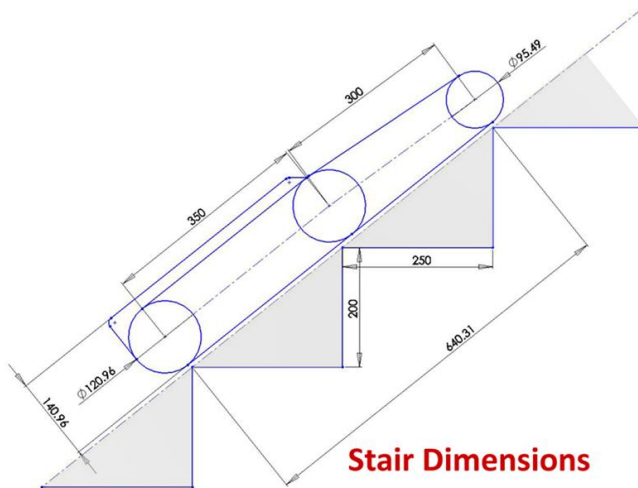


Figure 2 - Stair Climbing Dimensions

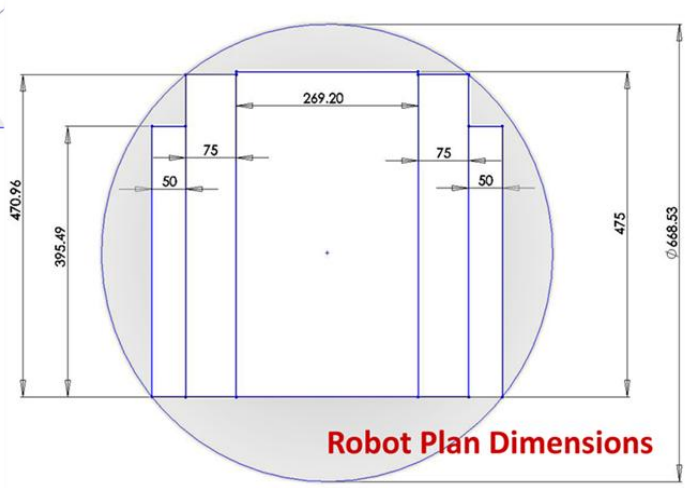


Figure 3 - Robot Dimensions

The dimensions of the stairs in competition are set as 200mm deep by 250mm high (40° incline). For the robot to be capable of ascending stairs with speed and stability, it requires a minimum of 2 points of contact at all times. Thus, setting the minimum drive train length to three points of contact (640mm) ensures the robot has a stable grounding to ascend and descend at all times. Setting drive train length to 640mm is within the maximum turning circle but would limit the robot's width to 191mm, this width would not be practical for differential turning or roll stability.

A practical alternative to a long, thin chassis and drive train is a folding one, as shown in figures 2 and 3. By utilising *Flippers arms* at the front of the chassis, the drive train length could be doubled for stairs or minimised for manoeuvrability. This orientation has mechanical design challenges not seen in a fixed-length drive train, but the roll-stability, spatial and turning advantages far outweigh the minor technical design issues. With the Flippers set beside the robot (*figure 3*) the entire robot fits within the maximum turning circle (668mm) specified previously. With the flipper arms extended the total drive train length becomes 745mm with a surface contact length of 640mm (*figure 2*).

During the competition the robot will need to ascend a 45° slope. This requirement sets some size-relation constraints on the robot dimensions. The higher the centre of mass (CoM), the longer the robot has to be, with the relative position of the CoM as far forward as possible. From *Figure 4 - Centre of Mass* it can be seen that with the CoM to the right of the stability line (line drawn vertically from last point of contact with slope) it will remain stable on the slope. However, the closer the CoM sits to the stability line, the more likely the robot is to flip when accelerating.

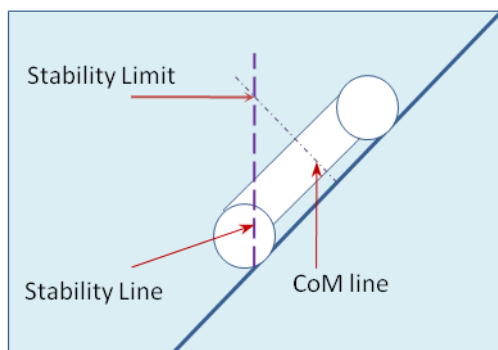


Figure 4 - Centre of Mass

With the main drive length specified as 350mm and the CoM estimated in the centre, the robot's CoM can be no higher than 175mm from terrain surface.

The minimum ground clearance will enable the robot to straddle the 15° sloped terrain (see *Figure 5 - Minimum Ground Clearance*) and manoeuvre without the chassis becoming grounded at any point. From *Figure 3 - Robot Dimensions* the external chassis distance is specified as 270mm (approx), this requires a minimum of 36mm ground clearance from surface to chassis underside (lowest point).

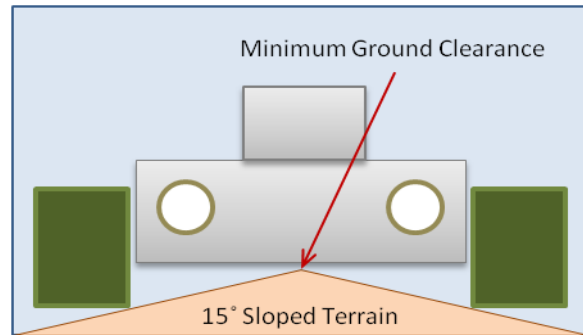


Figure 5 - Minimum Ground Clearance

3.2 ROBOT SPEED

Whilst in the Robocup Rescue maze there is no requirement for speed other than the need to negotiate the entire terrain under mission time constraints. However, this robot is being designed for deployment in an actual urban rescue terrain with human operators and rescuers. It is therefore imperative that the robot does not hinder human counterparts in speed or mobility and can maintain a brisk walking speed of up to 4.5mph (2m/s).

3.3 BACKPACK MOBILITY

The robot should be small and compact enough that a single person with all necessary operating equipment and spare batteries can carry it in a large winter backpack (up to 60lt capacity). Due to health and safety constraints, the total weight of the system must not exceed 40Kg.

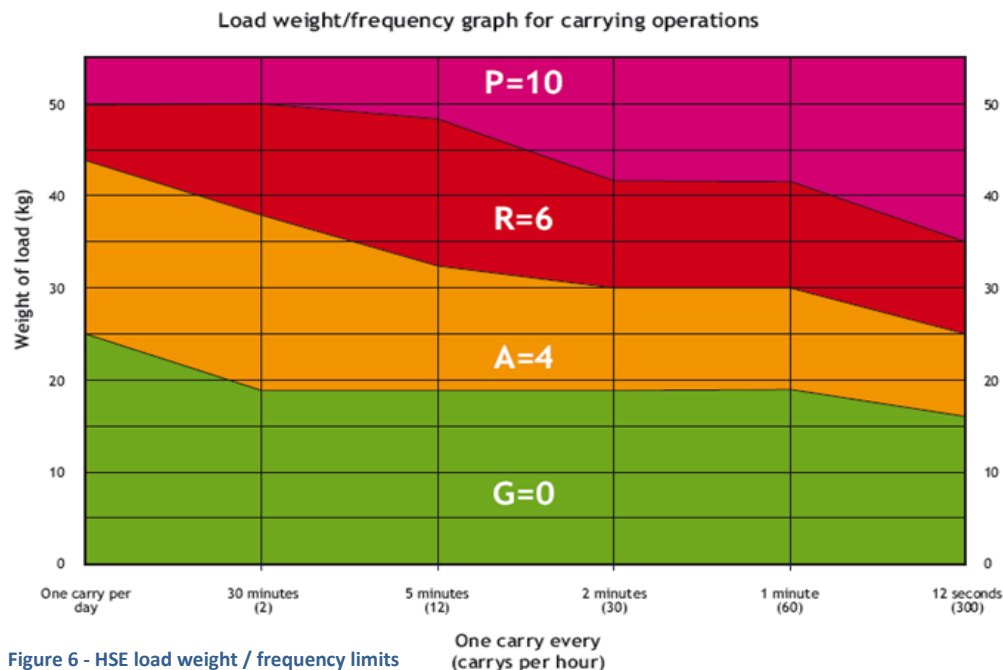
3.4 BATTERY DURATION

The robot's battery packs provide all the electrical power that the robot has available for use during any competition mission. The minimum robot runtime that the batteries have to sustain is therefore set by the duration of the longest competition trial; specified as **25 minutes**. In addition to this, a 15-minute set-up time is provided thus a battery runtime to **40 minutes** per trial would be desirable.

3.5 ROBOT WEIGHT

Due to the need for robot mobility, weight is a considerable factor in the specification. The robot will need carrying to location before deployment; driving it would use unnecessary battery life and accelerate aging of the cells and robot.

The competition trials last approximately 30mins (including set-up times), therefore it can be expected that the operator/s will need to lift the robot once every 30mins for a short distance of up to 10 meters (centre of terrain to start point). If the robot were to be deployed in the field it should be light enough for a single person to lift it for an extended period.



Using the *Manual Handling Assessment Chart (MAC)* from the HSE (Health and Safety Executive) website (HSE, 2008) the upper weight limit for the robot specifies 19Kg (green) and 38Kg (amber) for a single person lifting once every 30mins.

The green zone denotes a safe lift weight/frequency combination with very little risk of harm to the individual and the Amber zone denotes moderate risk, therefore proper lifting techniques must be applied. If the total lifting weight of the robot exceeds 38Kg certain lifting limitations are introduced, these require more than one person lifting the robot, special handles and distance constraints. Therefore, the upper weight limit of the robot is 38Kg. Target weight is set to 25Kg, the maximum that can be handled frequently by one person with moderate risks associated.

Other assessments that apply to the design of the robot include the hand distance from lower back, symmetry of the trunk/load and the grip on the load. A handle on the robot enabling it to be carried with a straight arm gives the best score in the *hand distance from lower back* assessment, but this could lead to a one-handed lift, giving the worst score in the *asymmetrical trunk/load* assessment. The weighting of the MAC scoring gives precedence to the former of these assessments, and hence a handled system is recommended. If the handle provided is 'good' (i.e. enables good grip, does not dig in), the best score in the *grip on the load* assessment will be achieved.

3.6 SPECIFICATION SUMMARY

The final specification for robot dimensions, weight and mobility are as follows:

- Maximum turning circle to be no greater than **670mm**
- Robot footprint to be no longer than **475mm**, no wider than **520mm**
- Minimum ground clearance to be no less than **36mm**
- Minimum drive track length when flippers extended to be no less than **640mm**
- Centre of Mass to be no higher than **175mm** and back no further than **175mm** from the last point of surface contact
- Robot sensor array must be capable of identifying **3** of the following signs of life;
- **Human form, Motion, Heat, Sound, CO₂**
- Sensor array should be capable of viewing into boxes through **15cm** holes
- Robot must have controlled illumination on sensor array
- Sensor array should be capable of detecting victims at a height of **90cm**
- Robot target weight of **25Kg**, maximum weight must not exceed **40Kg**
- Robot battery life must be **25mins minimum, 40mins desirable**
- Robot upper cruise speed to be no less than **4.5mph (2m/s)**
- Robot system (inc. operator terminal and spare batteries) to be no more than **40Kg**
- Robot system should fit into a **60lt** backpack for personal transportation

4.0 CONCEPT DESIGNS

4.1 LITERATURE REVIEW

The concept design process started with research into previous competition entrants, followed by commercially available products mainly targeted at the military, such as the Packbot (*Figure 8 - IRobot Packbot 510*) and the Wheelbarrow (*Figure 7 - Remotec Wheelbarrow MK8*).

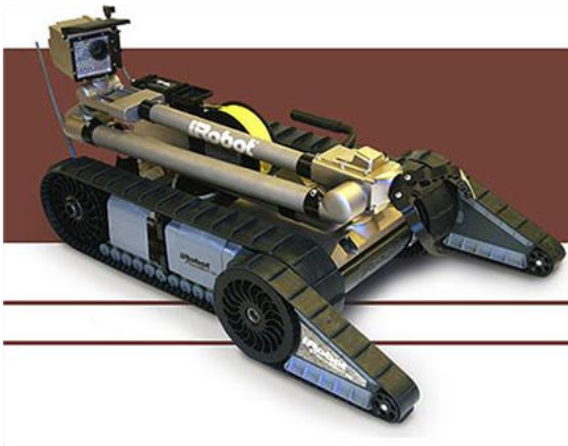


Figure 8 - IRobot Packbot 510 (IRobot Corp., 2008)



Figure 7 - Remotec Wheelbarrow MK8 (Remotec Unmanned Vehicle Systems, 2008)

These two robots have similar applications, both targeted at bomb disposal but with different merits. The Remotec Wheelbarrow is very durable, capable of withstanding a significant explosion and carrying a heavy payload, whereas the Packbot is designed to be very portable for use with military troops.

Their main drive systems rely on a differential drive arrangement which allows them to navigate rough, un-made terrain very successfully. The Packbot also uses two front flippers to self right itself and negotiate obstacles taller than its tracks; whereas the Wheelbarrow is large enough it can negotiate most obstacles using the main tracks alone.

4.2 COMPETITION RESEARCH

In addition to looking at commercially available products, extensive research was conducted into other robots entering the RoboCup Rescue competition. There is a distinct divide between the types of robots where some are aimed at fully autonomous mapping and navigation and others also have the ability to navigate over rougher terrain. The simpler robots mostly consist of 3 and 4 wheel chassis whereas the majority of the all terrain vehicles seen in previous competitions use caterpillar tracked, differential drive systems.

The focus for the WMR robot in its first year was to design and build a chassis capable of navigating over all the terrain, allowing future teams to develop the software for mapping and autonomous navigation on the previous year's platform. Developing the chassis to enter the competition within a year would also allow feedback as to the capability of the robot before further re-design. Out of all the existing robots we were able to study through photographs and team description papers from

previous events, there were several key features that influenced our design decisions. The main feature is the ability to manipulate the size and shape of the robot to allow it to navigate through small corridors and spaces yet still climb over the rough terrain and stairs. This is achieved by robots through the use of flippers in various places, usually the front, rear or both. For example the Resquake robot from the University of Texas (see Figure 9 – Resquake) has two pairs of flippers at the front and rear of their robot, allowing them to navigate the most complex terrain the competition environment has. Although this robot design has obvious advantages with its potential to span large distances, something fundamental to stair climbing it adds a large amount of complexity to the design and hence cost.



Figure 9 – Resquake (University of North Texas)

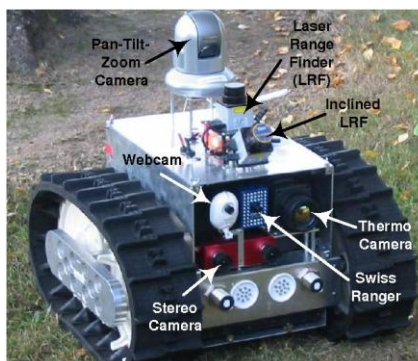


Figure 11 - Rugbot (Jacobs University)

Jacobs University in

Germany have designed a chassis known as the "Rugbot" (see Figure 11 - Rugbot) which consists of a much taller tracked drive than the PackBot or Resquake, allowing it to negotiate larger obstacles without the need for additional flippers. In comparison to the military Packbot the Rugbot is much taller in size; hence the centre of gravity is higher so it cannot climb stairs without additional help. Jacobs University have overcome this by implementing a flipper arrangement at the rear (see Figure 10 - Rugbot Stairs) extending their overall

length significantly. This technique allows them to negotiate stairs with ease, with the added benefit of providing assistance when climbing over rough terrain that could potentially prevent both tracks from achieving sufficient traction to move forwards.



Figure 10 - Rugbot Stairs (Jacobs University)

One of the difficulties with all these robots is their capability to be used in real life due to their large size and weight. To overcome this The University of New South Wales in Australia use a standard remote control car with flippers at the front and



Figure 12 - Redback Robot (University of New South Wales)

rear as some of their development platforms. This provides a very light weight package (approx 1.5kg). Although this provides a low cost solution for testing the basic capabilities of flippers and differential track drive there is little scope for improvement or space for sensors/control electronics.

Using research into the other robots entering the competition we were able to extract some of the best features from each to develop an ideal, concept design.

4.3 CONCEPT CHASSIS

The concept sketch designs were approached by splitting the design into two sections, Chassis and Robot Arm. The chassis concept was based around the two most challenging aspects of terrain, the Stairs and step fields (uneven surfaces). In order to negotiate the maze and navigate up such terrain the chassis needs to be capable of varying its length; hence the flipper concept.

The first prototype shown in (Figure 13 - Robot Prototype 1) has flippers at both ends to allow the Robot to be very compact, yet still negotiate tall obstacles.

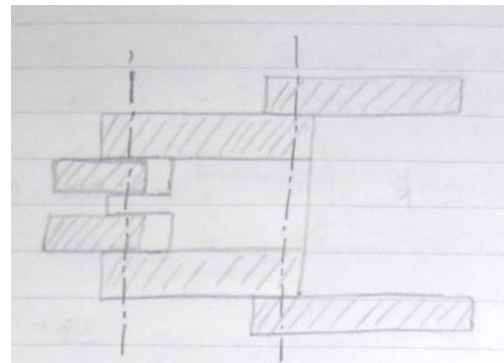


Figure 13 - Robot Prototype 1

Using this design allows the front flippers (left) to be retracted into the chassis, thus over 75% of the frontal area is covered by caterpillar tracks (Figure 14 - Robot Prototype 1 - Step-fields and Stairs), which should provide good traction over the step fields and the edges of obstacles.

With the initial sketches drawn on paper, 3D CAD models of the prototypes were built to test the viability of the design, in terms of physical size constraints and the space left inside for the control electronics and sensors. (Figure 15 - 3D CAD Model of Prototype 1) shows the 3D CAD model of the prototype sketches generated using SolidWorks, an industry CAD design package.

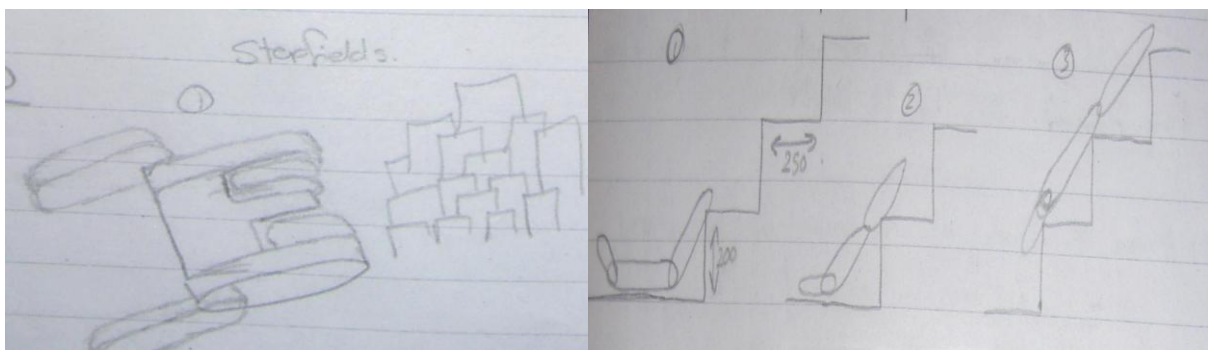


Figure 14 - Robot Prototype 1 - Step-fields and Stairs

Theoretically this model represents an ideal design, providing a platform capable of navigating obstacles larger than itself yet maintaining manoeuvrability in confined spaces.

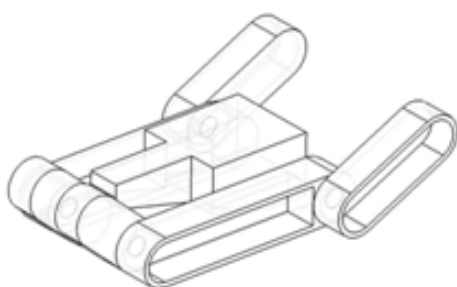


Figure 15 - 3D CAD Model of Prototype 1

The major problem with this solution is the complexity of the design, requiring two sets of flippers, motors and control electronics. This additional complication would incur significant cost overall chassis size increases. These issues were resolved by sacrificing some of the manoeuvrability and simplifying the design to use one larger pair of flippers.

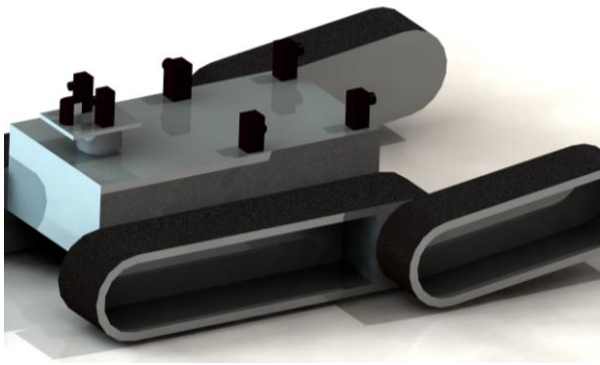


Figure 16 - 3D CAD Model of Prototype 2

(Figure 16 - 3D CAD Model of Prototype 2) shows the second revision of the design, essentially a simplified version of (Figure 15 - 3D CAD Model of Prototype 1) with a larger centre section for the Control systems.

Some of the key features of this design are the tracks overhanging the front and rear of the robot, ensuring they are the first feature to come in contact with obstacles. Thus encouraging the chassis to climb over obstacles rather than push toward them.

This design requires two drive motors to provide differential drive, allowing forward, backward and turning motions. By aligning the centres of the caterpillar track drive wheels the robot can be powered using two drive motors, one for each track/flipper pair. A third motor/drive assembly is required for the orientation of the flippers in parallel.

Alternatively a third and fourth motor/drive assembly could be used to allow independent movement of the flipper arms. However as the flippers main purpose is to navigate up stairs and tall steps it is likely they will be usually be used in parallel, hence a single motor/drive assembly will be used as it simplifies the design and reduces the overall weight.

4.4 CONCEPT ROBOT ARM

The competition requirements specify that victims are located in various locations at varying heights and life signs. For the robot to be successful at identifying all simulated victims, concept design had to focus on the most difficult/complex scenarios; ‘entombed’ victims with 15cm viewing holes raised above the ground in front of step fields.

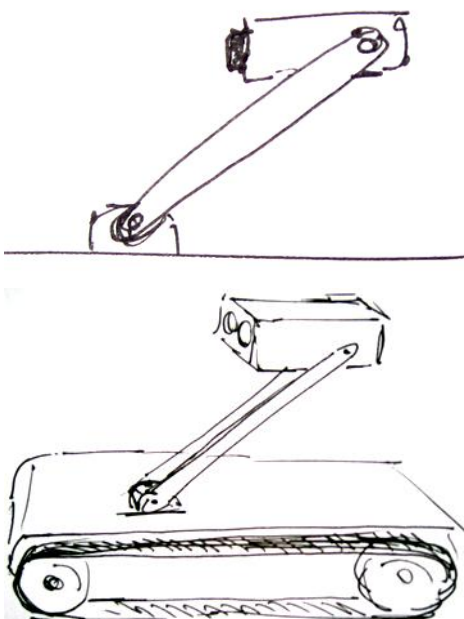


Figure 17 - Single Planar Robot Arm Concept

With the specified size constraints, it would not be possible for any sensory equipment mounted on the chassis to view into any of these boxes, hence the need for a versatile robot arm with a sensory array mounted at the end.

The first arm designs began with identifying the necessary heights for worst-case victim identification; 90cm. Although this amounts two box heights (competition specifies three), the viewing holes are located in the middle of the box faces. With the addition of height from the step fields in these scenarios, the necessary reach only amounts to 90cm. The first concept (Figure 17 - Single Planar Robot Arm Concept) uses a single link arm with tilt ability at the end. This approach is simplistic, easy to produce and control (with only two inputs). However, to obtain the necessary heights the arm has to span 60cm (the robot chassis can be used to provide the remainder), 12cm more

than the maximum specified chassis length. This would also sit outside of the maximum specified turning circle, thus not an acceptable approach. Another problem with this design is the lack of available manipulation. The arm cannot look directly in front of the robot chassis without being fully docked; in which case too far to read any text. Alternatively, it could be placed sticking out in front of the robot; extending its turning circle and risk of arm damage.

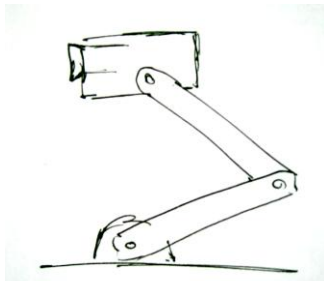


Figure 18 - Double link Planar Arm

The next stage was to incorporate a double link arm (Figure 18 - Double link Planar Arm) which provides a compact solution of approximately 30cm in length when docked and over 60cm when extended. This approach overcomes the control and visibility limitations seen with the single link design.



Figure 19 - CAD

Render Double Link Planar Arm

To assess the arms capability and reach it was modelled in CAD (Figure 19 - CAD

Render). This revealed further visibility limitations that required a 'pan' ability for use when the robot is side on or misaligned to a simulated victim box. The final concept stage saw the necessary introduction of pan control on the arm head (Figure 21 - Double Link Planar Arm + pan & tilt).

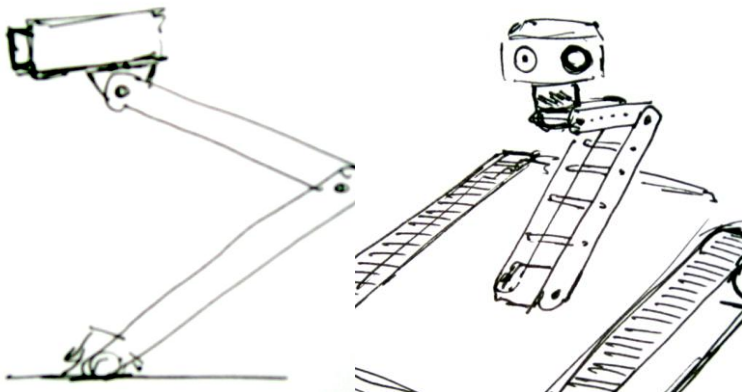


Figure 21 - Double Link Planar Arm + Pan & Tilt

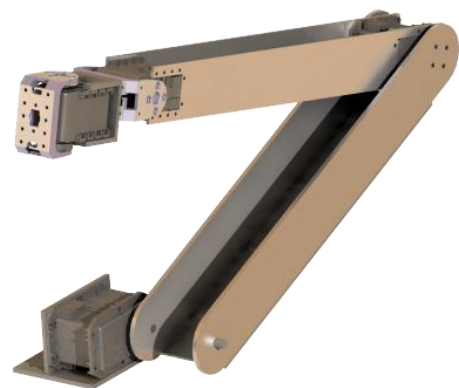


Figure 20 - CAD Render Double Link Planar Arm + Pan & Tilt

Whilst the operator is identifying victims using the head sensors, the arm will need to remain steady; this ability will require closed loop feedback control (servomechanisms) on each driving device within the arm. The various technologies that could be implemented to power the arm include electric, hydraulic, pneumatic and magnetic servomechanisms. However, the only source of power available on the robot without including compressors and storage tanks is electricity. With the robot using batteries the most suitable choice for the arm was DC servomotors

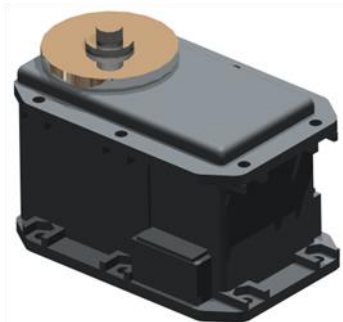


Figure 22 - RX64 Servomotor

(Figure 22 - RX64 Servomotor)

5.0 KEY COMPONENTS

For the design process to be successful several fundamental components were required. The caterpillar tracks were the first components to be specified and acquired; they specify the exact length of the chassis in addition to the type and power of the drive train required. The acquisition of these components took a significant amount of time as several international companies were used, resulting in a day's lag between questions and solutions.

5.1 CATERPILLAR TRACKS

Initial research conducted into caterpillar tracks investigated model and mobile robot stores. There are several versions on sale, such as the Traxster mobile robot platform shown in (Figure 23 - Traxster Robot), however, as with the Traxster (230mm x 203mm x 76mm), the tracks were too small for our requirements.



Figure 23 - Traxster Robot

The next point of research was conveyor belt manufactures, who provide a vast number of coatings on a wide range of belt widths and lengths. Literature was obtained from Gates Mectrol, a German company specialising in Polyurethane Timing Belts (see Appendix 15.2 Gates Mectrol)

Gates supply a range of timing belts with various teeth sections, surface coatings and a welded, endless construction, ideal for our application. The main concern with caterpillar tracks is the high side loads when turning; hence a method to centralise the belts was required. Fortunately Gates also sell a standard profile called 'T10V' (Figure 24 - Caterpillar Tracks T10V Section), a timing belt design with a central V-groove guide which allows high side loads, without the belts becoming misaligned.

T10V

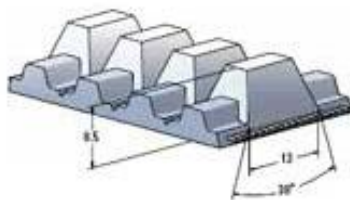


Figure 24 - Caterpillar Tracks T10V Section
(Gates Mectrol Limited, 2008)

There are many T10V pulleys available with the correct profile for the belt we used, however, as the central pulleys require two belts, thus two locating grooves, custom pulleys would be required.

In order to climb stairs and negotiate slippery obstacles, tracks with a high co-efficient of friction to grip onto the surfaces are needed. The main belts are manufactured from polyurethane and can be supplied with several different surface coatings. To guarantee the quality of grip we chose a "Rough Top", PVC coating with a kinetic co-efficient of friction; 1.3 against an aluminium surface. Figure 25 - Rough Top Timing Belts shows the rough top surface and the custom drive pulleys. The surface of the belt is made up of small rubber teeth approximately 3mm² which grip well onto any uneven surfaces.

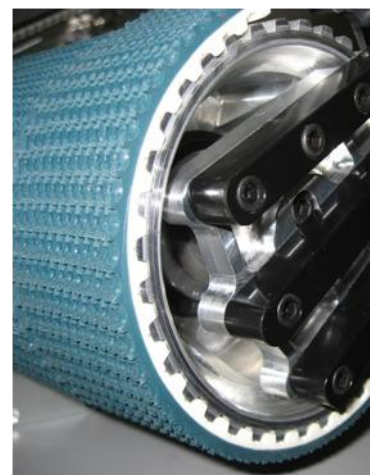


Figure 25 - Rough Top Timing Belts

5.2 MAIN MOTORS

Specifying the motors was based on two main factors; the performance characteristics required and the speed controller technology, the key aspects of this are;

- Maximum torque required at zero speed to allow the robot to start moving on any surface
- Efficient to prolong battery life
- Easily obtainable control systems due to short project lead time
- High power to weight ratio

The main two categories of motors are AC and DC, where both have significantly different performance characteristics; (*Table 1 - AC/DC Motor Comparison*) shows the key differences. The most important being the stall torque; the relative quantity of maximum torque obtainable when the motor shaft is stationary. Although the brushless AC motors provide better efficiency and higher power to weight, it is difficult to obtain off the shelf speed controllers with an RS232 serial interface. Additionally the low stall torque requires a higher gear ratio; thus brushed DC motors will be used.

Table 1 - AC/DC Motor Comparison

	AC	DC
Cost	High	Low
Power to Weight Ratio	High	Low
Stall Torque	Low	Full
Speed Controller Cost	High	Low

5.2.1 DRIVING POWER REQUIREMENTS

In order to specify the maximum power requirement we took the situation which uses the most power, thus when the robot is climbing the steepest slopes of 45° and the stairs. For the initial calculations we neglected the frictional forces of the drive train to calculate the minimum driving force to drive up a 45° slope. *Figure 26 - Slope Driving Force* shows the minimum force required to climb a 45° slope, although technically achievable by even the smallest motor this would require a very low gear ratio, thus increasing the mechanical complexity. Thus, based on a wheel diameter of 120mm the minimum torque required at the wheels is;

$$Torque = Fr = 173.4 \times 0.06m = 10.4Nm$$

Equation 1 - Minimum Torque

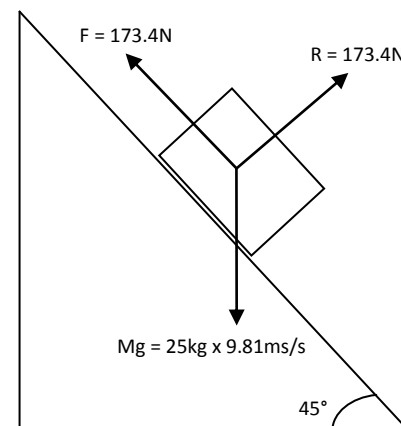


Figure 26 - Slope Driving Force

Using both tracks to negotiate up slopes reduces the maximum torque required from each track to $10.4Nm/2 = 5.2Nm$. Although this is a minimum torque to climb the slopes this only counts for a small amount of the robots use. Thus the motors could be overloaded while climbing steep slopes or steps, providing they are not overloaded continuously. This allows smaller motors to be used along with higher gearing to give higher top speeds. Additionally, to meet the requirement of travelling at

an equal velocity to a human at a walking pace the robot needs to be capable of travelling at approximately 4mph or 2ms⁻¹. To allow comparison of the different motor windings the required forward velocity can be shown as wheel velocity, thus allowing the winding to be chosen based on the simplest gear ratio required.

$$\text{Wheel Velocity } (\omega) = \frac{V}{\pi D} = \frac{2}{\pi * 0.12} = 5.3 \text{ revs}^{-1} = 318 \text{ rpm}^{-1}$$

Equation 2 - Wheel Velocity

5.2.2 MAIN MOTOR SPECIFICATIONS

To satisfy the requirements the motors were sourced from an American company, “Magmotor”, as they manufacture a range using neodymium magnets with a high Power-Weight ratio. They are able to supply the motors custom wound depending on the application. *Table 2 - Main Motor Characteristics* shows standard winding information from the manufacturer (see *Appendix 15.3*), followed by the theoretical Robot Speed and Driving Force based on the target size and weight.

Table 2 - Main Motor Characteristics

S23 Motor Range	E	G	I	K	Units
oz-in / amp	14.4	22.7	36.2	56.3	
Nm/amp	0.09	0.14	0.23	0.35	
Volts / krpm	0.6	16.8	26.8	41.5	
Terminal Resistance	0.5	1.9	2.5	5.5	
peak current	75	48	24	15	A
cont. Current	7.3	4.7	3	2	A
Theoretical Values					
rpm @ 24v	40,000.0	1428.6	895.5	578.3	
max V @ 130w	17.8	27.7	43.3	65.0	v
rpm @ max V	29,680	1,646	1,617	1,566	rpm
Torque @ cont. Current	0.66	0.67	0.68	0.70	nm
Gear ratio	9.00	4.00	9.00	9.00	none
Torque at wheels	5.91	2.67	6.11	6.33	nm
Cont. Driving force	118.26	53.345	122.175	126.675	n
Wheel velocity	3,297.8	411.6	179.7	174.0	rpm
Robot speed	17.27	2.16	0.94	0.91	m/s
Robot speed	38.85	4.85	2.12	2.05	mph
Peak torque at wheels	1215	545	977	950	nm

The table shows that winding style ‘G’ provides the closest match to the target velocity of 2m/s whilst still providing over ½ the torque required to navigate up 45° slopes within the continuous rating. Thus to climb the steepest slope the motors must be overrated by ~100% to achieve sufficient torque, well below the maximum current rating of 10 times continuous for short periods.

5.2.3 FLIPPER REQUIREMENTS

The terrain dimensions specify the flippers must be a minimum of 300mm long and the chassis a minimum of 350mm long, using the target chassis weight of 25kg allows the motor/gearbox combination torque to be calculated. Figure 27 - Flipper Torque Calculations shows the worst case scenario for the flipper motor where ½ the robots mass is elevated at the maximum length of the flipper arms, causing the highest moment of torque to act on the flipper arms and drive train.

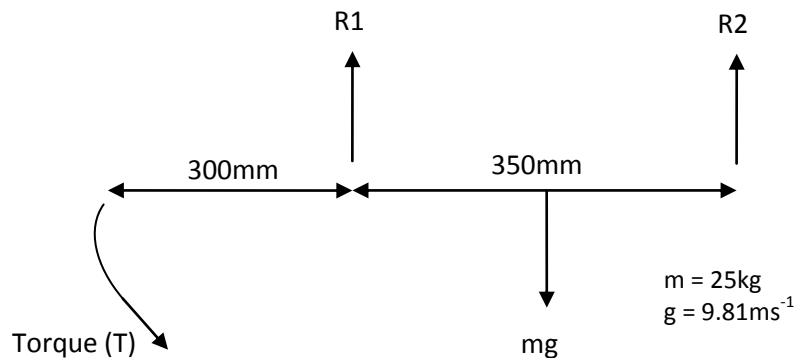


Figure 27 - Flipper Torque Calculations

Assuming the centre of mass acts about the centre of the robot chassis the resultant forces R1 and R2 in *Figure 27 - Flipper Torque Calculations* are equal, therefore;

$$R1 = R2 = \frac{mg}{2} = \frac{25 * 9.81}{2} = 122.6N$$

Equation 3 - Flipper Resultant Forces

Using the flipper lengths taken from the diagram in *Figure 27 - Flipper Torque Calculations* the torque required at the base of the flippers can be calculated as;

$$T = F.D = 122.6N * 0.3 = 36.8Nm$$

Equation 4 - Flipper Torque Required

The speed of the flippers is a compromise between how much they can be used, which is dependent on their deployment time and how large the drive motor assembly is. During the majority of the robots use the flippers will be folded either alongside the robot or pointing vertically up, thus they will usually need to be rotated a maximum of 90 – 180° when climbing over obstacles. To allow the flippers to be utilized fully they need to be capable of moving to their desired position in 5 – 10 seconds to prevent delays to the mission.

5.2.4 FLIPPER MOTOR SPECIFICATION

The requirements state the flippers must be capable of 36.8Nm of torque at a minimum of 6 revolutions per minute; hence the drive system must be capable of the same unless additional gearing is added between them. As space is very limited in the chassis a belt driven arrangement will be used with a 1:1 gear ratio. The key choice to be made when looking at small motor and gearbox combinations was the type of gearing used; either a worm and pinion or a planetary drive system, both with their advantages and disadvantages.

The worm gearbox allows a very high gear ratio in a single gear train, hence they tend to be lower in cost and have the added benefit they can only be moved by the drive end. Thus, once the motor has driven the flippers to the required position power can be removed and the flippers will maintain their current position. This may cause problems if the robot is dropped onto the flippers they will have no compliance and it is likely to damage the gearbox or other components in the drive train.

The planetary gearbox is much more complex with a multi stage gear train; however the package is still very small and capable of providing the torques required. The disadvantage with this method is closed loop feedback is required to keep the flippers in the required position when they are under load. Although the control system is more complex it is still achievable with off the shelf electronics.



Figure 28 - Planetary gear motor (Parvalux, 2008)

The gearbox was specified from Parvalux, a gearbox manufacturer who specialise in small drive systems. The model chosen, (see in Figure 28 - Planetary gear motor) consists of a 4 stage planetary reduction, providing a final torque of 30Nm at 12rpm, requiring a power input of 59 watts. Although this is not sufficient to meet the 37Nm of torque required, the gearbox can be overloaded by up to 50% for short periods.

5.2.1 MOTOR CONTROL

To allow speed control of the Main Drive Motors and positional control of the Flipper arms two sets of electronic speed controllers were required. Due to the short development time of the robot, off the shelf speed controllers were used to link between the software and the drive train hardware. Using 24V DC as the main power source and 24V DC motors allowed access to a wide range of standard hardware used commercially and for remote control vehicles.

Both controllers were specified from the same range from Roboteq, an American company specialising in robot control for domestic, commercial and military applications. This reduced the amount of interfacing required between the computer program and the electronic speed controllers as the code could be re-used.

The speed controllers are from the AX-Family of motor controllers which have an RS232 interface, closed loop feedback through encoders or analogue position sensor and temperature based current limiting. They also incorporate heartbeat functionality for additional safety in the case of communications failure.

5.2.1.1 MAIN MOTORS

The AX3500 speed controller (see Figure 29 - Roboteq AX3500 Motor Controller) has two channels, each capable of 60A peak and 30A continuous, easily capable of powering the main motors 4.7A continuous current, shown in Table 2 - Main Motor Characteristics.

The main motors each have encoder feedback with 1000 pulses per revolution; this allows precise monitoring of the track movements, hence the robot displacement. Although this information is relatively accurate in a straight line move due to the nature of the differential drive there is a large amount of slippage during turning. An additional benefit of the encoders is to allow the speed controller to hold the main tracks in a constant position, (I.E. to allow a 'soft' handbrake) or to allow accurate distance movements of each track.



Figure 29 - Roboteq AX3500 Motor Controller (Roboteq)

5.2.1.2 FLIPPER MOTOR

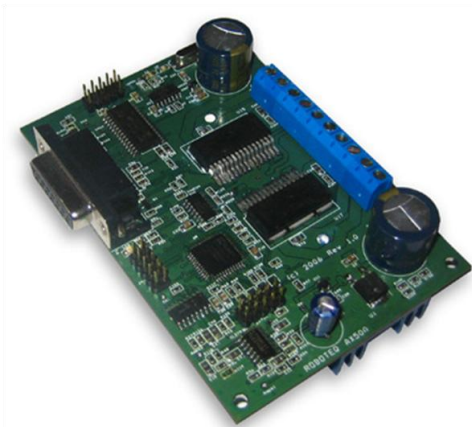


Figure 30 - Roboteq AX500 Motor Controller (Roboteq)

The flipper motor controller can be considerably smaller than the main motor controller as it only requires a single channel control of 59 watts. The AX500 (see Figure 30 - Roboteq AX500 Motor Controller) from the Roboteq can provide 7.5A or 180watts at 24v for one hour, easily capable enough of driving the flipper motor as the robots target run time is only 30 minutes. The AX500 also has a 0-5V analogue feedback input to provide closed loop control for accurate positioning.

The analogue encoder must be capable of endless 360 degree movement, output 0-5V over the full range and fit into a very small footprint. Typically an absolute encoder would be used for this purpose; however the vibration the chassis will suffer exceeds the limits of most optical encoder devices, not to mention their large size. This was solved using a non-contact, magnetic, angular sensor from Novotechnik (see Figure 31 - Novotechnik RFC4800 Magnetic Sensor) which measures the poles of a magnet attached to the drive shaft. The sensors allows up to 3mm lateral offset from the shaft which is more than sufficient on a machined chassis with a tolerance <1mm. Additionally the sensor datasheet claims a positional accuracy of $\pm 1^\circ$ which will allow positioning of the flipper arms to;

$$\pm 1^\circ + \text{Speed controller accuracy}$$

Equation 5 - Flipper Accuracy



Figure 31 - Novotechnik RFC4800 Magnetic Sensor (Novotechnik, 2008)

5.3 POWER REQUIREMENTS

The robot's battery packs provide all the electrical power that the robot has available for use during any competition mission. The minimum robot runtime that the batteries have to sustain is therefore set by the duration of the longest competition trial; specified as **25 minutes**. In addition to this, a 15-minute set-up time is provided thus a battery runtime to 40 minutes per trial is desirable.

5.3.1 CAPACITY

The capacity of the batteries is set to the power required for components to run for the minimum runtime. The loading conditions of each component will vary greatly throughout a trial, i.e. Drive motors will fluctuate between full-load, no-load cycles repeatedly, while the computer, and sensor arrays will have near constant power requirements. To estimate the minimum capacity needed, a power data sheet was compiled which lists every type of electrical component in the robot and its corresponding electrical requirements.

Table 3 - Component Power Requirements

Power Requirements	Efficiency	Quantity	Power (w)	Voltage	Full Load Current	Load Factor	Total (W)
Mini ITX		1	35	12		100%	35
LADAR		1	2.5	5	0.5	100%	2.50
Sonar		10	0.001	5	0.002	100%	0.01
Network Camera		2	2.5	5	0.5	100%	5
Flir Thermal Imager		1	2	5	0.4	100%	2
WLAN/Switch		1	12.5	5	2.5	100%	12.5
Fans		5	2.5	12	0.21	100%	12.5
LED lighting Array		3	6	24	0.25	100%	18
Services Total							87.51
Drive Motors		2	1152	24	48	9%	200
Drive Controller	20% drive						40
Flipper Motor		1	70	24	8	30%	21.00
Speed Controllers	20% arm					100%	4.20
						0	0.00
						Total	346.71

The motors will use the majority of available capacity but their needs vary largely on the terrain, i.e. stairs could use up to 100% load (2.3kW) whilst horizontal travel could use as little as 5% load (115W) @ 50% speed. Knowing how long the robot will spend in each condition is vital to specifying the correct battery capacity. Analysis of the competition terrain suggests an estimate of 1 minute of the trial under full load and the remainder at 5% is suitable to describe the load conditions, which results in a combined load factor of 8.88% (1min@2.3kW & 24min@115W = 200W approx). With a sustained power requirement of 353W, the robot's batteries have to hold approximately 235Wh of usable energy to provide a 40-minute runtime.

5.3.2 BATTERY CHEMISTRY TECHNOLOGIES

The chosen batteries have to be capable of delivering high currents (96A total) to the drive motors without inducing damage or notable distortion, therefore they must be rated for high performance with a high C value (where C is the peak rated draw current for a cell). The battery technologies that can sustain this typical loading are Ni-Cd (Nickel Cadmium), Ni-MH (Nickel-Metal Hydride) and Li-Poly (Lithium Polymer).

	Nickel-cadmium	Nickel-metal-hydride	Lead-acid sealed	Lithium-ion cobalt	Lithium-ion manganese	Lithium-ion phosphate
Gravimetric Energy Density (Wh/kg)	45-80	60-120	30-50	150 - 190	100 - 135	90 - 120
Internal Resistance in mΩ	100 to 200 ¹ 6V pack	200 to 300 ¹ 6V pack	<100 ¹ 12V pack	150 - 300 ¹ pack 100-130 per cell	25 - 75 ² per cell	25 - 50 ² per cell
Cycle Life (to 80% of initial capacity)	1500 ²	300 to 500 ^{3,4}	200 to 300 ³	300 - 500 ³	Better than 300 - 500 ⁴	>1000 lab conditions
Fast Charge Time	1h typical	2 to 4h	8 to 16h	1.5 - 3h	1h or less	1h or less
Overcharge Tolerance	moderate	low	high	Low. Cannot tolerate trickle charge.		
Self-discharge / Month (room temperature)	20% ⁵	30% ⁵	5%	<10% ⁵		
Cell Voltage Nominal Average	1.25V ⁷	1.25V ⁷	2V	3.6V 3.7V ⁸	Nominal 3.6V Average 3.8V ⁸	3.3V
Load Current peak best result	20C 1C	5C 0.5C or lower	5C ⁹ 0.2C	<3C 1C or lower	>30C 10C or lower	>30C 10C or lower
Operating Temperature¹⁰ (discharge only)	-40 to 60°C	-20 to 60°C	-20 to 60°C	-20 to 60°C		
Maintenance Requirement	30 to 60 days	60 to 90 days	3 to 6 months ¹¹	not required		
Safety	Thermally stable, fuse recommended	Thermally stable, fuse recommended	Thermally stable	Protection circuit mandatory; stable to 150°C	Protection circuit recommended; stable to 250°C	Protection circuit recommended; stable to 250°C
Commercial use since	1950	1990	1970	1991	1996	2006
Toxicity	Highly toxic, harmful to environment	Relatively low toxicity, should be recycled	Toxic lead and acids, harmful to environment	Low toxicity, can be disposed in small quantities		

Figure 32 - Battery Chemistry Comparison Table (Mr Isidor Buchmann)

1) Internal resistance of a battery pack varies with mAh rating, wiring and number of cells. Protection circuit of lithium-ion adds about 100mW.

2) Based on 18650 cell size. Cell size and design determines internal resistance. Larger cells can have an impedance of <15mOhms,

3) Cycle life is based on battery receiving regular maintenance. Failing to apply periodic full discharge cycles may reduce the cycle life by a factor of three.

4) Cycle life is based on the depth of discharge. Shallow discharges provide more cycles than deep discharges.

5) The self-discharge is highest immediately after charge, and then tapers off. The capacity loss of nickel-cadmium is 10% in the first 24h, then declines to about 10% every 30 days thereafter. High temperature increases self-discharge.

6) Internal protection circuits typically consume 3% of the stored energy per month.

7) The traditional nominal voltage is 1.25V; 1.2V is more commonly used to harmonize with lithium-ion (3 in series = 3.6V).

8) Lithium-ion is often rated higher than the nominal 3.6V, based on average voltage under load.

9) Capable of high current pulses; needs time to recuperate.

10) Applies to discharge only; charge temperature range is more confined. Delivers lower capacity at lower temperatures.

11) Maintenance may be in the form of 'equalizing' or 'topping' charge to prevent sulphation.

Ni-Cd, Ni-MH and Li-ion/poly cells have relatively fast recharge times, a vital attribute during competition and field deployment. Sealed Lead-acid has relatively slow recharge times thus multiple spare packs would be required to sustain operation in the field.

Battery cycle life is very high for NiCd (in excess of 1500 cycles) and relatively high for Lithium and Ni-MH (between 300-1000 cycles). Again, Sealed Lead-Acid cells do not perform comparatively well in this category with cycle life below 300 cycles.

It is important for the robot's peak load current to be at least matched, or outperformed by the chosen battery chemistry, otherwise robot performance limitations will occur. Ni-Cd and Li-Mn / Li-Po have the best peak current performance, well beyond what is required for the robot. Ni-MH and sealed Lead-acid have more appropriate peak current limits but higher C rated cells would be better-suited (7C). Li-Co is not suitable for this application.

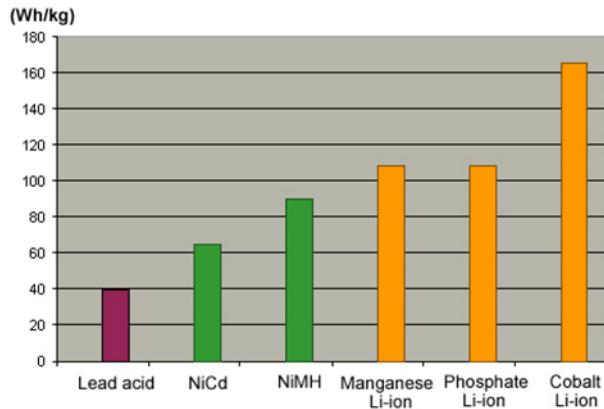


Figure 33 - Energy Density of Battery Chemistries (Mr Isidor Buchmann)

The robot should be as light as physically possible, yet have sufficient battery life to meet the runtime requirements. Therefore, Energy density is a considerable factor when choosing battery chemistry. Both Lead acid and Ni-Cd have a relatively low energy density; their use would result in an unacceptable weight penalty. Although the Li-Co has the highest energy density it is also the most unstable and explosive of the battery chemistries, therefore not acceptable either. The most appropriate chemistries for this application are Ni-MH, Li-Mn and Li-Po. They are all thermally stable, have relatively high cycle lives, short recharge times and relatively moderate energy densities.

5.3.3 CELL COST AND WEIGHT

For the appropriate chemistry to chosen, two final comparisons are needed, cell cost and their respective weight penalties at the required capacity.

Cell Type	Per Cell Voltage (V)	Amp hours (Ah)	Capacity (Wh)	Weight (Kg)	Cost (£)	Quantity	Total		
							Cost (£)	Weight (Kg)	Capacity (Wh)
Li-Po	11.1	3.2	35.52	0.3	55	6	330	1.8	213.12
Ni-MH	1.2	10	12	0.154	8	20	160	3.08	240
Lead Acid	12	7.5	90	2.8	25	2	50	5.6	180

Figure 34 - Cost vs. Weight Comparison at required capacity

Li-Phosphate cells have the most appropriate cell chemistry for this application, fast recharge, excellent cycle life and high energy density. However, the cost of this technology is prohibitive considering the need for multiple battery packs. Ni-MH offers the best value to weight ratio in addition to an appropriate capacity as specified above. The total 240Wh will provide the robot approximately 45 minutes of runtime, 20 minutes beyond the specified minimum of 25. This estimate, based on the assumption that the batteries will provide their rated capacity, is highly dependent on loading conditions. The highest capacity, non-custom Ni-MH cells (produced by Ansmann) are 10Ah, D type cells. Using 20 cells (2 packs of 10) rated at 1.2 Volts and 10Ah, creates a 24V rail capable of delivering 10 Amps continuous and 70Amp peak; which is sufficient to run the robot in a max load condition. The robot will typically draw power at 0.7C, which lowers the battery efficiency and available capacity (10Ah @ 0.2C) to approximately 9Ah (see Appendix 15.4 Annsman Battery Data Sheet). One full set of batteries will cost £160 and weighs 3.1kg

5.3.4 PACK DESIGN

The design of the battery housing focuses on low weight and quick removal using a minimum of components. The top and bottom plates, made from Nylon 66 (Impact resistant) use aluminium bracing bars to tie the packs together. A non-conductive material is essential for the top and bottom plates for two critical reasons, the battery terminal locations and the high risk of shock. The terminal link-cables run through the top and bottom plates in track-ways (see *Figure 35 - Battery Pack Design*). Another consideration is the means of pack connection to the robot. By using shrouded connectors, short circuit is prevented.



Figure 35 - Battery Pack Design

5.3.5 POWER SYSTEMS

In addition to the main drive and flipper motors, the on-board PC is powered directly through the 24V rail whilst all additional components will draw power through reduced voltage rails, e.g. 18V, 16V, 12V and 5V.

The electrical services components listed in the power calculation table consume the majority of the services power. The devices not listed are servomotors; used in the robot arm, USB TV capture card and USB to Serial converter. The USB devices will draw their 5V power through the PC, hence not listed as separate devices. The servomotors all require their own power rails (18V, 16V and 12V), but will only operate a fraction of the time spent on a mission, thus their power use is negligible relative to constant load devices.

5.3.6 CHARGE AND DISCHARGE CHARACTERISTICS

Correct battery maintenance is essential if the Ni-MH cells are to perform as designed and reach high cycle life. Their chemistry is less prone to memory effect (crystallization) than Ni-Cd and fewer exercise cycles are required, however the cells require full charge/discharge cycles **every 60-90 days**. Self-discharge rate is typically 50% higher than equivalent Ni-Cd at 30% per month. Sustained heavy discharge currents can prematurely age the cells reducing the cycle life below 300. Ni-MH cells cannot tolerate overcharge, thus algorithm-controlled chargers are required to maintain the cells.

Battery manufacturer, Ansmann stipulates a maximum charge voltage of 1.5Vs per cell, equating to a per-pack voltage of 30V. Maximum fast charge current is 5Amps, charging the cells in 2.2 hours. Maximum continuous discharge current is rated as 10Amps between 20°C and 50°C but peak current is in excess of 50Amps per cell. See graphs below for charge and discharge characteristics.

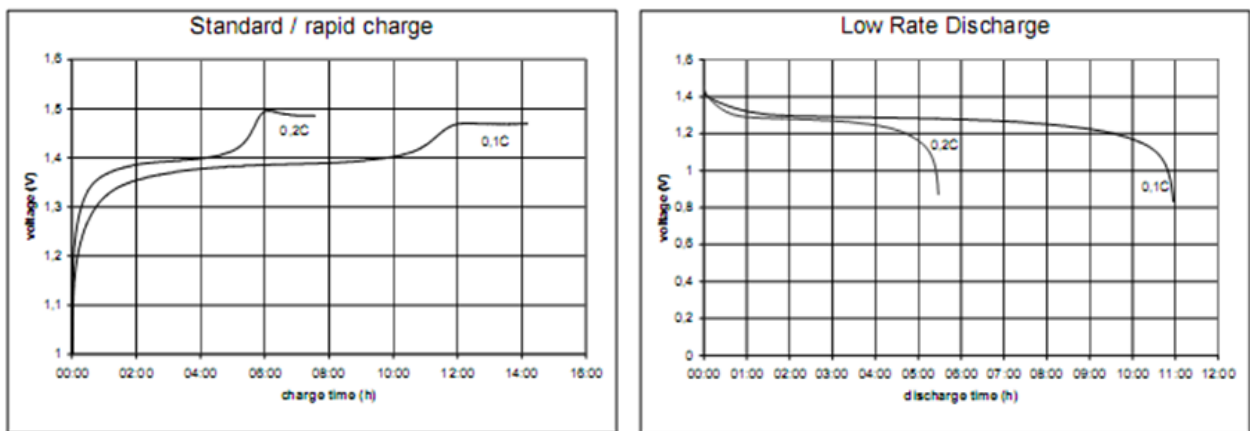


Figure 36 - Battery Charge and Discharge Characteristics (Gramlich, 2005)

5.3.7 CHARGING

Fast charging high capacity battery packs requires high power charging equipment. A cost effective charger capable of delivering 10Amps at 24Volts and fast charging a set of batteries inside 2.2 hours is the Robbe Power Peak, Infinity 3 (see *Figure 38 - Robbe 12v Battery Charger*). The majority of compact chargers in this price range use a 12V DC input which the Ripmax Pro Peak Power Supply provides, (see *Figure 38 - Ripmax Pro-Peak Power supply*).



Figure 38 - Robbe 12v Battery Charger (Robbe, 2006)



Figure 38 - Ripmax Pro-Peak Power supply (Ripmax, 2007)

5.4 BEARINGS AND SEALS

The concept chassis design using differential drive requires bearings capable of standing high thrust loads. This is relatively easily achieved using several different bearing types; however the target weight and size in our application limit the range significantly. Other aspects to consider include lubrication and sealing against dust and dirt from the terrain. Initial research considered rolling element type bearings including; Deep Groove Roller Ball, Angular Contact and Spherical Roller Thrust Bearings.

5.4.1 ROLLER BALL BEARINGS

Roller ball bearings are the most common in industrial electric motors and are capable of handling moderate radial and axial loads. They consist of a hardened inner and outer race with a series of metal balls which can rotate freely (see Figure 39 – Deep Groove Ball Bearing. They provide a low friction solution capable of moderately high speeds and misalignment. A standard ball bearing has a relatively shallow groove to guide the balls without causing excessive friction whereas deeper groove in these bearings allows higher axial loads.

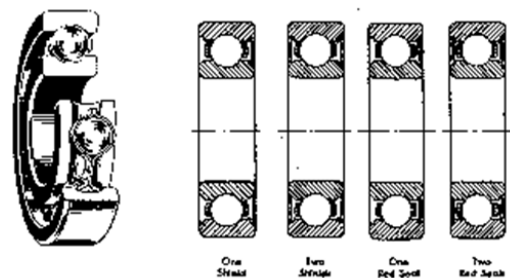


Figure 39 – Deep Groove Ball Bearing (US motors)

By locking a single bearing onto a shaft they constrain all translational movement but still allow rotation, to overcome this they are usually used in pairs, one each end of the shaft. This application requires a dense solution which can be achieved by using a double row of balls contained in the same housing (see Figure 40 - Double Row Angular Contact Bearing).

5.4.2 DOUBLE ROW ANGULAR CONTACT BEARINGS

Angular contact bearings use asymmetric races where axis loads pass in a straight line through the bearing as opposed to a roller ball bearing where the force tries to separate the inner and outer races (Machine Design). The larger the contact angle, typically 15 - 40° increases the axial load the bearing can withstand. The figure (see Figure 40 - Double Row Angular Contact Bearing) shows a double row angular contact bearing which constrains all axis of movement except rotation about the central axis. This type of bearing is capable of withstanding the loads from the differential drive but is relatively.

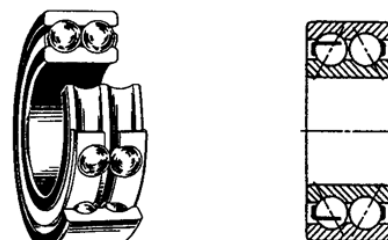


Figure 40 - Double Row Angular Contact Bearing (US motors)

5.4.3 SPHERICAL THRUST ROLLER BEARINGS

Spherical Roller Bearings are capable of withstanding extremely high axial and radial loads but they are generally much larger than other rolling element types. Preload springs are required to supply minimum down thrust at start up to prevent bearing skidding; hence this type of bearing has a lower efficiency than others. They are also large in size as two are required back to back and typically have a contact angle of 45° (US motors).

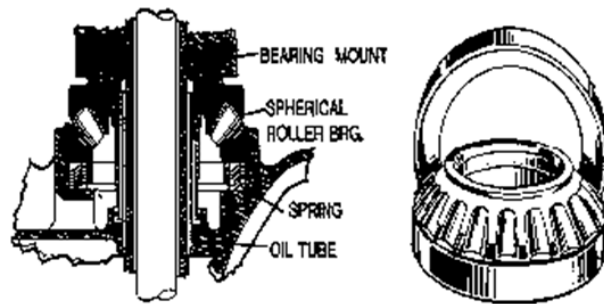


Figure 41 - Spherical Roller Thrust Bearing (US motors)

5.4.4 NEEDLE ROLLER BEARINGS

Needle Roller bearings use a set of cylindrical rollers, significantly smaller than the shaft they are rotating. As the rollers are much smaller than a traditional ball bearing they are much more compact. They have a significantly larger contact area than ball bearings hence, are less susceptible to imperfections in the bearing journal surface. A typical roller bearing consists of an inner and outer race with the needle rollers in the gap, where hardened shafts are used the inner race is not necessary, thus the overall bearing size is further reduced.



Figure 42 - Needle Roller Bearing (ToyoBearings, 2008)

5.4.5 POLYMER BEARINGS

Polymer bearings rely on a different technology, where they have a low friction surface for the shaft to revolve within. The advantages of polymer bearings are their light weight, low cost and high corrosion resistance, where their main disadvantage is higher friction due to the constant sliding of the bearing surface over the shaft (IGUS). IGUS are a manufacturer of a self lubricating polymer bearing materials which are available in a huge range of different sizes. Thermoplastics can have lubricants embedded into the surface and can mechanically reinforced with technical fibers to provide better wear resistance and lower surface friction (IGUS). The IGUS iGlide bearing range is suitable for running directly onto Aluminium shafts with a very thin walled design. One of the additional benefits of Polymer bearings are they can be manufactured with a flange at one end which can act as a thrust race.

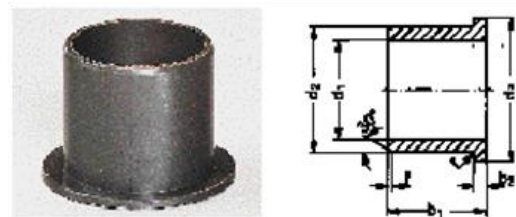


Figure 43 - IGUS iGlide Polymer Bearing

One of the disadvantages of Polymer bearings is the shaft itself acts as one of the bearing surfaces, thus the surface finish and hardness is more critical than other bearings that have an inner race.

5.4.6 BEARING COMPARISON

A table was produced showing the key variables for each bearing, using a sample bore of 50mm (see *Table 4 - Bearing Comparison*), an approximate size taken from the concept shaft through shaft design. After consideration of the requirements, especially size and weight the IGUS Polymer bearings are a significant advantage despite their higher tolerance requirement for shaft surface finish. The added advantage of the Polymer bearing is the lack of lubrication, requiring no continuous maintenance or servicing even within the terrain environment with dirt and dust.

Table 4 - Bearing Comparison

Bearing Type	Make	Part Number	Bore (mm)	Size (mm)		Mass (g)	Lubrication	Seal	Cost (£) Ex VAT
				OD	Width				
Roller Ball	NKE	NU210ETVP	50	90	23	580	Grease	None	36.97
Angular Contact	NKE	3210B2ZTV	50	90	30	740	Grease	Metal	49.54
Spherical Roller	NKE	22210EC3W33	50	90	23	580	Grease	Rubber	48.12
Needle Roller	NKE	NKI5025	50	68	25	270	Grease	Rubber	36.12
Polymer	IGUS	GFM-5055-10	50	55	10	18	Dry	N/A	4.28

Table 4 - Bearing Comparison shows a comparison between each of the types of bearings discussed in this section, where the following requirements are shown in order of importance.

- Thin wall thickness
- High thrust loads (Consequence of Differential Drive)
- Resistant to dust and dirt
- Light weight
- Low rolling resistance

In terms of physical dimensions the IGUS polymer bearings are far superior with only a 2.5mm wall thickness and less than 10% of the total weight. With the additional advantages of requiring no lubrication, hence no maintenance and being significantly cheaper they were a definite choice for this application. The key disadvantage to this type of bearing is the quality of surface finish and hardness which is discussed in the manufacturing section of this report.

6.0 MECHANICAL DESIGN

Modern day design and manufacture is largely done with the assistance of 3D CAD modelling. This allows realization of paper sketches to create a complete virtual model of the assembly before time and money is spent in manufacture. Once the concept design was completed and the drive train design began it became apparent just how complex the final chassis design would be.

The main design challenge within the chassis was the layout of the track and flipper drives as they both need to travel through the same axis. The solution to this was a “shaft inside a shaft”, where the inner shaft rotates independently to drive the flippers and the outer, tubular shaft drives the main tracks.

The first concept (*Figure 44 - Concept Drive Train 1*) has both the main drive and the flipper motors at the front of the chassis, in an attempt to keep the Centre of Mass (CoM) as far forward and as close to the flipper axis as possible. Thus reducing the torque required to actuate the flipper arms. However the initial design sketches in *Figure 44 - Concept*

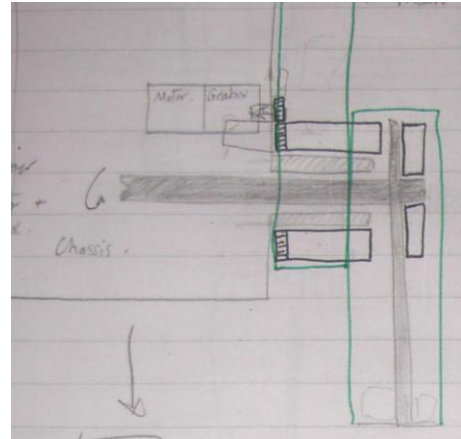


Figure 44 - Concept Drive Train 1

Drive Train 1 do not represent the true dimensions of the motors. Due to the size of the Parvalux flipper gear motor alone the main motors would have to be mounted above or below, increasing the CoM of the robot. This would increase the difficulty of negotiating up steep slopes where the CoM dictates the tipping point; hence the maximum slope the robot can climb.

6.1 DESIGN APPROACH

Computer Aided Design (CAD) has revolutionised the modern day design approach, allowing designers to create virtual models of components and insert them into large assemblies to ensure everything fits together correctly. The addition of tools such as Finite Element Analysis (FEA) allows verification of component strength and how they will distort under load, allowing optimisation of components and assemblies long before manufacture.

The University of Warwick benefits from a site license for SolidWorks, a CAD design, FEA, Motion and Flow simulation package. It is also the first choice for all of the designers working on this project, thus the entire chassis was designed and tested using this package.

As with most large projects, there were several designers working on different aspects of the assembly which caused problems with versioning of files. For the purpose of this project the files were stored on a single machine. Microsoft SyncToy was used to synchronise updates between the central database and a USB flash drive for each designer. Although SyncToy is able to determine when server designers have modified the same file, it is not able to merge changes, leading to some conflict which was overcome by discussion between designers.

To allow a uniform design approach there were several key design features that were agreed before the CAD models were created with the aim of standardising the tools and equipment required to manufacture and assemble the components.

6.1.1 CHASSIS CONSTRUCTION

The first major design decisions were materials and the main type of construction and fixing methods, where one of the key aspects is the ability to modify components by adding holes and additional fixing points as this is the first prototype.

One of the key features to the chassis is weight where the target is 25kg (*see 3.5 Robot Weight*), thus lightweight materials were required whilst still maintaining a rigid chassis. The materials also need to be resistant against corrosion unless finishing processes are used on the venerable components, where the disadvantage is modifications will expose the raw material, hence will need re-finishing.

Aluminium was specified as the main material due to its light weight, ease of machining and availability in any size required (*see section 8.0 for material selection*). The first design consideration was the method for constructing the main chassis;

6.1.1.1 SOLID BILLET CHASSIS

The complete chassis design could start as a solid block of in the CAD model. The key mounting points could then be drawn in, followed by removing material where necessary to fit the control electronics, motors and sensors into. One of the advantages of this method is the ability to FEA the entire structure at the end as one model to reduce the overall weight as much as possible. However this method would require an expensive billet of aluminum large enough and huge amounts of machining time to remove excess material, not to mention consideration for how to machine the internal mounting locations.

6.1.1.2 FABRICATED CHASSIS

This type of construction involves using flat sheet material cut to shape and formed using bending and press tool equipment. Fabricated construction typically uses joining processes such as welding or riveting to fix the formed parts together. This method of construction is usually difficult to take apart as welded and riveted joints have to be destroyed to take them apart. The advantage of this construction is it is simple to manufacture the components using processes such as laser cutting and the result is very rigid and lightweight. Despite these advantages fabricated construction is very time consuming to design and does not lend itself well to the modifications undoubtedly required in a prototype design.

6.1.1.3 PLATE CONSTRUCTION

This is the approach the design process took, where the chassis is built up from flat plates which can be easily machined and joined together. Although there are several joining techniques the majority of the chassis is bolted together using CAP head screws, this allows over 90% of the chassis to be constructed using only a single set of Allen Keys. The main side plates of the chassis were designed around 12mm plate, as this provides sufficient depth for tapped threads perpendicular to the plate. This also allows M6 threads tapped into the ends of the plate whilst still maintaining sufficient strength. Although 12mm plate appears heavy in solid form, the component parts can have pockets removed where the strength is not required to reduce the overall weight.

6.1.2 FIXINGS AND HARDWARE

Once the type of construction was decided the design team agreed a specification for holes, clearances, tolerances and counter bores was devised with the aim of standardising part design. As discussed in the plate construction section CAP head screws were the standard choice of fixing throughout the chassis using counter bored fixing holes to prevent interference.

Corrosion resistance is important to prevent threads jamming. This was overcome using Stainless Steel bolts. Despite the lower strength of Stainless steel this was neglected as the tapped Aluminium holes are significantly weaker still. Key components such as motors, electronics and sensors were mounted using a combination of Nylock nuts, shake proof washers and Loctite to prevent them vibrating loose during operation.

6.1.3 SOLIDWORKS DESIGN AIDS

SolidWorks has a number of inbuilt features to simplify and standardise the addition of common features within CAD models, two of the key features used throughout this project were the hole wizard and the sheet metal toolbox;

Hole Wizard

This allows the user to select the type and size of the fixing required, specify the location and SolidWorks will automatically calculate the hole dimensions. When using tapped holes SolidWorks calculates the size of the tap drill, draws a double ring representing the peaks and troughs of the thread and assigns a cosmetic thread pattern to the hole. When importing the solid model into the machining software it automatically detects the threaded holes and sets up the drilling and tapping operation automatically, thus saving time and reducing the possibility of errors.

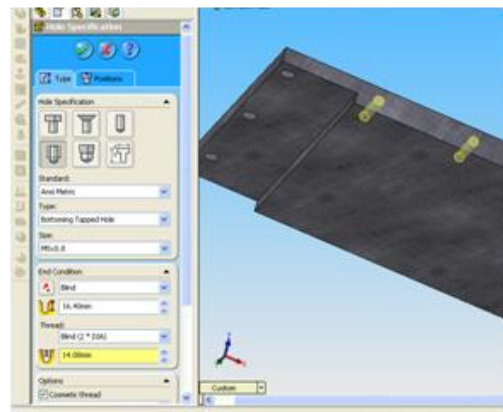


Figure 45 - SolidWorks Hole Wizard

Flat Plate design

One of the problems when designing parts to be folded from flat plate is to consider the bend radius and the material bend factor, i.e. how much material length is used in within the bend. Usually parts are designed and an allowance is made for each bend depending on the thickness of the plate and the angle of the bend. SolidWorks has a sheet metal toolbox which allows plate parts to be modelled in 3D (see Figure 46 - SolidWorks *Folded and Unfolded Sheet Metal*) then a flat sheet cutting pattern can be generated including all of the bend tolerances, thus reducing the design and development time.

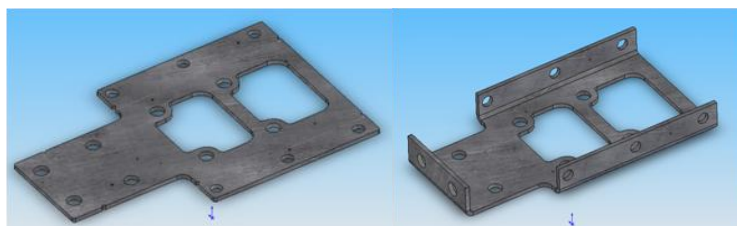


Figure 46 - SolidWorks *Folded and Unfolded Sheet Metal Bracket*

6.2 CAD DESIGN APPROACH

In order to ensure the chassis could be assembled every significant component in the robot was modelled in SolidWorks allowing the designers to check everything will fit. Additionally several tools such as Allen keys were also modelled to check certain bolts could be reached and tightened. Modelling the electronic components in 3D also helped consideration of the cooling for each section as the heat sinks are clearly visible for the major heat producing components.

The design approach for the main chassis components all followed a similar pattern which allowed the chassis to be assembled in CAD to check the fit of components before time was spent optimising components for strength and weight.;

Draw the outline of the part (e.g. side plates)

Major fixing points (e.g. connection to the rest of the chassis)

Component fixing points (e.g. motor fixing points)

Component clearance (e.g. pockets or cable holes)

Weight reduction (e.g. removing excess material to save weight)

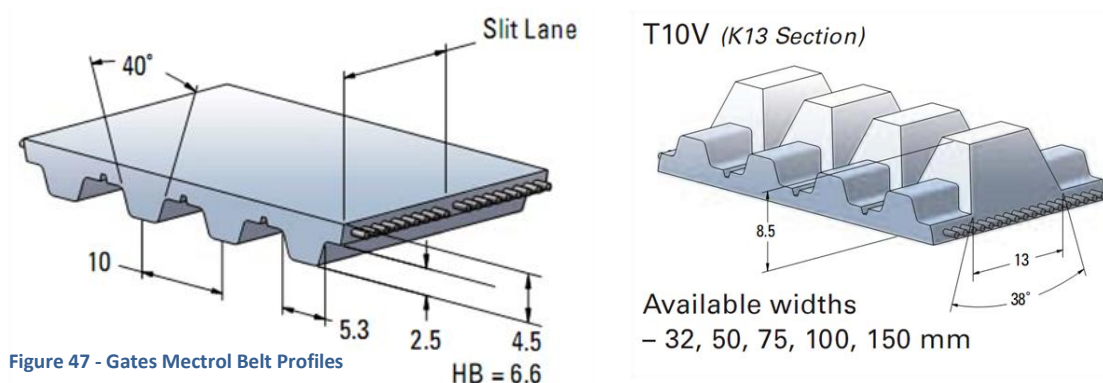
One of the key flaws with many of the other rescue robots is the vulnerability of their sensors, in an aim to overcome this, the sensors were some of the first components modelled in 3D so the front and rear chassis plates could be designed around them.

NB: See the CAD Drawings Report for detailed drawings of all the custom manufactured parts.

6.3 PULLEY DESIGN

With the caterpillar tracks specified and the general chassis and drive system conceptualized, the next task was to design custom pulleys for the drive, compound drive and flipper arms. The pulley tooth profiles were designed using the Gates Mectrol Catalogue (*see Appendix 15.2*).

The T10V belts with a PVC coating have a minimum bend radius of 90mm, therefore the smaller front flipper pulleys had to use the next available size, $300\text{mm}/\pi = 95.4\text{mm}$ pitch diameter. The pitch diameter of the belts is taken from the fibres contained within the belts; these form the neutral axis, 1mm from the either side. As the belts bend around the pitch diameter the shape of the teeth distort and fatten as a function of the bend radius. This requires the sockets they sit in to be larger,



thus the tooth profile on the flipper pulleys were designed to accommodate. Instead of a 17° chamfer on the pulley sockets, 25° was required with the socket root remaining the same. This resulted in 'sharper' teeth on the pulley.

With all belts using the K13 V-groove, the front pulleys could be either a single pulley with a V-groove profile or split pulleys with chamfered edges. To ensure as little material as possible was placed outside of the belt the flipper design used a central link arm with identical split pulleys either side (as can be seen in Figure 48 - Front Flipper Pulleys).

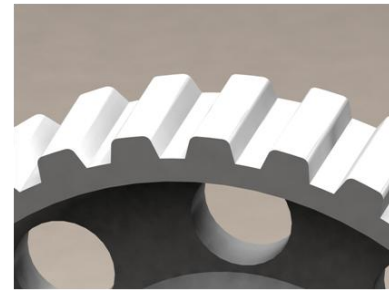


Figure 49 - Flipper Pulley Tooth Profile

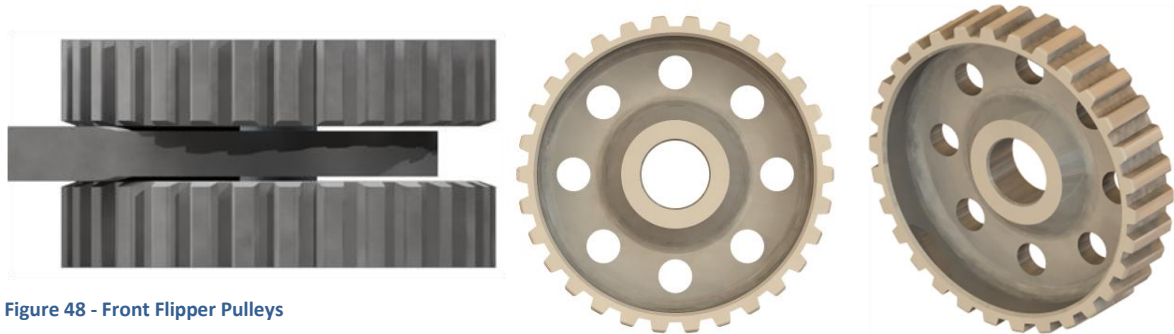


Figure 48 - Front Flipper Pulleys

Weight saving is a key issue in all components so as much material was removed as possible with FEA analysis showing acceptable distortions of $\pm 0.1\text{mm}$ under worst case loading (50% target chassis mass axially and compressively loaded).

In contrast to flipper pulleys, the rear and compound drive pulleys were all machined from single billets of aluminium and could not be separated along the groove line, thus a K13 V-groove was required. With the front pulleys carrying two belts they needed two V-grooves. Again, using the Gates catalogue the specific dimensions were incorporated into the CAD models (Figure 50 - K13 V-Groove Profile) and the material compression issue was accommodated with a 1mm change in socket depth.

To simplify design a single pitch diameter was used for all the chassis mounted pulleys (rear drive and compound drive), (38 teeth, $380\text{mm}/\pi$) 120.96mm. This larger diameter relative to the flipper pulleys resulted in a less compressive tooth distortion on the belts. A 20° chamfer from socket root position was used instead of the standard 17°.

The production design for the compound drive pulleys; which transfer belt drive from the rear to the front, is shown below in Figure 51 - Compound Drive Pulley. During the design process FEA analysis showed that a shock load (50% target weight) normal to the driving pulley face would result in an oval distortion to the cylinder shape. The prevention method was to add support material radiating out from the centre.

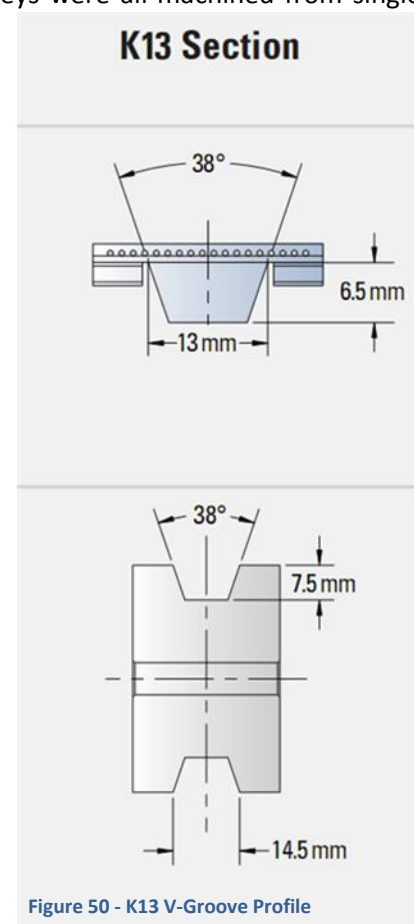


Figure 50 - K13 V-Groove Profile

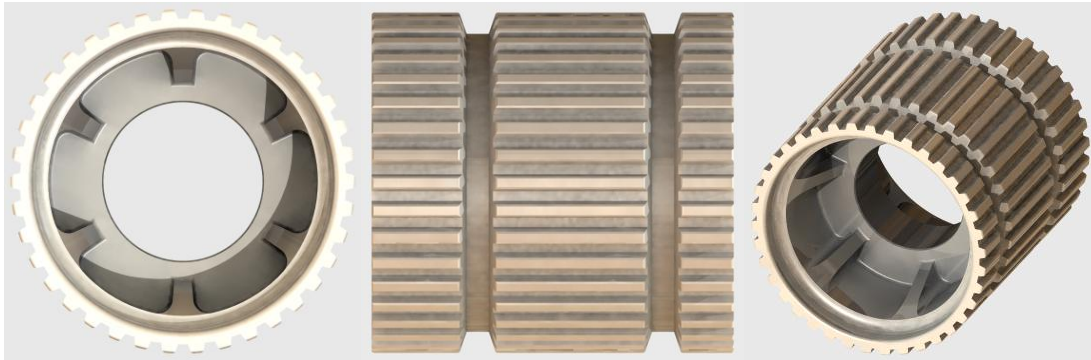


Figure 51 - Compound Drive Pulley

6.4 REAR DRIVE TRAIN DESIGN

After various iterations of the concept designs it was decided to drive the tracks with the rear pulleys, using the middle pulleys as idling wheels to transfer drive to the flipper tracks. Another important consideration in the design was the fixing method to hold the pulleys in place with enough rigidity to support the high thrust loads encountered while turning.

One of the key mechanical components in the drive train is the bearings; these provide the ability to rotate the pulleys about their shafts. As discussed in the previous section Polymer bearings were chosen as the most suitable for this application, their low wall thickness allowed more freedom in the design and stronger shafts and pulleys.

The next design feature for the rear drive is the method for fixing the wheels in place and resisting the high thrust loads the tracks exert during turning. The maximum force the robot can exert is the product of its weight and the co-efficient of friction on the surface below them, hence on a smooth surface the maximum force is equal to; $m * \mu = 25\text{kg}$.

A typical method for fixing a bearing on a shaft is to drill and tap the end of the shaft and use clamping bolt across the front of the bearing face, this is was not possible at the front of the chassis due to the shaft through shaft design. Another way of achieved the clamping would be to put an M50 thread on the end of the shaft and make a large diameter locking nut but this is susceptible to loosening with vibration.

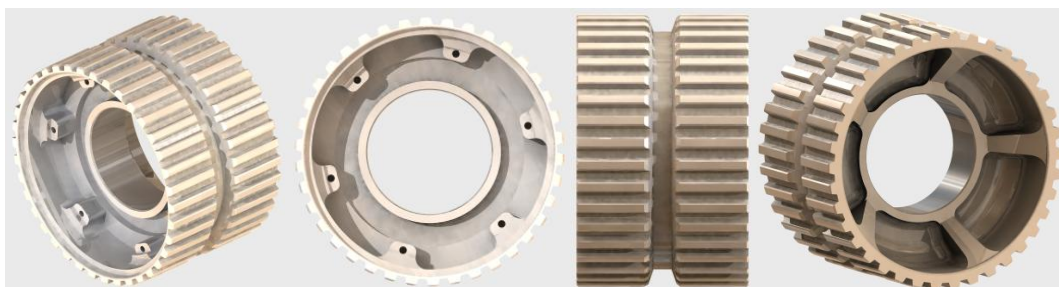


Figure 52 - Rear Drive Pulley

6.4.1 CIRCLIP FIXING METHOD

The solution to holding the bearings and pulleys onto the shafts was to use a circlip. Manufactured from high strength spring steel they are very strong and highly resistant to vibration. For example, using a steel shaft of yield strength = 200N/mm^2 , a 50mm Circlip is capable of carrying a load of 38KN (Roy Mech), significantly higher than any forces the robot is likely to experience.

Figure 53 - External Circlip Fitting shows a 50mm Circlip opened up using a pair of external circlip pliers, thus allowing it to be slid into the matching groove on the shaft.



Figure 53 - External Circlip Fitting

6.4.2 MOTOR POSITIONING

Space inside the centre of the chassis is at a premium as there is a large amount of processing, control and sensor components that need to be mounted internally. The first consideration for motor placement was between the drive tracks as they are quite wide and this space serves little purpose. As the motors are quite long they would have to be placed in line with the chassis from front to back. This would require a 90° drive to transfer power from the motors to the pulleys. Although

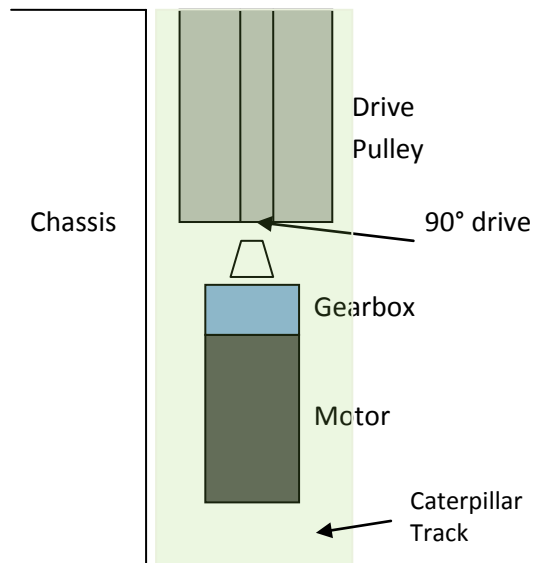


Figure 54 - Drive in track concept

possible this would require a bevelled gear pattern to be machined into the outside of the pulleys, as shown in Figure 54 - Drive in track concept. This type of gear pattern would be possible using 5-axis machining, however it would require a high strength material as the gear teeth are relatively small but need to be capable of withstanding the full torque of the drive system.

Although the drive train could not fill the gap between the tracks, the twin battery packs fit with little space to spare and have the additional benefit of being easily accessible. Thus, the motors were mounted inside of the chassis whilst still leaving a large enough space in the centre section for the control electronics.

6.4.3 GEARBOX

The motor gear ratio is specified by the choice of main motors in Table 2 - Main Motor Characteristics, where the gear ratio needs to be approximately 4:1 to achieve the required torque at the wheels. The first design was to use drive belts between the drive pulleys and the motor shafts as they are easily obtainable and in a wide range of different sizes. The disadvantage to using belts is the necessity for the additional space for the tensioning mechanism, thus fixed ratio gears were purchased as off the shelf components and the custom components were designed around them.

The concept drawing in *Figure 55 - Concept Drive Train 2 – Rear Pulleys* shows the flanged bearings pressed into either end of the rear pulleys to provide support for rotary bearing and end thrust loading. The drawing also highlights the use of circlip grooves at the ends of the shaft to hold the assembly together, NB: The thrust washers spread the load of the bearing onto the circlip, thus preventing the contoured shape of the circlip damaging the face of the bearing.

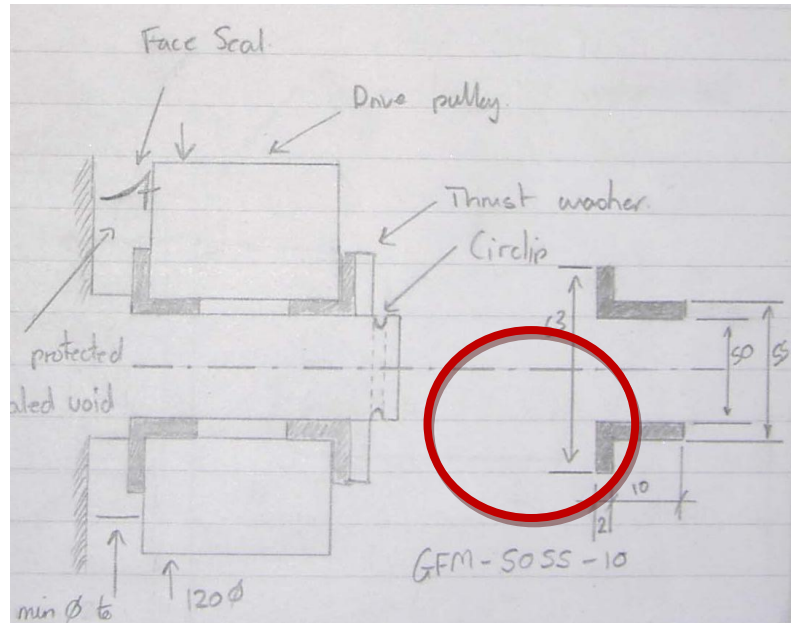


Figure 55 - Concept Drive Train 2 – Rear Pulleys

To prevent the drive train using up excess space within the main chassis an internal annulus gear ring was embedded into the rear pulley design, allowing the gearbox components to be kept out of the chassis. This has the additional benefit of keeping the gearbox grease contained within the pulleys. To prevent contamination of the grease a method is needed to seal them away from the outside world, *Figure 55 - Concept Drive Train 2* shows a face seal highlighted in red, which prevents dirt from entering the gear train cavity within the pulleys.

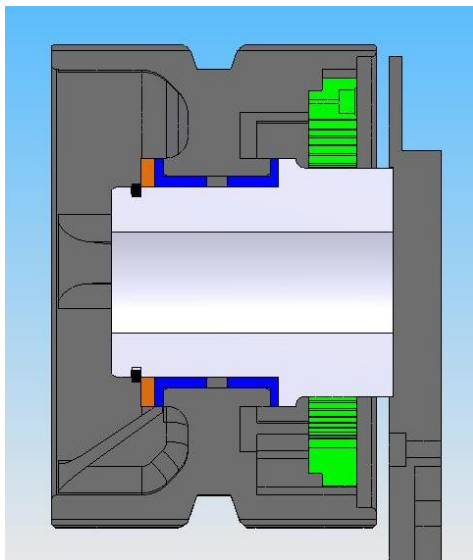


Figure 56 - Rear Drive cut-through

Both halves of the gear train, the spur and the internal gear were purchased from HPC gears to ensure they would mesh together. The internal gears are designed to be shrink fitted into a location which causes difficulty disassembling components, thus 5 counter bored holes were drilled around the outside edge of the gear to allow them to be bolted to the pulleys. To achieve the desired ratio the largest internal gear that would fit was used, thus allowing the most scope to further reduce the gear ratio at a later date if required. Using an 80 tooth internal and 20 teeth spur gear gave an exact ratio of 4:1, identical to the requirements in *section 5.2.2*.

The final layout for the rear drive train can be seen in *Figure 56 - Rear Drive cut-through*. The flanged bearings can be seen in blue between the outer pulley and the central stub shaft, with a bronze thrust washer and black circlip sitting in a groove to hold them in place. The internal annulus gear can be seen in green with the spur gear meshing behind the stub shaft. The motor is bolted to the opposite side of the side plate on the right hand side.

One of the requirements of such a small chassis is to separate noisy electronics from the computer processing equipment, thus the speed controller was mounted directly above the motors in the rear

section. This allows the entire rear section of the chassis to be connected up using a single power rail and RS232 serial connection.

Figure 57 - Rear drive CAD VS Photo shows the similarity between the rendered CAD model on the left and the final assembly of the rear section on the right. The CAD model excludes cable routing and some of the final fixing screws as these slow the computer model down with little benefit. The internal and spur gear mesh can be seen through the transparent drive pulleys in the CAD model.

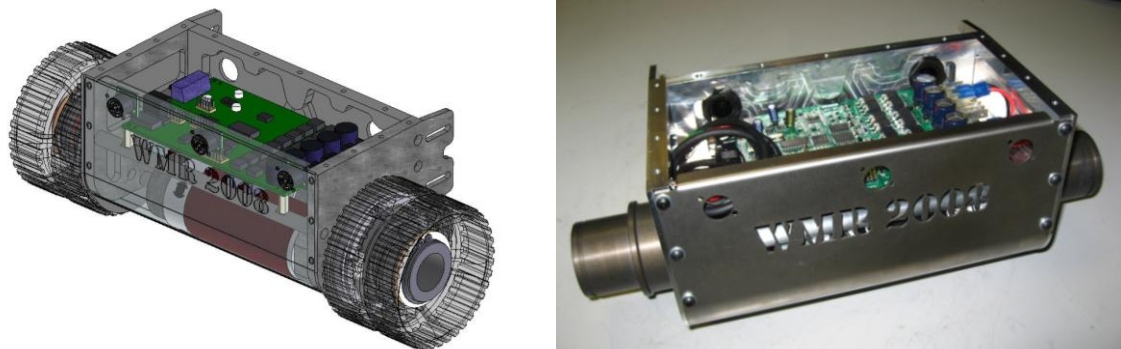


Figure 57 - Rear drive CAD VS Photo

6.5 FLIPPER DRIVE TRAIN DESIGN

The flipper arms are controlled by a common shaft passing through the centre of the front pulley stub shafts which is connected to the gear motor specified in *5.2.4 Flipper Motor Specification*. The mechanical construction of this section is similar to the rear, using flanged polymer bearings either side of the pulleys with a thrust washer and circlip to prevent them sliding off the stub shaft.

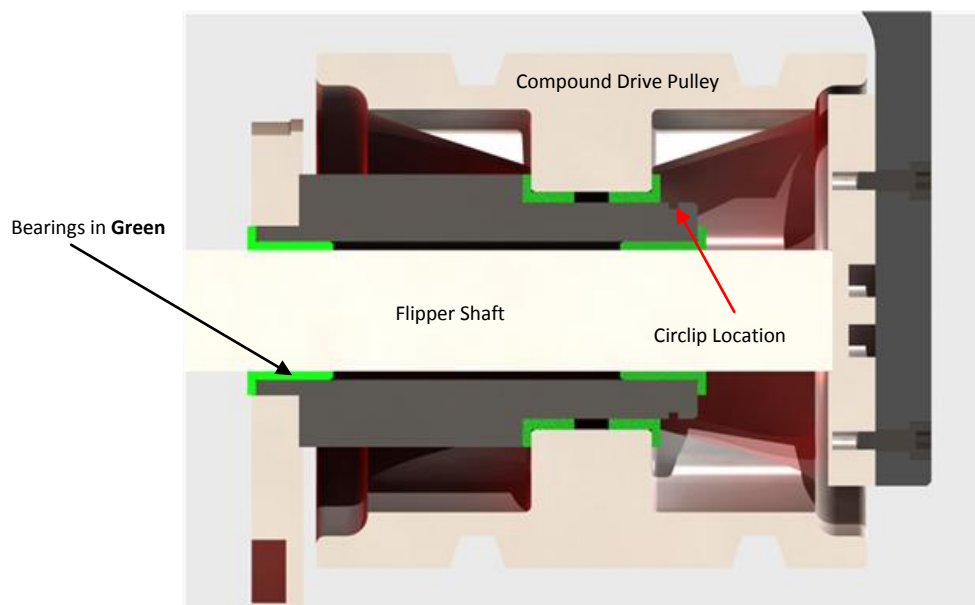


Figure 58 - Concept Drive Train 2 - Compound pulley

The additional shaft through the centre of the stub shaft requires a method to constrain its movement along the central axis of the shaft and the capability to withstand high bending loads from the flippers. This was achieved using two smaller polymer bearings, one each end of the front stub shafts and two locking collars up against flanges of the internal bearings.

6.5.1 FLIPPER MOTOR AND SHAFT DRIVE MECHANISM

The flipper arms are powered via a belt drive from the Parvalux gearbox and motor. The Parvalux shaft is keyed (3mm) so a keyed tapered bush has been used to fasten the belt pulley (34 tooth, T5 profile) in place. This approach was the only suitable solution due to the size constraints within the front chassis area. The Parvalux motor, gearbox and drive shaft is over 227mm long, whilst the internal width of the chassis is only 225mm. As the flipper arms require closed loop feedback and no encoders were available built into the motor, an external non-contact magnetic positional encoder was used. In order to fit the 12mm thick encoder and motor, the chassis side plates had 10mm profiled sections machined into them, providing the vital space needed to locate the motor and encoder (see *Figure 59 - Flipper Drive Assembly* and *Figure 67 - Flipper*).

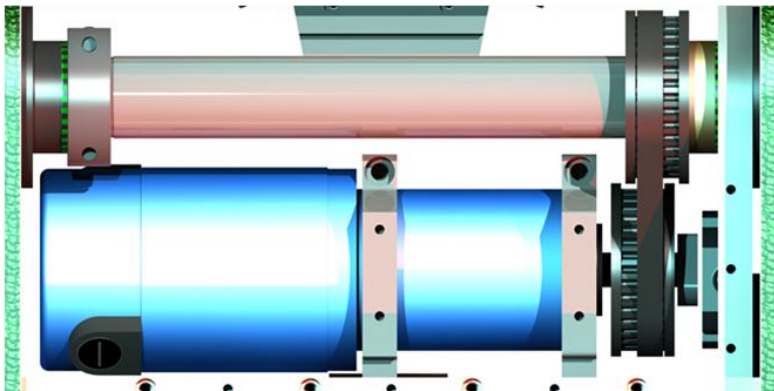


Figure 59 - Flipper Drive Assembly



Figure 60 - Flipper Motor & Pulley

Due to the restricted space available once the motor assembly is in place, a custom-made magnet holder was machined from nylon to hold a reduced size bar magnet needed for the encoder feedback. This was fixed to the end of the motor shaft through a M3 tapped hole.

Note for Assembly: The magnetic encoder needs to be positioned first, once the motor is located and the belt tensioned, the encoder has to be centralised to the magnet fastened to the end of the motor shaft (*Figure 61 - Magnetic Encoder*).

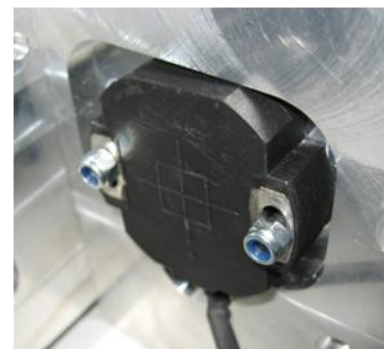


Figure 61 - Magnetic Encoder

To hold the flipper motor in location within the chassis, two locking collars were machined to clamp over the gearbox housing (*Figure 60 - Flipper Motor*), these collars doubled up as the belt tensioning mechanism when placed against the central chamber front wall (*Figure 62 - Flipper Motor Belt Tensioning*). By using 4x M6 Cap heads and tapping threads into the locking collars the motor can be pulled away from the flipper shaft, therefore tensioning the drive belt.

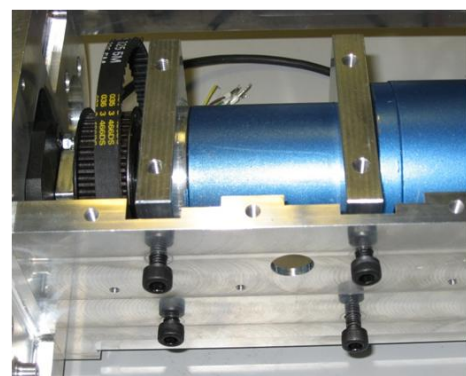


Figure 62 - Flipper Motor Belt Tensioning



The flipper shaft uses the same keyway, tapered locking bush and belt pulley combination (28mm ID bush, 8mm Key, 36 tooth pulley) as the motor assembly. To ensure the flipper shaft did not slip a split locking bush was used on the opposite side to the belt pulley (*Figure 59 - Flipper Drive Assembly*). This also allows for lateral adjustment of the shaft when aligning the belt on the pulleys.

Figure 63 - Flipper Shaft Components

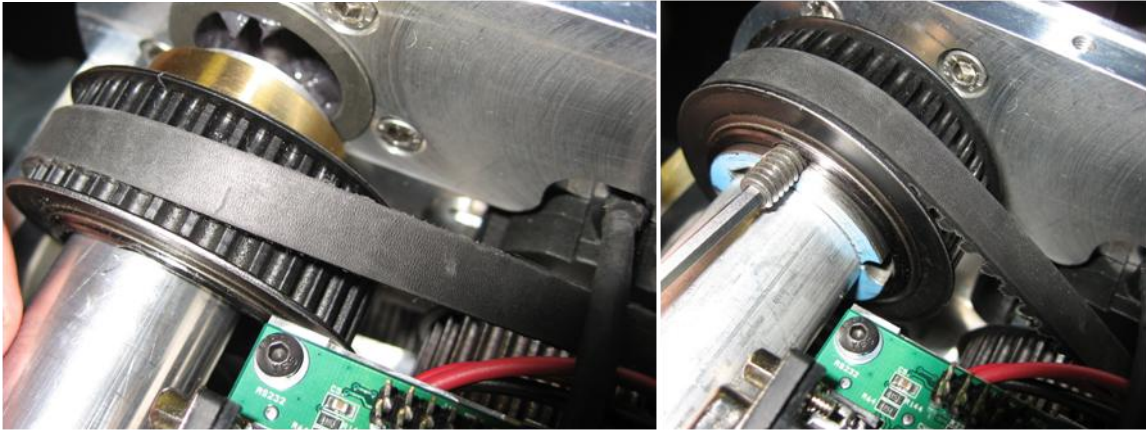


Figure 64 - Positioning Flipper Motor Belt

By transferring drive through a belt whilst using bearings and bushes to locate the shaft, the flippers can effectively turn endless 360° cycles. However, with the belt pulleys using a non 1:1 ratio the encoder becomes out of sync if the arm is turned past the 0-360° barrier, therefore, a pulley change is required on the flipper shaft to provide a matched ratio. The motor pulley cannot be changed as it already uses the largest pulley available for a 12mm taper-lock bush.

6.5.2 FLIPPER ARM EXPLODED VIEW

The exploded view below shows the concept flipper arm before production began, several changes were made to simplify this design; the Tensioning Bracket was brought to the front side, the Centre Arm thinned to remove weight and the Bracing Arms simplified and strengthened (extra cross section).

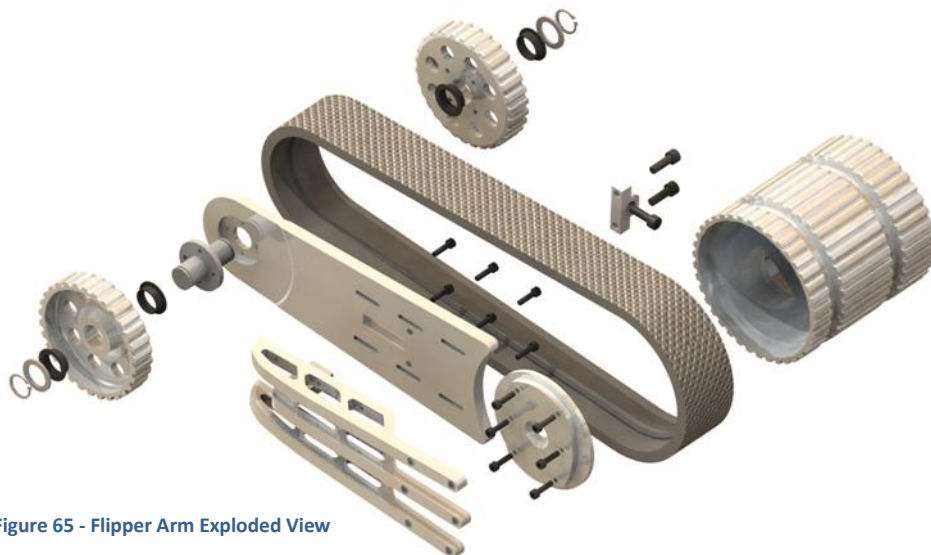


Figure 65 - Flipper Arm Exploded View

6.5.3 BELT TENSIONING

All belts stretch during use (varies on load, age, conditions) and the same is true of the drive tracks purchased from Gates for this robot. Therefore, a tensioning mechanism is required for the both the flipper arms and main chassis.

The chosen design solution uses a single M8 thread to tension the arm (*Figure 66 - Flipper Arm Tensioner*) and 8x M5 Cap heads to hold location once tensioned. By using slots on the arm plate, the entire flipper assembly can stretch and shrink (-10mm, +15mm).

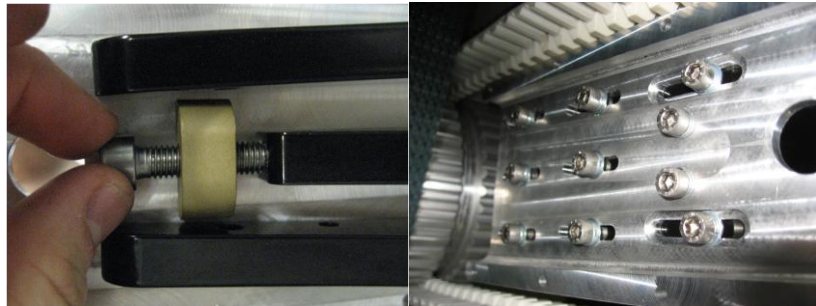


Figure 66 - Flipper Arm Tensioner

The minimum belt length that could be purchased from Gates was 940mm (94 teeth), this limitation resulted in the flipper arms being longer than required. The knock on effect was the extra power needed to drive them and lift the robot. Centre to centre, the flipper arms span 310mm, taking into consideration surface contact they span 330mm (approx), requiring 10% more power from the motor than expected.

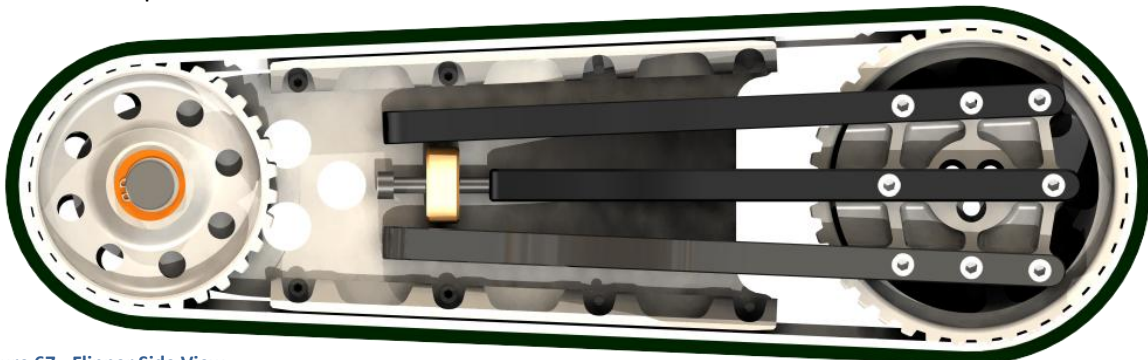


Figure 67 - Flipper Side View

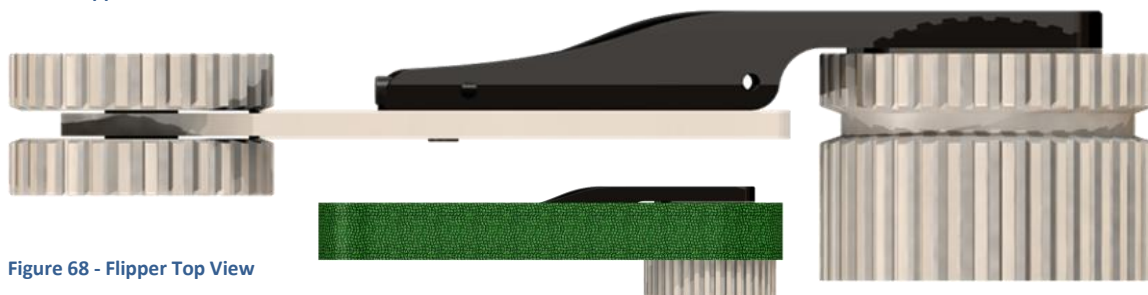


Figure 68 - Flipper Top View

Looking at Figure 68 - Flipper Top View, an alternative, more complicated design approach could have used a split-pulley on the compound drive leaving an idle pulley on the outside instead of the current single part with two v-grooves. This approach was avoided because of the unknown shear resistance of the belts and their stability if only one side of a pulley was driven. However, not employing this method has resulted in extra material being located outside of the belts extremes (flipper armatures), which can be caught on terrain.

6.6 CENTRE CHASSIS SECTION

6.6.1 BELT TENSIONING

To simplify the drive train and gearbox the entire rear drive assembly is self contained and fixed. By treating the rear and the central chassis as separate units they only require a selection of cables to pass between them for operation. Taking advantage of this feature allows a simple tensioning mechanism to be implemented using the same principal as the flipper arms. Slot are located in the sides of the rear drive chassis which can slide on 'pinching' bolts treaded into the central chassis (see *Figure 69 - Chassis Tensioner Side View*).



Figure 69 - Chassis Tensioner Side View

To tension the belts three M8 bolts are located inside the central chassis (*Figure 70 - Chassis Tensioner Plan View*). By adjusting the bottom two, any discrepancies in belt lengths can be removed. The top bolt is the tensioning bolt (always easily accessible) as it uses the bottom two as a fulcrum. With the belts tensioned to specification the remaining six external bolts can be fastened with washers and star washer/spring washers for security.

By mounting the necessary adjustment bolts in easily accessible locations any field changes (such as removing the belts or replacing them) can be made quickly and simply.

Track skids have been placed below the central chassis (above main tracks) to prevent over stretching (resulting in excessive loading on the drive motors) of the drive belts when the robot is traversing uneven terrain and step fields. The inherent disadvantage with skids is the extra frictional loading on the drive motors when the tracks are in contact.

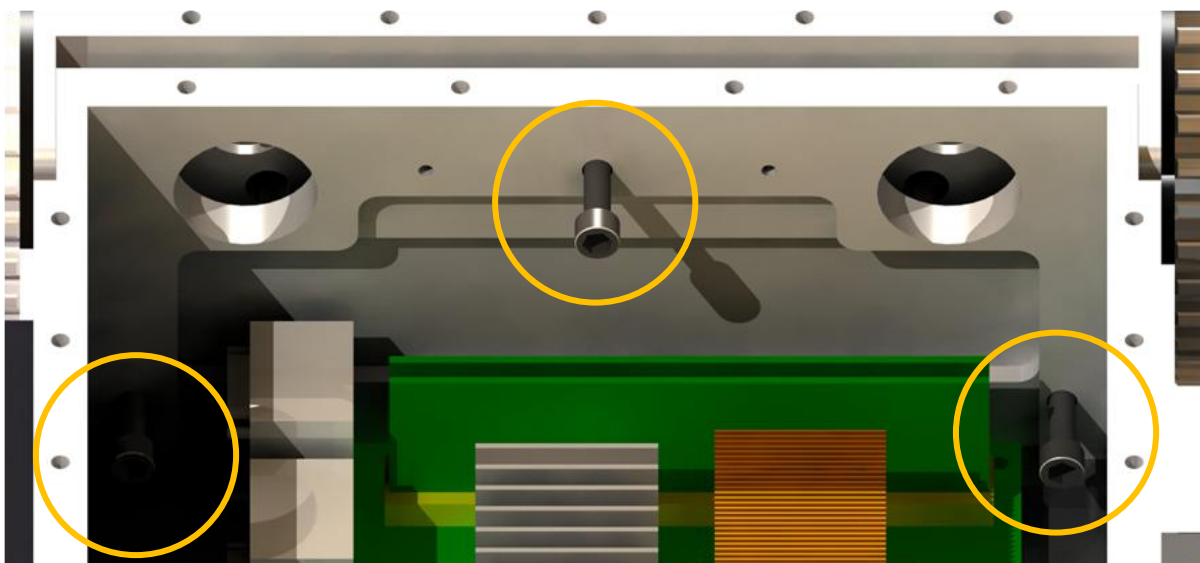


Figure 70 - Chassis Tensioner Plan View

6.7 SUB-ASSEMBLIES

Once the major of the drive components were modelled in SolidWorks, the designers experienced problems with slow performance due to the number of component parts. Additional problems were caused when both designers modified the single assembly file. To overcome this, chassis construction was broken down into several sub assemblies; Rear drive, Centre chassis, Flipper arms, Robot Arm and Batteries. This allowed the designers to each work on the smaller sub assemblies whose changes were automatically imported to the overall assembly of assemblies.

6.8 ROBOT ARM

For the best chance of identifying victims the sensory array located at the end of the arm should house as many sensors as possible, unfortunately this approach carries the greatest weight penalty. The guaranteed signs of life in all cases are; human form, heat and CO₂. To identify form and motion both a thermal imaging and video camera are suitable, but only a thermal imaging camera can identify a heat source. Although it would be possible to drive a robot using a thermal camera, it would not be easy negotiating terrains with little thermal gradient (inside of buildings), therefore a video camera is also necessary. Since weight is at a premium, the justification was made that just a thermal camera and lightweight network camera would be sufficient for the tasks of navigation and identification. Section 9 outlines the possible choices of device.

As discussed in section 4.4, the method for robot arm power is DC digital servomotors. With the head sensors known (thus the approximate masses known) and a pan and tilt function needed, the servo torque requirements could be calculated.

Figure 71 - Robot Arm Sketches shows initial loading calculations for the robot arm. The lengths and masses were modified as the devices were specified.

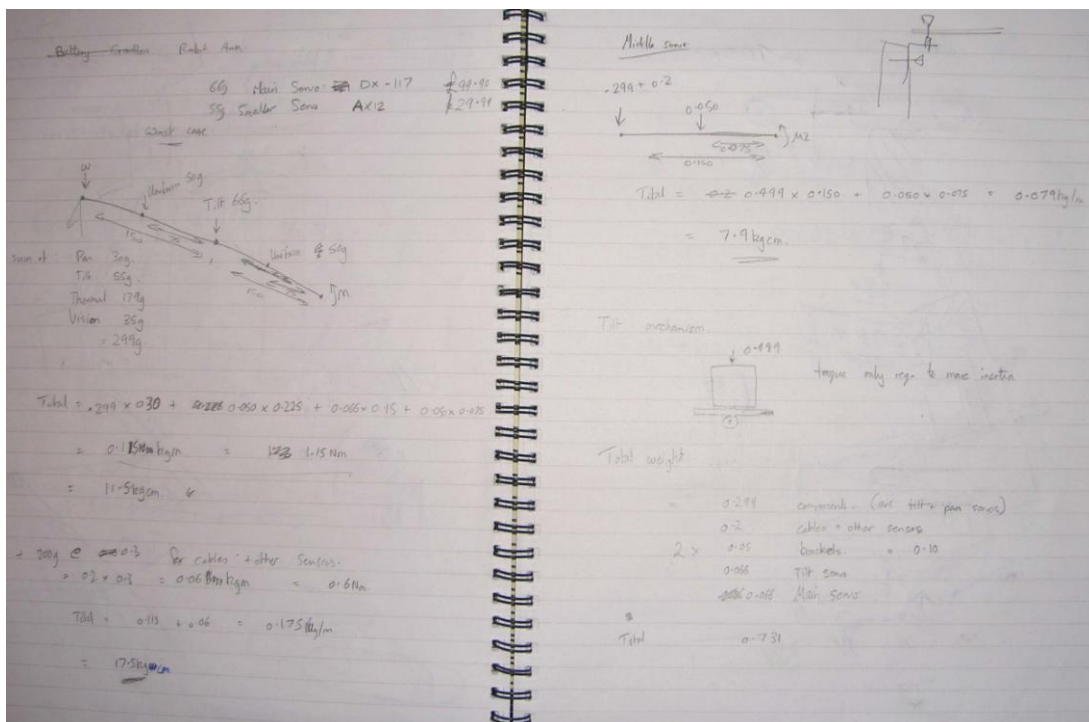


Figure 71 - Robot Arm Sketches

The robot head assembly (including pan and tilt servo) has an estimated mass of 400g (175g IR camera, 75g Network camera, 2x 60g RX10 Servomotor, 30g aluminium plate). At the arm elbow this mass would require 11kgcm (0.275m*0.4Kg) of torque (kgcm is the unit of torque specified by servo manufactures), which does not including middle arm mass. Assuming 80g for the mass of the linking plates and bolts, the elbow servo should be rated a minimum of 12kgcm. However, servo manufactures rate their devices with a holding torque, not the starting torque. After investigation with some servos a general rule emerged that starting torque was approximately half the rated holding torque, therefore the elbow servo was specified at 24kgcm minimum.

Following the same approach the base servo motor was specified at 60kgcm (arm mass 600g acting over 50cm).

Table 5 - Robot Arm Torque Calculations

Arm Lengths		Torque				Total Torque	2xRX64 load	RX28 load	Total mass
Base	Top	Bottom plates	Top plates	Mid Servo	Head				
0.225	0.275	0.016875	0.058	0.010125	0.235	0.32	67%	72%	0.87

A selection of servos matched the specified holding torques but the RX64 (64kgcm) and RX28 (28kgcm) from Robotis of South Korea were chosen over the competition because of their ability to daisy-chain power rails and the Serial Bus.

Two RX64 servos were selected to power the arm shoulder (although one would suffice) to ensure that more devices can be added in future development (PTZ camera, CO₂ sensor, etc).

To save weight all plates within the robot arm were Laser cut. For strength all the main arm links plates have been made from 1.2mm stainless, reinforced with crossbars and torsion winglets. As there are no structural loads applied the head, all parts used folded 1mm aluminium sheet for maximum weight saving.

The Roll cage around the arm serves three purposes; fixes the arm to the chassis top plate, protects the sensor array in case the robot inverts and acts as a carry handle, specified as necessary in the HSE guide.

Brass masses have been added to the rear of the elbow joint to reduce the load the RX28 servo has to exert. Their presence moves the CoM of the head from 200mm to 140mm from the axis, increasing the speed with which the arm can respond.

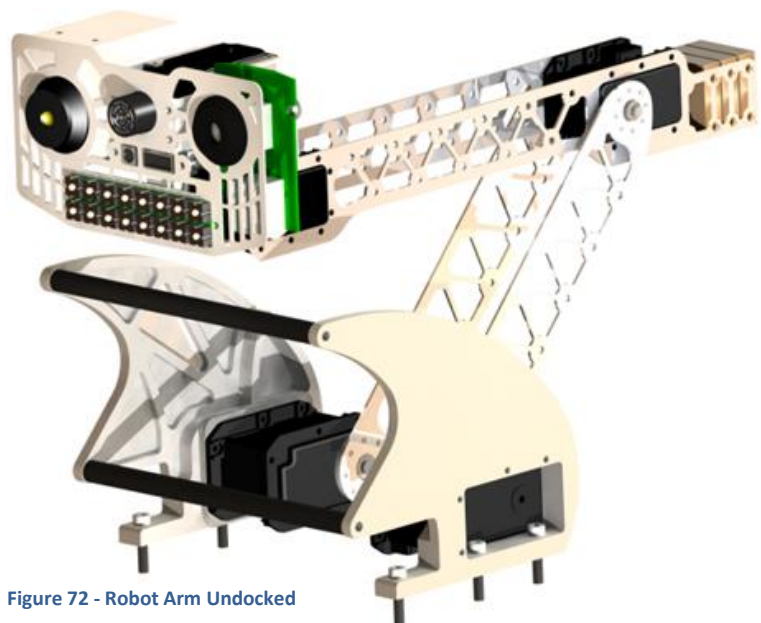


Figure 72 - Robot Arm Undocked

Figure 75 - Docked Robot Arm Side View

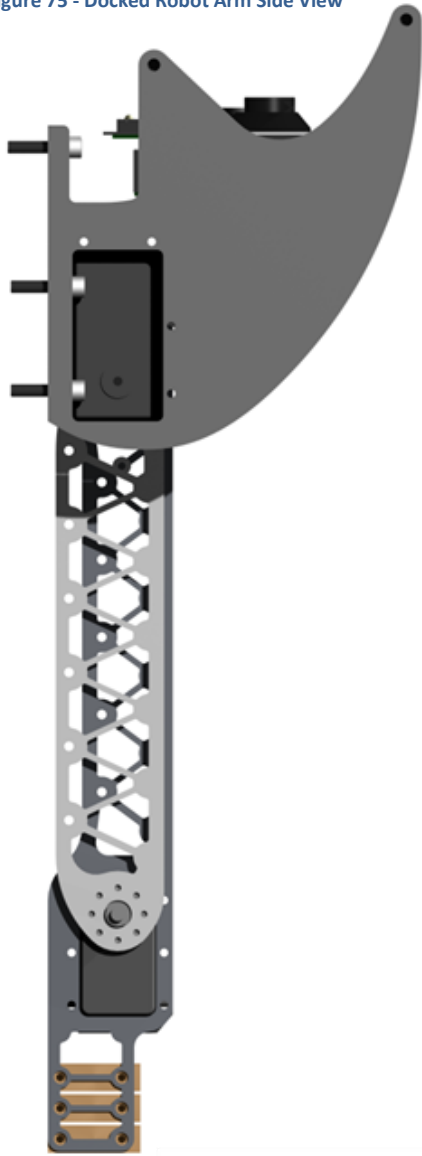


Figure 73 - Robot Arm extended to 60cm (Line of Sight)

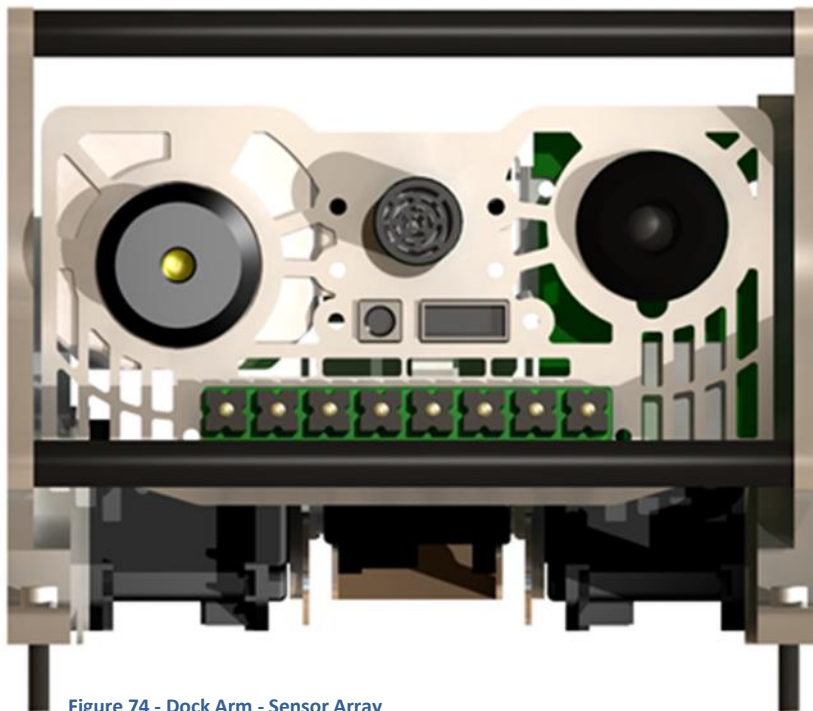


Figure 74 - Dock Arm - Sensor Array

7.0 MANUFACTURING

7.1 DESIGN FOR MANUFACTURE

Modern day CAD design allows very complex designs to be created but encourages designers to neglect the manufacturing processes required to achieve such designs. To ensure components did not require redesign the design approach was discussed with the machinist regarding the equipment available. Most of the components in the chassis are milled from Aluminium billets. The machines available are capable of 5 axis machining however most of the components require only 3 axes with the exception of the pulleys which require 3+2.

One of the main issues with milled components is the high forces exerted on the raw billets in comparison to a process such as laser cutting thus, the more complex components required jigs to hold them in place (*see 7.2 Part Manufacture for details*).

7.2 PART MANUFACTURE

7.2.1 PULLEY MACHINING

One of the difficulties machining the larger pulleys was machining the outer diameter on the DMG milling machine as they range between 75 and 130mm high, too long for most milling operations whilst still leaving a clean surface finish. This was overcome by machining the outer profile of the pulleys using a turning centre before the billet was placed into the mill (*see Figure 76 - Flipper Pulley Turning*). The turning centre was also used to turn the taper onto the inner supporting ribs of the pulleys.

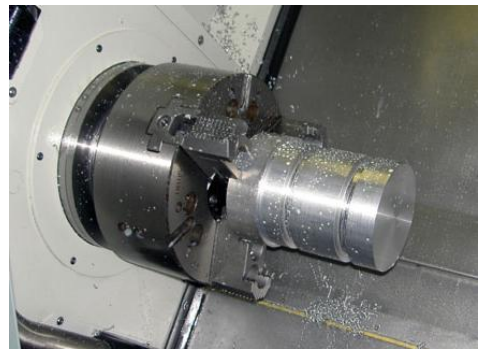


Figure 76 - Flipper Pulley Turning

The second stage of the larger pulleys was to machine the 38 grooves to match the profile of the T10V timing belt tracks. Typically this type of cutting would be achieved using a hob cutter the same process as used for gears. As this is a prototype construction the grooves were machined using a milling machine as it is very flexible and requires no custom

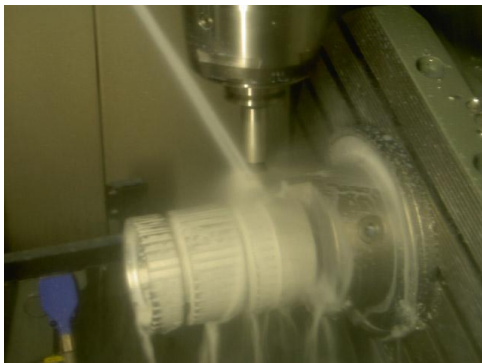


Figure 77 - Flipper Pulley Teeth Machining

tooling. Although the DMG milling machine is capable of 5 axis machining the pulleys only require constant 3 axis movement with an additional rotation about the centre of the pulley once each tooth has been cut (*see Figure 77 - Flipper Pulley Teeth Machining*). This manufacturing process was very effective with each pulley taking on average one day to machine the final part.



Figure 78 - Small Flipper Pulley Billet

The smaller pulleys were machined directly from billets using the DMG mill, firstly machining the pulley inner detail and teeth from one side followed by cutting the billet to length using a chop saw. A pair of custom machined jaws in the lathe was used to hold the pulleys while the sawn side was finish machined (see Figure 80 - Custom Lathe Jaws).

The finish machined pulleys can be seen in Figure 79 - Finish Machined Pulleys which show the stub shafts in the far left and two medium sized pulleys. The figure also shows the annulus and spur gear mesh in the back of the rightmost medium sized pulley.



Figure 80 - Custom Lathe Jaws



Figure 79 - Finish Machined Pulleys

7.2.2 FLIPPER SHAFT MACHINING

The flipper shafts is difficult to machine as it is over 500mm long as has 3 tapped holes in either end which are timed to one another. Thus, the shaft must be either machined all in one fixture or repositioned between processes.

The first stage of shaft manufacture was to turn the ends of the shaft down to size using a turning centre. To ensure the accuracy of the end holes a jig was machined to support the flipper shaft horizontally on the bed of a 5 axis DMG mill, where the C axis rotates the centre table. Figure 81 - Flipper shaft machining shows the jig bolted down to the table and the machining head tilted over at 90° ready to drill and tap the 3 M6 holes in each end. The gauge blocks underneath the jig ensure the machining head doesn't come in contact with the table on the lowest hole.

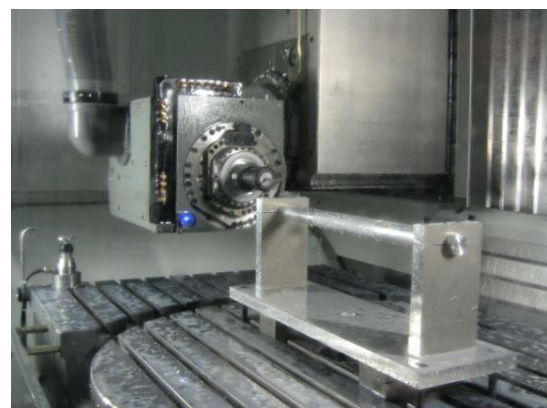


Figure 81 - Flipper shaft machining jig

7.2.3 PLATE MACHINING

As with all other machining operations using a milling machine, a method is required to hold the material in place while it is machined. The difficulty with plate machining is there is no part of the plate untouched, thus the clamps must be moved part way through. A sacrificial block was placed underneath the work piece which is held down using tool clamps (see *Figure 82 - Robot Arm Plate Fixture*). This allows the holes in the component to be drilled through and tapped into the sacrificial plate, thus the component can be bolted in place and the tool clamps removed.

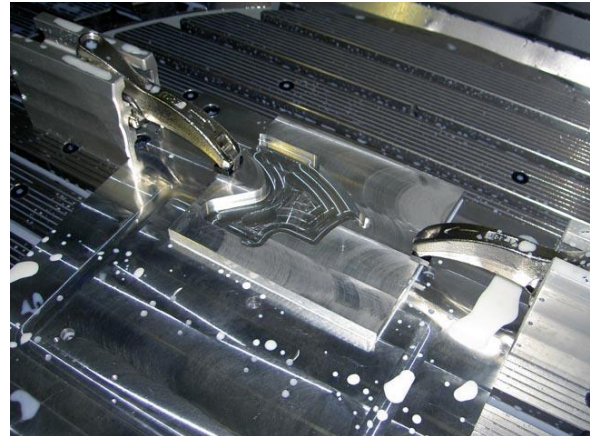


Figure 82 - Robot Arm Plate Fixture

7.3 FINISHING

The majority of the components were machined from aluminium, hence required no surface finishing preventing corrosion when only exposed to air. Several of the components are manufactured from plain steels such as the flipper drive pulleys and main drive gears, however as they are coated in grease they do not require additional finishing processes.

Aluminium has a high strength to weight ratio compared to steel but lacks the high surface wear resistance when used as a bearing surface. This was apparent after the first test run of the drive components where grooves were worn into the surface of the stub shafts. These grooves are shown as lines on the shaft between the circlip groove and the thrust face, shown in *Figure 83 - Stub Shaft Wear*.



Figure 83 - Stub Shaft Wear

After some discussion with bearing the manufacturer, IGUS, it was discovered the surface of Aluminium 6082 (the grade used for all chassis components) is not sufficiently hard enough. A hard anodising process was used to increase the surface hardness of the components whilst still maintaining structural strength without becoming brittle.

The anodising process has the effect of increasing the thickness of the surface which causes problems on bearing surfaces as parts must be machined with sufficient tolerance (approximately 25 microns for hard anodising). This was fortunate as it allowed the stub shafts to be machined down by 50 microns on diameter, removing almost all of the bearing grooves.



Figure 84 - Anodised Stub Shafts

The natural colour of hard anodising is dark grey which can be coloured using dyes but it reduces the hardness of the surface, thus all the chassis components were kept in their natural colour as shown in *Figure 84 - Anodised Stub Shafts*.

Several of the aluminium chassis components were powder coated for a variety of different reasons including; hiding a small amount of tool vibration and aesthetic style. The process is simple; the component is statically charged opposite to the power particles thus, they are attracted to the surface. The powder coated component is placed in an oven at $\sim 200^{\circ}$ which melts the powder into a high gloss finish.

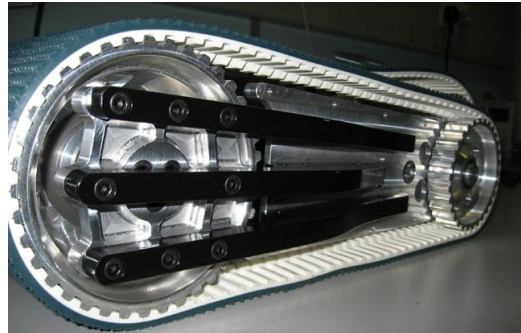


Figure 85 - Powdercoated Flipper Arms

7.4 MANUFACTURED COMPONENTS

There are over 100 custom manufactured parts which all have an associated 3D CAD model, (see *Appendices 15.1 CD of CAD Models*, the majority of which also have an associated 2D drawing detailing material specification, quantity and key dimensions for inspection. An image of every chassis component can be seen in *Figure 86 - Overview of Chassis Components*, taken a few days before the final chassis assembly. An overview of the image is listed below;

Top left: Electronics including; processing, radio communications, storage, control electronics, power electronics, power supplies and cooling.

Top middle: Centre chassis plates, rear chassis plates, front chassis plates, front wrapper plate, rear gusset plates and supporting bars.

Top right: Parvalux flipper motor, top plate, sensors, flipper drive belt, LED arrays and reset buttons.

Bottom left and bottom right: Rear drive motors, track pulleys, main belts, flipper belts, anodised stub shafts, flipper arms and anodised track runners

Bottom middle: Robot arm plates and servos, battery casings, roll cage bracing bars, flipper shaft.

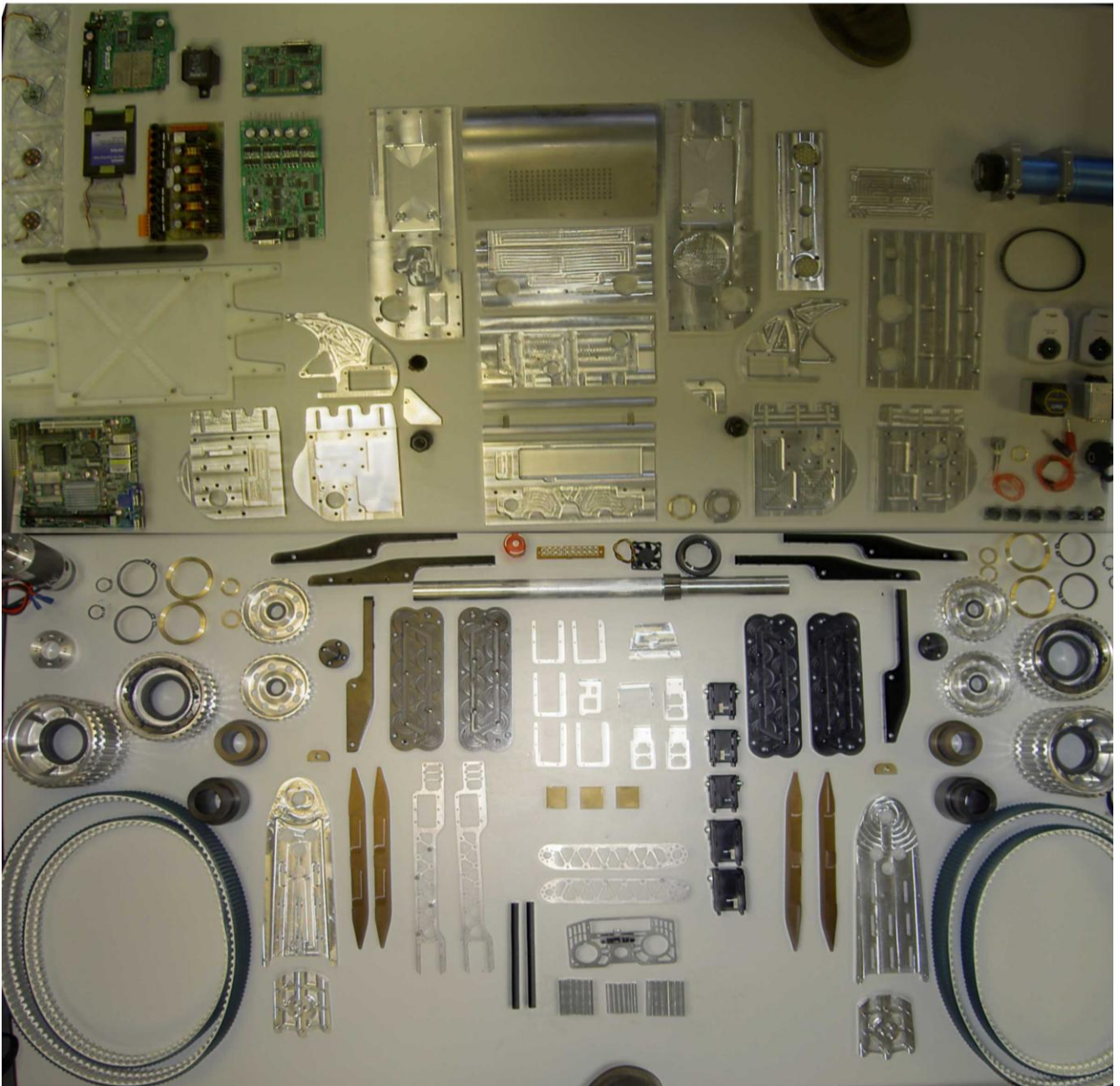


Figure 86 - Overview of Chassis Components

7.5 RE-DESIGN FOR MASS PRODUCTION

The major floor with the prototype design is the large number of parts and they are mostly custom made for this project. Although CNC milling is very cost effective for prototype design it is very slow in comparison to plastic moulding and casting. The following section lists a few key designs that would most likely be used in mass production;

7.5.1 PULLEY MANUFACTURE

The pulleys are machined from solid billets of aluminium, this is very time consuming with each billet taking approximately a day to turn into the final part. One of the key features of this pulley is its over engineered design, a typical problem with first prototypes. The first stage to mass production would be to reduce the wall thicknesses of the part and the thickness of the bracing ribs as they are far in excess of what is required. This can be achieved efficiently using FEA analysis to allow material removal while ensuring component rigidity is not compromised.

In addition to redesign the pulleys would be better manufactured from a polymer such as nylon to allow them to flex slightly, absorbing heavy shocks to prevent them travelling throughout the chassis. In mass production the pulleys could be injection moulded from a polymer, reducing the cycle time from a day to a few minutes. This would require further optimisation to ensure even wall thickness and the addition of draft angles to allow removal from the tool.

7.5.2 CHASSIS MANUFACTURE

The plate style construction of the chassis is a very modular design that is easy to dismantle, ideal for a prototype where modifications are constantly required. In mass production such construction would not be viable, for similar reasons to the pulley manufacture, namely time and cost. This could be overcome by redesigning the chassis to use a different manufacturing technique whilst still using the same mounting points and drive systems. Perhaps the most effective mass production technique for space frame type construction is a welded fabrication, similar to modern car manufacture. This is discussed in more detail in *6.1.1.2 Fabricated Chassis*.

8.0 RAW MATERIALS

8.1 ALUMINIUM VS POLYMER

Aluminium is the material of choice on the robot for the majority of machined parts. It has approximately 1/3 the density and stiffness of steel (USSAutomotive, 2008), easier to machine and corrosion resistant due to its high reactivity forming a surface oxide layer. With the robot intended to search areas that could have damp or hazardous atmospheres corrosion and chemical resistance is vital.

The majority of usable Polymers, such as polycarbonate, nylon and ABS have a lower density than aluminium, higher fatigue resistance, no corrosion issues (but susceptible to hydrocarbon based solvents) and a much poorer temperature resistance. (AEM, 2007)

Aluminium provides an appropriate balance between low cost steel with long machining times and expensive polymers that can be moulded to form shapes not achievable with machining.

Machining Aluminium can achieve good surface finish results (Figure 87 - Aluminium Surface Finish) with little effort or finish passes. Other advantages are the ability to surface harden using anodising and surface colouring. Swarf re-processing sells the waste off-cut/swarf back to supplier, thus reducing waste costs.



Figure 87 - Aluminium Surface Finish

8.2 ALUMINIUM SPECIFICATIONS

Aluminium can be obtained in various billet and plate sizes, all aluminium used in the robot is graded 6082. The robot pulleys used 5" (125mm) and 4" (100mm) bar with an extra 25mm per component for machine holding and parting-off added onto each billet.

The robot chassis, roll cage and flipper arms all use 1/2" (12.5mm) plate in various dimensions (all plate sizes can be seen in part drawing section).

See Appendix XXX for Aluminium physical properties

8.3 POLYMER SPECIFICATIONS

Due to electrically conductive nature of Aluminium, it is not suitable for the battery housings or the base of the central chassis (motherboard mounts). Instead, Black and White 1/2 "Nylon 66 (Impact resistant grade) plate was used. The base of the central chassis pan was cutaway, removing excess material, providing airflow under the motherboard and location posts for the motherboard mounts.

See Appendix XXX for Nylon 66 physical properties

9.0 ELECTRONICS

This chapter investigates the electronic design of the robot. This is split into five parts: power regulation from the batteries; communication between the PC and PCB through the use of microcontrollers; design of LED lighting; testing of the rotary encoder for the robot arm; and the choice of router for communications.

There were difficulties encountered during the design process, which were mainly due to the tight time schedule and the restricted space requirements within the robot. This chapter will discuss how the majority of these difficulties were overcome.

9.1 POWER CONTROL PCB

The power control circuit was originally designed as a single PCB. The schematic for this is provided in *Appendix E1*; all of the sub-circuits contained within this schematic can be found in subsequent appendices. It was however, decided early on in the design stage that this circuit may not fit in the allocated space within the robot, so it was split into two separate PCBs that were connected via a 14-pin ribbon cable. This separated all of the power control onto one PCB, and the microcontroller components onto the second PCB, and gave the option of stacking the PCBs if needed to reduce the space requirements. This section examines the design decisions behind the main power control board.

9.1.1 MOSFET SWITCHING

The robot is required to switch between mains and battery power supply. This switching, however, has to be instant. If there is even a short delay, then many of the sensors and outputs will shut down, including the PC and router. It is important that this does not occur, as it would result in communication to the robot being lost for over a minute whilst the PC and router restart.

The resolution to this problem was to create a sub circuit that instantaneously switched between mains and battery. If both mains and battery were present, however, the mains would take precedence in powering the board to conserve battery life for as long as possible. The desired solution to solve this problem was to produce a switching circuit using MOSFETS. The schematic for this is provided in *Appendix E2*.

The basic operation of this circuit is to use comparators and MOSFETS to compare the battery and mains inputs. The top half of the circuit compares the mains input, and the bottom half compares the battery input. If either input has power, the respective comparator will output a low value, thus switching on the MOSFET and allowing power to flow to the rest of the PCB.

It is also important to note that the circuit is designed to prioritise mains over battery power if both sources are available to prevent the batteries being drained when there is alternative power available. This condition was achieved by connecting the input of the 330 k Ω resistor in the top half of the circuit to the battery input. The MOSFET switching was tested with two power supplies. The first was set to 25 V and replicated the mains supply, and the second was set to 20 V to simulate the battery pack. These were then switched on and off in a variety of combinations to obtain the following results:

Power Supply Input 1 (Mains)	Power Supply Input 2 (Battery)	Output	Result
25 V	0 V	25 V	Working Correctly
0 V	20 V	20 V	Working Correctly
25 V	20 V	25 V	Working Correctly
15 V	20 V	20 V	Working Correctly

Table 6- Testing MOSFET Switching Circuit

The above table illustrates that the switching works as required and that the mains supply is the preferred power source (as shown in the third line of the table; the output comes from the mains supply even though both sources are present). The last line of the table also provides evidence of the switchover when power supply 1 drops low, as the output switches to the 20 V battery supply.

This circuit was tested in the Remotec bomb disposal chassis (see main group report) to prove the switchover is quick enough for the computer and router to remain constantly operational as the robot changes inputs from mains to batteries (or vice versa). Unfortunately the circuit requires more space than is available so it needed to be redesigned when incorporated into the final robot.

It was decided that the comparison between mains and battery could be omitted and only the diode would be used for the fast switching. The disadvantage of this is that the mains supply no longer has priority over the batteries. This is not an issue, however, because the diode will always take the largest input. As the mains supply is at approximately 27 V and the batteries are approximately 24 V, this means that the diode will use the mains anyway, and only power from the battery if the mains source is removed.

9.1.2 POWER SUPPLIES

The main input from the batteries is at 24 V (or slightly higher at approximately 27 V for the mains). However, many of the sensors and motors run at a lower voltage. It was, therefore, necessary to reduce this input to enable 18 V, 16 V, 12 V and 5 V outputs. The solutions considered for this were:

- 1) Use power supplies with 24 V input and a regulated output
- 2) Use an IC chip to regulate the 24 V input
 - a. With a switching regulator
 - b. With a linear voltage regulator

The first option was used in the Remotec test robot. This worked very well and gave a constant output at the required values. However, the power supplies were very large in size and would be unable to fit inside the final robot. This makes power supplies unsuitable for this application, so the option of voltage regulators had to be investigated. A table showing the relative advantages and disadvantages of the two types of regulator is provided in *Appendix E10*. The final decision after considering this comparison was to use the LM2576T switched regulator. This was mainly due to the very high efficiency, and the reduced power dissipation, which leads to a lower heat sink requirement. This ultimately results in a smaller area being used on the main PCB, which was one of the most crucial factors for every aspect of the design. The sub-circuit for voltage regulation can be found in *Appendices E3, E4, E5, and E6*, with the relevant calculations in *Appendix E11*.

9.1.3 EMERGENCY-STOP

Safety is an extremely important factor in every aspect of the robot design. In terms of electronics, this means that it should be very easy to instantly shut down all power to the robot if there is a problem. To maximise safety, an emergency stop was designed through both hardware (with an E-stop switch) and software (over wireless communication).

The hardware safety circuit has two components; an emergency stop and a reset button. The design for this circuit is provided in *Appendix E7*. As the schematic shows, the robot will not start until the emergency stop is released. If this condition is true, then pressing the reset switch will turn on the small relay, which will subsequently switch on the large relay and enable power to the motors. The large relay is kept off board due to the very high current that the main motors draw. If the relay was on-board then this current would be too much and would destroy the PCB tracks.

If the E-stop is pressed at any time, power to the motors will instantly be cut and the robot will stop. The circuit is designed in such a way that the motors will not start again until the E-stop is released and the reset button is pushed. The following table shows the results of testing all configurations of the E-stop and reset button:

Current Condition	E-stop State	Reset State	Resulting Condition	Notes
Motors off	0	0	Motors off	motors will not start whilst E-stop is pushed in
Motors off	0	1	Motors off	motors will not start whilst E-stop is pushed in
Motors off	1	0	Motors off	system ready and waiting for reset to be pushed
Motors off	1	1	Motors on	E-stop ready; pressing reset will start motors
Motors on	0	0	Motors off	pressing E-stop will cut power
Motors on	0	1	Motors off	pressing E-stop will cut power
Motors on	1	0	Motors on	as motors are already running the state of reset does not matter
Motors on	1	1	Motors on	as motors are already running the state of reset does not matter

Table 7 - Testing all combinations of the E-stop and Reset button

An explanation of the E-stop and reset states is provided below:

Switch State	Explanation
E-stop 0	E-stop has been pressed (off)
E-stop 1	E-stop is out (on)
Reset 0	reset is off
Reset 1	reset has been pushed

Table 8 - Explanation of switch states

This shows that the motors will only switch on when the E-stop is out, and the reset button is pushed. If the motors are already on, however, the state of the reset does not matter and the motors will continue to run until the emergency stop is pressed.

9.1.4 HEAT SINKS

Some of the components require heat sinks to dissipate power. These components are listed in *Appendix E12*, which also includes calculations for the required size of the heat sink. In order to have as much standardisation as possible, the majority of components use the same heat sinks. This means that some of the components will actually be better at dissipating heat than that required from the calculations. This is advantageous, though, because it means the temperature of those components will be further reduced, which increases both life and performance on an exponential scale. The final PCB design incorporated heat sinks at 5 °C/W for the U30D20C diode and 12.9 °C/W for each of the LM2576 voltage regulators.

9.1.5 CONNECTION TO MICROCONTROLLER PCB

As mentioned at the beginning of this chapter, the power control board was on a separate PCB to the microcontrollers and so these needed to be connected in some way. A few options were considered, but it was decided that the most practical would be to use a ribbon cable. The biggest advantage of this is space, as a ribbon cable is very compact. When compared to other alternatives (for example, using wires and a connector block), the area on the PCB is largely reduced.

Current was one consideration that had to be taken into account when deciding upon the best connection to use between the boards. As the ribbon cable cores are very thin, they have a low maximum current rating. However, the microcontroller board is only connected to the two PICs, which draw very little current (a maximum of 40 mA per pin (Atmel Corporation, 2004)), so this was not an issue that affects this project.

9.2 MICROCONTROLLER PCB

The microcontroller PCB provides the interface between the PC and the main power control circuit board. The main two elements of this PCB are the serial to USB conversion (to communicate between PCB and PC) and the two PICs (which are programmed to provide the safety functionality for the board). The PICs chosen were only available as SMD components, which led to the decision that the whole board should be surface mount. This is partly to achieve standardisation, but more importantly it is to address the space issue. Surface mount components are many times smaller than their through-hole counterparts, so it enables a more compact PCB to be designed.

9.2.1 SERIAL TO USB CONVERSION

The PCB board uses the two PICs to communicate with the onboard computer. This communication is achieved through the USB port. In order to make this possible, a serial to USB converter was required. There were two options for this conversion. One possible method was to use a serial to USB cable. However, cables are large and would require more space in the robot, so it was decided that this method should not be used. Instead, the conversion was designed to take place on-board. This uses a FT2232L UART chip, which was chosen because it is capable of performing a conversion to two serial ports. This is ideal for the robot, as the circuit is required to connect to two serial ports (one port for each PIC) through a single USB connection. The sub-circuit for this conversion is displayed in *Appendix E8*.

9.2.2 PROGRAMMABLE INTERFACE CONTROLLER (PIC)

The board contains two PICs. This is to keep the safety controller separate from the reset functions, which minimises the possibility of an error occurring. The initial objective was for one of the PICs to be designated for safety control, containing a “heartbeat” function that is capable of shutting off the motors if communication with the PC is lost. The second PIC is programmed to be a software reset that is linked to the sensor outputs, thus enabling individual sensors to be switched on and off remotely.

The PICs chosen were Atmel Atmega64-16AU chips. The reason for this choice was that these are the PICs used in robot football, so this allowed previous knowledge and experience to be transferred across to the rescue robot. For example, code had already been written in robot football to initialise serial communications, etc; this was adapted for use in the new robot.

There were, however, a number of difficulties with this microcontroller part of the design. The main problem was achieving enough power to switch the MOSFETS on and off. As a result, the design had to be adapted from the initial schematic. This will be discussed in more detail in the next section.

9.3 PCB ALTERATIONS

There were some alterations that needed to be made to the original designs. Some of these modifications have already been mentioned previously (for example, removing the amplifiers in the MOSFET switching circuit). The rest of the changes are mentioned in this section.

It was decided that there were too many fuses in the original design to fit in the available space. Therefore the less important ones had to be taken out. As the voltage regulators are current regulated at 3.0 A, the fuses on the regulator outputs could be omitted. Some of the outputs were also joined together to be supplied by a single fuse (for example, the webcams were joined so that they now require one fuse instead of three).

The biggest modification to the PCB design was on the microcontroller board. The MOSFETS on the power control board require over 20 V to switch on properly, so the output from the PICs on the microcontroller board had to be amplified (they are currently at 5 V). The option of using op-amps was considered to achieve this, but the final decision was to use a Darlington driver connected to the 24 V battery supply. This is simply an array of BJTs that allows the 24 V supply through to the power board when switched on by the PIC. The main advantage of this over using op-amps is that it takes up less space on the PCB.

When the microcontroller circuit was built, there was a problem with the Darlington driver (it failed to operate), which meant that the PICs were unable to connect to the power control board. This issue was resolved by using the onboard relay (labelled relay2) to ensure that the safety heartbeat still worked. The relay connections were edited to connect to the PIC and to 24 V. The PIC output was used to activate the coil, which switched on the 24 V supply to the 14 pin header (which then went to the motor emergency stop on the power board). This adaptation meant that the safety E-stop could still be programmed and used in the robot; this is paramount due to the importance of the safety function.

As only 2 relays are present on the PCB, there are not enough to repeat this modification for all of the MOSFET switches. The switching operation, therefore, was not fully working. This is of less importance, though, because the main aim of the switching is to conserve power by switching components off when they are not in use. This is not as critical as the software E-stop, which was a top priority to get working. It should also be noted that the LED indicators for switching on the power control board were disconnected and removed, as they will not turn on if the MOSFET switching is not present.

The revised schematics, including the PCB footprints, are provided in *Appendix E13 to E16*.¹

9.4 LED ARRAY DESIGN

The LED arrays were designed to run directly from the batteries, meaning they have a 24V input. The reason for this choice is to minimise the load on the switching regulators by using a direct connection to the batteries wherever possible. This is advantageous because a lower load on each of the regulators will result in a lower operating temperature, therefore increasing their life and reliability.

Two LED arrays were designed for the robot; one to provide overall lighting, and one to provide lighting for the camera on the robot arm. Both of these designs are provided in the *Appendix E17*. The main considerations for these LED arrays were luminosity and circuit design.

9.4.1 LED LUMINOSITY

In an earthquake situation it is very likely that there will be a power cut to the collapsed building. This means the rescue may have to be carried out in complete darkness, or with only very low levels of emergency lighting. When considering this, it was concluded that the LEDs used in the array need to be as bright as possible. Viewing angle is also a consideration because it is desirable to light as much of the surrounding area as possible. A table comparing the possibilities of different LEDs is shown below with the important information from the datasheets:

¹ Mr Jonathan Meadows assisted with the power control PCB and microcontroller PCB
Mr Michael Tandy assisted with the microcontroller PCB
Mr Ian Griffith assisted with making the microcontroller PCB

LED	LM520A	TLWW9600	HLMP-CW70-LP000
Manufacturer	Seoul	Vishay	Avago
Farnell Part Number	1494477	8311161	8577153
Size	5 mm	5 mm	5 mm
Colour	Warm White	White	White
Viewing Angle	20 Degrees	60 Degrees	70 Degrees
Luminous Intensity	7000 mcd	1760 mcd	1150 mcd
Forward Current	30 mA	50 mA	30 mA
Forward Voltage	3.2 V	5.2 V	4.0 V
Price ²	£0.77	£0.99	£0.49

Table 9 - Comparison of LED options

It was decided that the LM520A LED has too restrictive a viewing angle, and would not illuminate enough of the area. It was also found upon testing that the warm white colour had a yellow tint to it and was not as clear as the white of the other two LEDs, so this option was rejected.

The TLWW9600 LEDs were used in the robot arm. The reason for this choice was that they have a narrower viewing angle (although still a wide enough angle to be useful, unlike the LM520A) so the beam of light will be more concentrated, which is beneficial when the robot arm is exploring boxes and enclosed spaces. It is also brighter than the Avago LED, which is important because small enclosed boxes are likely to be the darkest areas that the robot encounters. The final benefit of this choice is that the square shape of the LED enables them to fit together very compactly in an 8x2 rectangular array on the arm.

The other LED array that was required is for the front headlights. As these are used for general exploration of the surrounding area, it was decided that the wider 70 degree viewing angle would be better. Therefore, the Avago HLMP LEDs were selected for this purpose. These are nearly as bright as the robot arm lighting array, and require less than half the power. They are also cheaper, so this selection results in both power and cost saving benefits. The robot will have two front headlights, each of which contains 19 LEDs.

² Prices correct on 27/04/2008

9.4.2 LED CIRCUIT DESIGN

The design alternatives for the circuit were as follows:

- 1) All LEDs placed in parallel
- 2) All LEDs in series
- 3) A combination of parallel and series LEDs

The problem with designing all the LEDs in parallel is the high power dissipated across the resistor, as shown with the following calculations:

For the TLWW9600 LED;

$$P = IV$$

$$P = 0.05 * (24 - 5.2)$$

$$P = 0.94 W$$

For the HLMP LED;

$$P = IV$$

$$P = 0.03 * (24 - 4.0)$$

$$P = 0.6 W$$

Equation 6 - LED dissipation power

This indicates that a resistor with a power rating of 1W or above would be required for the arm array, and 0.6 W or above for the front headlight array. Higher rated resistors are larger in physical size, so this leads to issues with space on the PCB. A circuit of this type would also require an individual resistor for each LED, which results in an undesirable number of resistors.

If all LEDs were in series, then only one resistor would be required. This would save space on the PCB and therefore reduce cost. However, this is not possible with a 24V input due to the voltage drop across the LEDs being too large (the drop would be $5.2 \times 16 = 83.2 V$ for the arm and $4.0 \times 19 = 76 V$ across each headlight). Arranging the circuit in this way is likely to result in the LEDs not switching on at all. Another disadvantage is that if one LED were to break then all of the lighting would switch off. In a parallel circuit, however, only the broken LED would switch off and the remaining LEDs would stay lit.

The most suitable option is to use a combination of parallel and series LEDs. The arrangement for this is shown in *Appendix E17*. This method of combining parallel and series LEDs also addresses the issue of space, as only one resistor is needed per parallel branch in each circuit. The required power rating is also reduced to 0.24 W for the headlights and 0.096 W for the robot arm, so smaller sized resistors can be used. The other advantage of this arrangement is that it is possible to still have light if an LED fails, as only the LEDs in series with the broken one will switch off. If this were to occur, the array would still be lit by all the LEDs in parallel to the broken one, which would be adequate enough to continue the search and rescue operation.

9.5 ROTARY TESTING

As described in the mechanical section, the robot has a moveable arm with a rotary encoder to provide flipper feedback. The model purchased was a Novotechnik RFC 4800-600 series. This was analysed with a test rig to determine its suitability for the robot. A diagram of the test rig is shown below:

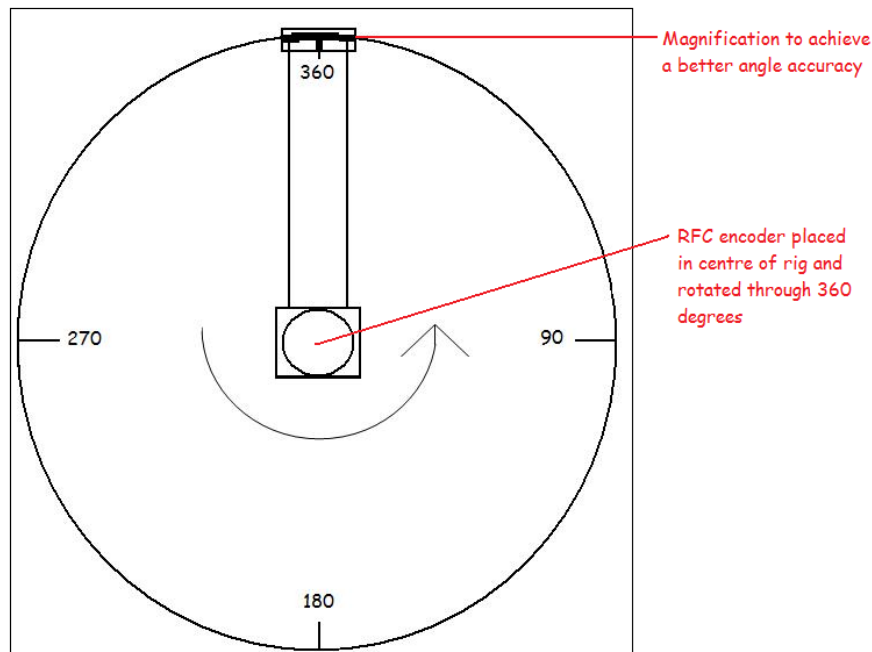


Figure 88 - Diagram of rotary encoder test rig

The test rig was essentially a circular board labelled with the angles from 0 through to 360 degrees. The encoder was placed in the centre with the sensor fixed in position. The magnetic component of the RFC was placed on top and allowed to rotate freely around the circle, as shown in the diagram. The voltage reading at a selected range of angles was then recorded; these readings vary from a minimum of approximately 0 V (at 0 degrees) to nearly 5 V (at 360 degrees). The end of the rig was magnified to assist with seeing the angles more accurately. The table of results from these tests are provided in *Appendix E18*.

The graphs on the following page were obtained from *Appendix E18*. The straight line equation is similar for both results;

$$\text{Angle} = 83 * \text{Voltage} - 21$$

The error from the predicted value is a maximum of $\pm 1.8^\circ$ in both graphs. On closer inspection, though, the voltage vs error plots are found to be similar for both graphs and fluctuate at similar voltage levels. This implies that there could be a systematic error with the encoder rather than a random error. Systematic errors are better than random errors because they can be predicted more easily, and so the program code could actually be written to account for them.

It was concluded that the results from these tests are accurate enough for the required application in the robot arm, so it was decided that this encoder should be used in the final robot design.

Results from Test 1

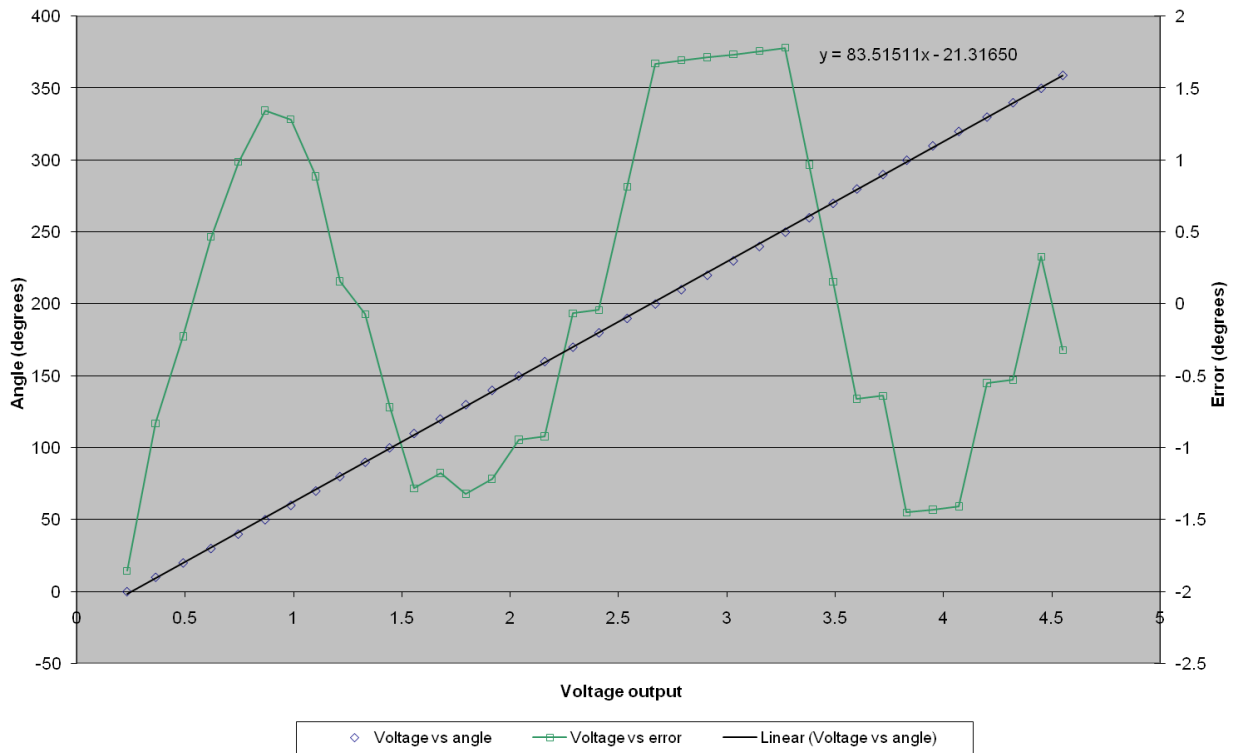


Figure 89 - Results from test 1 of the rotary encoder

Results from Test 2

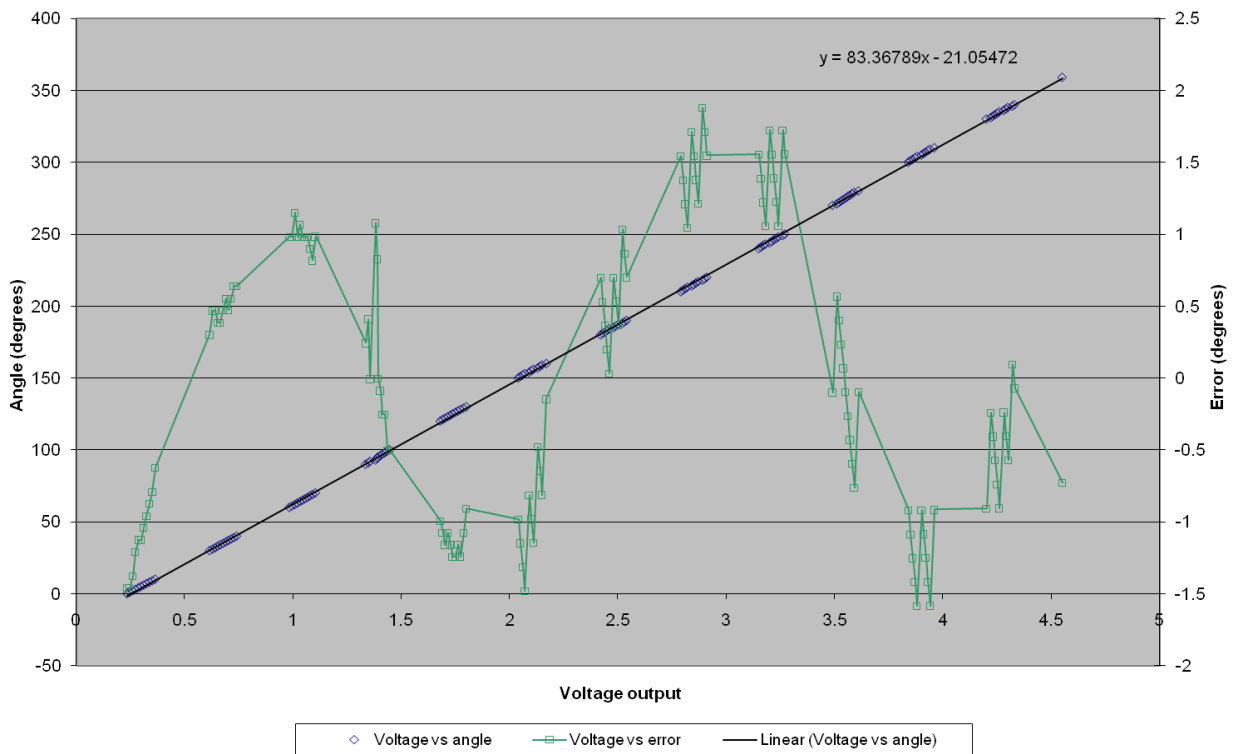


Figure 90 - Results from test 2 of the rotary encoder

9.6 COMMUNICATIONS

The first design decision for communications was to choose which method to use. There were four options to choose from:

- 1) No communication: The aim of this method is to have a completely autonomous robot that can be released into the disaster zone to search for survivors. It will return to the start point to provide results after the search is complete.
- 2) Wired communication: This method incorporates a tether on the robot that is reeled out as it moves along.
- 3) Wireless communication: A router is used to create a network for communications.
- 4) Both wired and wireless: This option combines the previous two methods. The main advantage is that a backup is present if one communication technique fails.

These methods are analysed quantitatively in *Appendix E19*, where it was found that wireless communication is the best technique. Having no communication was not advised as it is paramount that the robot returns. If it gets stuck or breaks down during the search and rescue, no information will be obtained. The main reason for rejecting the wired option was the mechanical issues with placing a long heavy cable on the robot. As weight and space are very important considerations for the robot design, this is not the most practical method. This was also the major factor in rejecting the option of both wired and wireless communications.

A Linksys Wireless-N Gigabit Router was purchased for the test robot. This made use of the 802.11n standard, which has very low latency compared to other standards. The Linksys router also has a more stable connection, and a faster data rate, due to MIMO (Multiple In, Multiple Out) technology; this works by overlaying the signals of multiple radios to increase speed.

Unfortunately, the wireless-n standard is not allowed in the rules of the RoboCup Rescue competition. The rules stated the preferred network standard to be 802.11a, so a Buffalo Wireless-A&G MIMO BROADBAND ROUTER was purchased. This is capable of operating under the required 802.11a standard. Although this does not have the same range as the Linksys one, it still performed adequately during the competition.

9.7 TESTS FOR CHECKING CIRCUIT WORKS

Once the PCB was produced, numerous checks were performed to ensure the circuit was properly working. The first was a visual inspection of all tracks, components, and solder connections. Once it was ensured that these were all correct, the circuit was given power (without connecting the sensors). The next series of tests involved checking each output to ensure it was providing the correct voltage (the fuses needed to be installed before making this check).

The outputs from each of the PICs were also tested, and a visual inspection was performed on the indicator LEDs to check that they were all lit. The final test was to connect all the sensors and motors, and ensure they were functioning correctly.

Safety is an important factor in the robot. It was necessary, therefore, to examine the failsafe systems. The first of these was the hardware emergency stop, which could easily be checked by

pushing it and ensuring that the power had been switched off. The USB cable on the microcontroller board was also pulled out whilst the robot was running; this simulated a communications failure with the PC, and was to check that the PIC switched off power to the motors, as was required. A table of the results from testing is provided below:

Table 10 - Electronics test cases

Test	Condition	Result	Pass / Fail
Visual Inspection	Visually inspect all tracks / solder connections / components	No errors found	Pass
Outputs without sensors	Insert fuses but do not connect sensors. Check voltage outputs	All of the voltage regulators are working correctly and providing the expected output	Pass
Indicator LEDs	Check all indicator LEDs are lit	All connected LEDs are switched on	Pass
Connect all outputs	Connect all sensors / motors etc	All outputs run correctly and work as expected	Pass
PIC output for switching	Check the reset functionality of the MOSFET switches	MOSFET switching does not work as intended	Fail
Communications failure	Pull out USB cable from PC to simulate failure	The robot motors cease	Pass
Software E-stop	Ensure the remote software emergency stop works	Software E-stop does cause the motors to cease	Pass
Hardware E-stop	Press the E-stop button whilst the robot is running	E-stop button does cause the motors to cease	Pass

These tests show that the robot is working as required as all of the tests were passed except for the sensor reset functionality. This is expected due to the redesign and modifications described in the earlier section on *9.3 PCB alterations*.

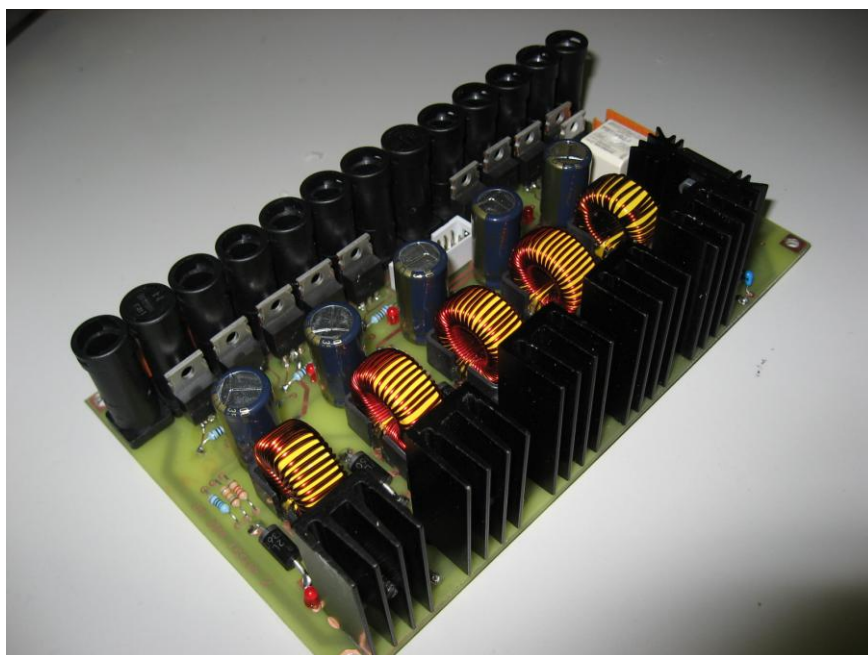


Figure 91 - Main Electronics Board

9.8 MAIN PROCESSOR

All the sensory feedback on the robot needs to be processed by an onboard computing solution. After analysis of the available market units, including; Mac mini, Various Laptop Computers, Embedded PCs, Gumstick boards running Linux OS and Mini ITX custom systems it became apparent that a custom system was required if processing needs, low power consumption and durability issues were to be satisfied. With the chassis size constraints, the maximum size the motherboard could take is 200mm², thus the only available solution was a solid-state Mini ITX based System.

- Mainboard: Commell MiniITX LV-676D (170mm²)
- Processor: Intel Core 2 Duo T5600 (2MB L2 Cache)
- Memory: 2GB Corsair XMS2 PC6400 (667Mhz DDR2)
- Hard Drive: 16GB Samsung Solid State Hard Drive
- Micro PSU 120W – Silent 20V-32V Input
- The full system uses 35W (idle), 65W (load)



Figure 92 - Mini ITX Motherboard

9.9 WHAT COULD GO WRONG?

Several issues have been identified which could interfere with the performance of the board, the main concern is the high current drawn by the PC, motors, and some of the sensors. This issue has been minimised by including fuses to prevent over current. The copper tracks on the board were also specified to be as wide as possible to increase their current carrying capacity.

Another issue is protecting the sensors. In order to minimise this risk, fuses were included on all outputs connecting to sensors, thus a fuse will blow if a problem should arise before the sensors are permanently damaged. Each power supply also contains an auxiliary output which is left unconnected which can be used as a spare for replacement or additional devices if necessary.

9.10 ELECTRONICS CONCLUSION

The main aim of the electronic design of the robot was to regulate the 24 V battery input to suitable output levels, and to provide a way of switching between battery and main without losing power. These objectives were both fully achieved. The safety aims were to provide both a hardware and software emergency stop function. Both of these E-stops worked, but the software E-stop was not connected as intended in the original design; it was adapted to work through a relay because of the failure of the Darlington driver. Although the software safety function did work on the robot, it is highly recommended that this is investigated and improved in the future. The MOSFET switching was also an area identified as a high priority for future investigation, as this was only part of the PCBs that did not work sufficiently.

The remaining electronics within the robot are the LED arrays and the communications device. Both of these were tested and found to be fully operational. They were also used in the competition in Germany, where they worked with very few issues. The only problem was that the router lost a few packets of data every so often, but this was to be expected when considering the number of networks present in the competition hall. Although this has been identified as an issue, it was not actually detrimental to the performance of the robot.

9.11 SENSORS

9.11.1 LASER SCANNER

The rules of the RoboCup Rescue competition require a map of the area to be handed in at the end of a rescue mission. This map can be created either automatically from sensors or drawn by hand from information delivered by the robot. It was decided that drawing the map autonomously would offer a much higher accuracy of the map, and would offer the most potential to be used by future generations of the project, for example in implementing Simultaneous Localisation and Mapping (SLAM).

Different mapping sensors were investigated. These included sonar and laser rangefinders. The conclusions drawn from this investigation was that the quality of the maps produced by a laser rangefinder would far exceed that of a map produced by sonar sensors. Most commercially available laser rangefinders give output data that is designed to be used for mapping data, whereas sonar sensors would need extra automation to give data that could be used for mapping. The RoboCup Rescue competition requirements state there are acoustic tiles made from sound-absorbing foam. These would severely disadvantage a sonar mapping device. Hence it was decided that a laser rangefinder was the most appropriate sensor for mapping



Figure 93 - Hokuyo URG-04LX

The model chosen was the Hokuyo URG—04LX (see due to its wide scanning area of 240° and high refresh rate of 10 Hz. Although this unit can only scan a 2D plane it can be tiled up and down using an additional motor and controller to produce a 3D scan.

9.11.2 VISION CAMERAS

The current rescue robot is not capable of navigating autonomously, and is driven remotely by an operator. The main sensors to allow remote navigation the robot are digital video cameras, mounted on the robot chassis. Initially multiple Unibrain firewire cameras were connected directly to the on board computer which compressed the raw image data and sent it over the network. This requires a huge amount of computer processing power, over 50% of the available capacity for the two cameras an unacceptable overhead considering the additional tasks the computer has.



Figure 94 - Unibrain Fire-i Camera (Unibrain, 2008)

In order to remove the video compression load from the main processor IP cameras were used which have on board processing and Ethernet connectivity to allow direct transmission of video to the clients over the wireless IP network. Two axis IP cameras were purchased from 20x range, both the 206 and 207 have 640 x 480 resolutions at 15 frames per second, additionally the 207 has a microphone to decent sound. They have a fixed focus lens which is manually adjusted, requiring the cameras to be focused at a specific distance. With a focal range of approximately 1m they are more



Figure 95 - Axis 207 IP Camera (Axis, 2008)

than sufficient for the competition environment. One of the difficulties observed when using the cameras on the Remotec test platform is their narrow angle lens which requires them to be positioned as far back as possible to allow the operator to see the robots extremities in the FOV.

To allow the operator to visualise forward and rear facing obstacles the cameras were directed in opposing directions. As the WMR robot chassis is much smaller than the Remotec test platform it is not possible to move the camera as far backwards to increase the FOV, thus the forward camera is mounted on the robot arm. One disadvantage to the IP cameras is the visual frame data can only be captured in a compressed format, hence the firewire cameras may still be required if vision processing is used.

9.11.3 THERMAL IMAGING CAMERA

The rules of the RoboCup Rescue competition state that two methods of identification are required to designate a victim as 'found'. One of the more reliable signs of life in the competition is the heat emitted by pads in victim's clothing where the temperature of the pads is between 35°C and 39°C.

The two types of thermal sensor considered were pyrometers and thermal cameras, where pyrometers are typically considerably cheaper due to their lower resolution. A thermal camera is similar in output to a video camera where a 2D array of pixels represents temperature as opposed to colour or intensity (see Figure 97 - Photon Thermal Image) .

Two types of thermal camera were tested, an Irisys IRI 1002 which is essentially thermal array with 16 x 16 pixels of data, however this low resolution makes targeting victims over long distances very difficult. Hence this type of sensors main use would be to identify a victim's heat source at close range. The next level up was to use a more typical thermal imaging camera with resolutions starting at 120 x 160 pixels. Flir imaging offer an uncooled core in a much smaller case than typical designs which, although expensive is far superior to any thermal array and offers accurate positioning and shape identification even at longer ranges.



Figure 97 - Photon Thermal Image of a Rescue Arena Victim



Figure 96 - Flir Photon Thermal Imaging Camera (Imaging, 2008)

9.11.4 SONAR SENSORS

The digital cameras on board the robot provided suitable information for a user to navigate the rescue robot, however the information obtained was inevitably limited by viewing angle and the shape of the robot. Sonar sensors on the extremes of the robot help avoid collisions with the environment. Many of the competing RoboCup rescue teams use the MaxSonar range of sensors, thus several were purchased which provided good results. In total 7 of these sensors, with varying dispersion patterns are used on the robot, 3 forward facing, 3 rear facing and one on the robot arm.



Figure 98 - MaxSonar EZ3 (MaxSonar, 2008)

Another challenge faced by the project was a way of accurately aligning the robot arm with the opening to an enclosure before entering. This is important since the robot arm holds many valuable sensors and any collision due to misalignment could be very expensive. The solution used two more sonar sensors; a MaxSonar EZ3 and an EZ0. The EZ0 has a wider detection range. When using both together, the two sensors will give an indication of when the robot arm is aligned with an enclosure opening, as shown in *Figure 99*. *Figure 96* shows the detection ranges of the two sensors.

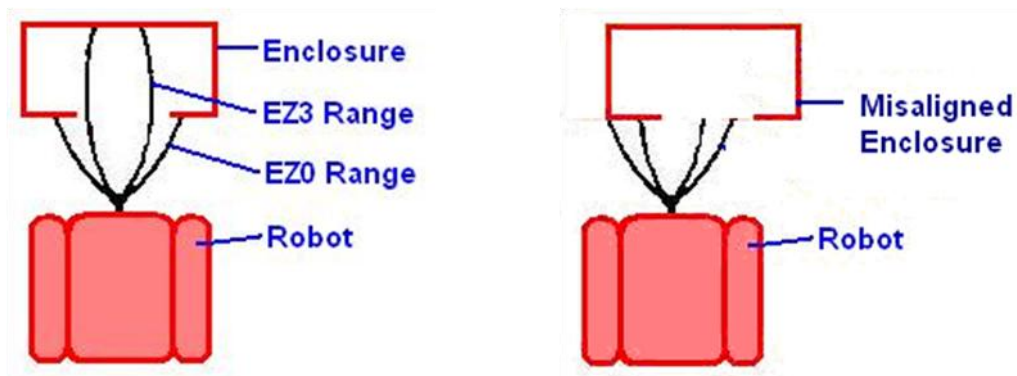


Figure 99 - The sonar sensors detecting a correctly aligned opening (left) and a misaligned opening (right)

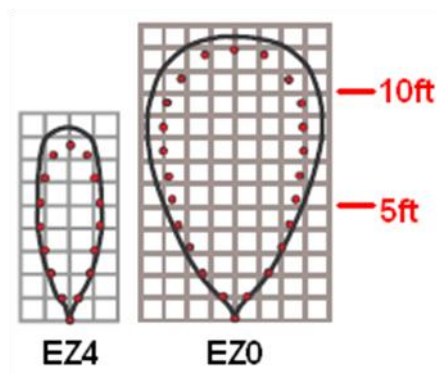


Figure 100 - MaxSonar EZ0 and EZ3 Detection Range (MaxSonar, 2008)

9.11.5 DIGITAL COMPASS

The requirement for a digital compass is for two reasons; to allow the operator to watch the general direction of the robot as it is easy to become disoriented in tight spaces and the second is to aid in mapping. One of the difficulties with a compass is they lose accuracy when tilted; this was overcome by using a compass with integrated pitch and roll measurement to allow electronic compensation.

The compass interfaces through RS232 serial and uses the international NMEA standard for heading information, thus once the computer interface is written it can be used for many different sensors using the same standard. Initial testing showed the compass was very susceptible to magnetic noise, an obvious consequence of its method of operation, thus it was kept away from motors, moving surfaces and noisy electronics.

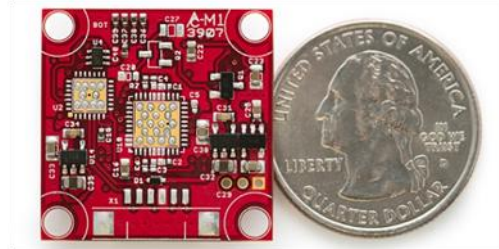


Figure 101 - OS5000 Digital Compass (OceanServer, 2008)

9.11.6 6DOF INERTIAL MEASUREMENT UNIT

The compass unit is capable of giving direction, pitch and roll in addition to this accurate measurements of displacement were required. Accelerometers allow accurate measurement of the acceleration of the sensor relative to the world co-ordinate system, integration of these values with respect to time gives the displacement. This type of measurement is inherently noisy; however initial testing needed a platform to base development on, thus a 6 axis inertial measurement was purchased, giving 3 axes of accelerometers and 3 axes of gyro measurement.



Figure 102 - 6 DoF Inertial Measurement Unit

10.0 ASSEMBLY

The robot chassis components are so compact it has a fairly specific sequence of assembly, to emphasize the quality of design a photographic walkthrough is provided in the Photo Log Technical Report. The photo log details the entire final assembly process which took approximately 7 12 hour days to complete, including wiring and calibration of the sensors.

Assembly was constructed in a logical order, similar to that of building a house;

Stage 1) Assemble the shell of the chassis (*see Figure 103 - Chassis Pan Assembly*).

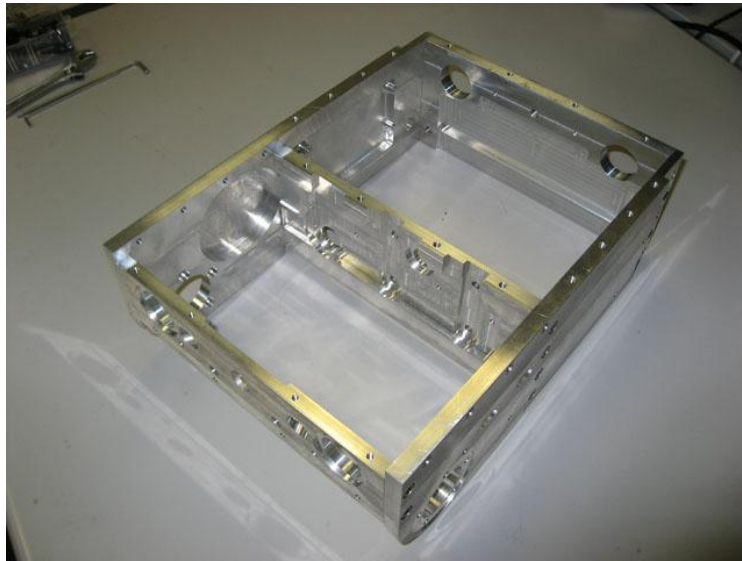


Figure 103 - Chassis Pan Assembly

Stage 2) Fit key components, e.g. motors and stub shafts (*see Figure 104 - Key Component*

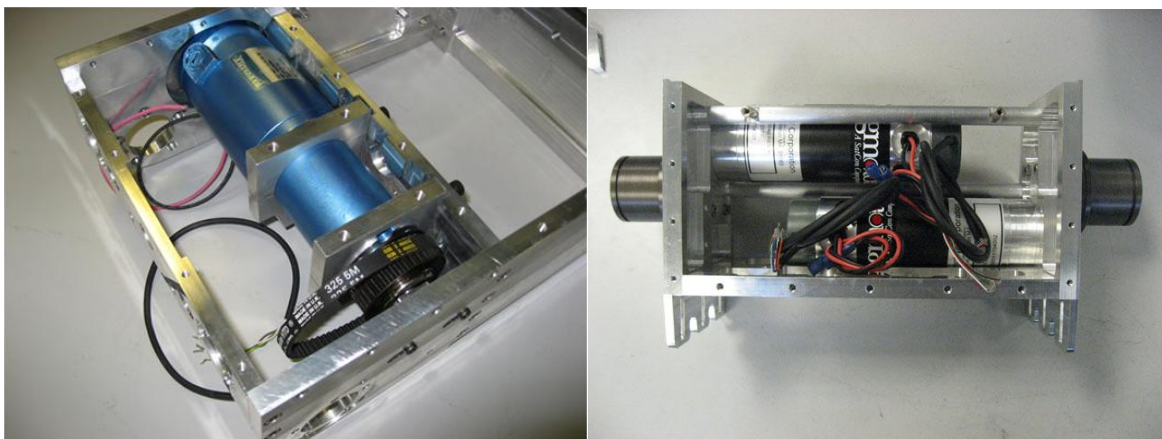


Figure 104 - Key Component Assembly

Assembly).

Stage 3) First fit wiring, power rails and difficult to reach cabling once fully assembled (see Figure 107 - Centre First Fit Wiring, Figure 106 - Rear First Fit Wiring and Figure 105 - Front First Fit Wiring).

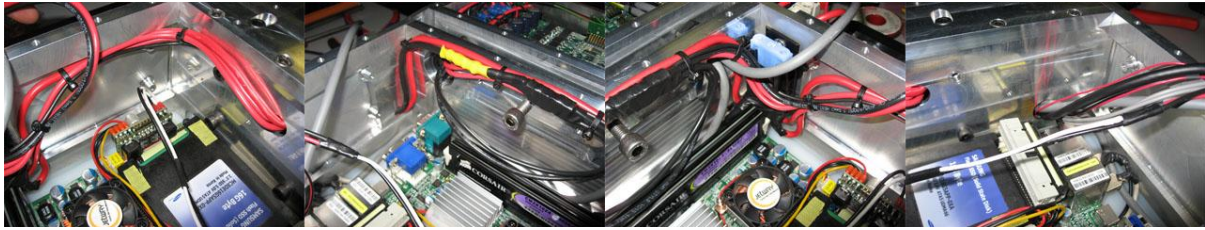


Figure 107 - Centre First Fit Wiring

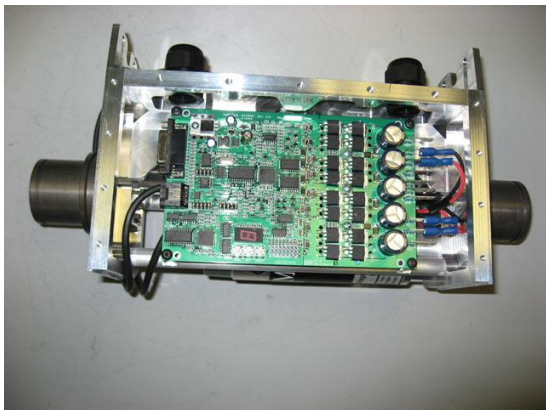


Figure 106 - Rear First Fit Wiring

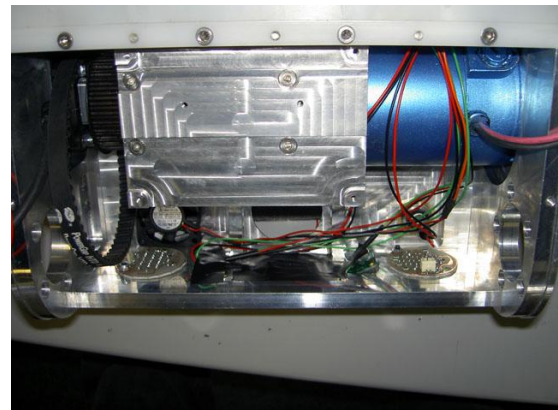


Figure 105 - Front First Fit Wiring

Stage 4) Final addition of components, addition of sensors, control buttons etc (see Figure 109 - Centre Section Component Assembly and Figure 108 - Front Section Component Assembly).



Figure 109 - Centre Section Component Assembly

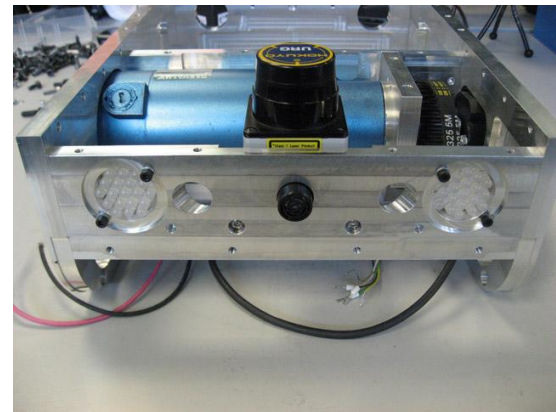


Figure 108 - Front Section Component Assembly

Stage 5) Second fit wiring and additional infrastructure to support remaining components.

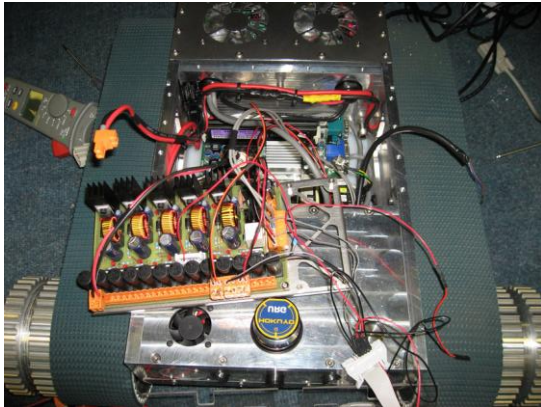


Figure 111 - Centre Section Final Wire

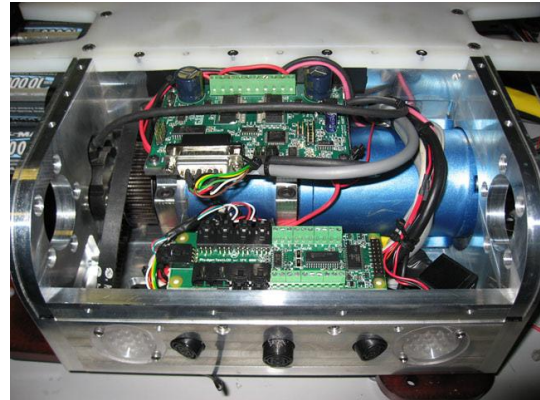


Figure 110 - Front Section Final Wire

Stage 6) Fit all of the covers, roll cage and robot arm.

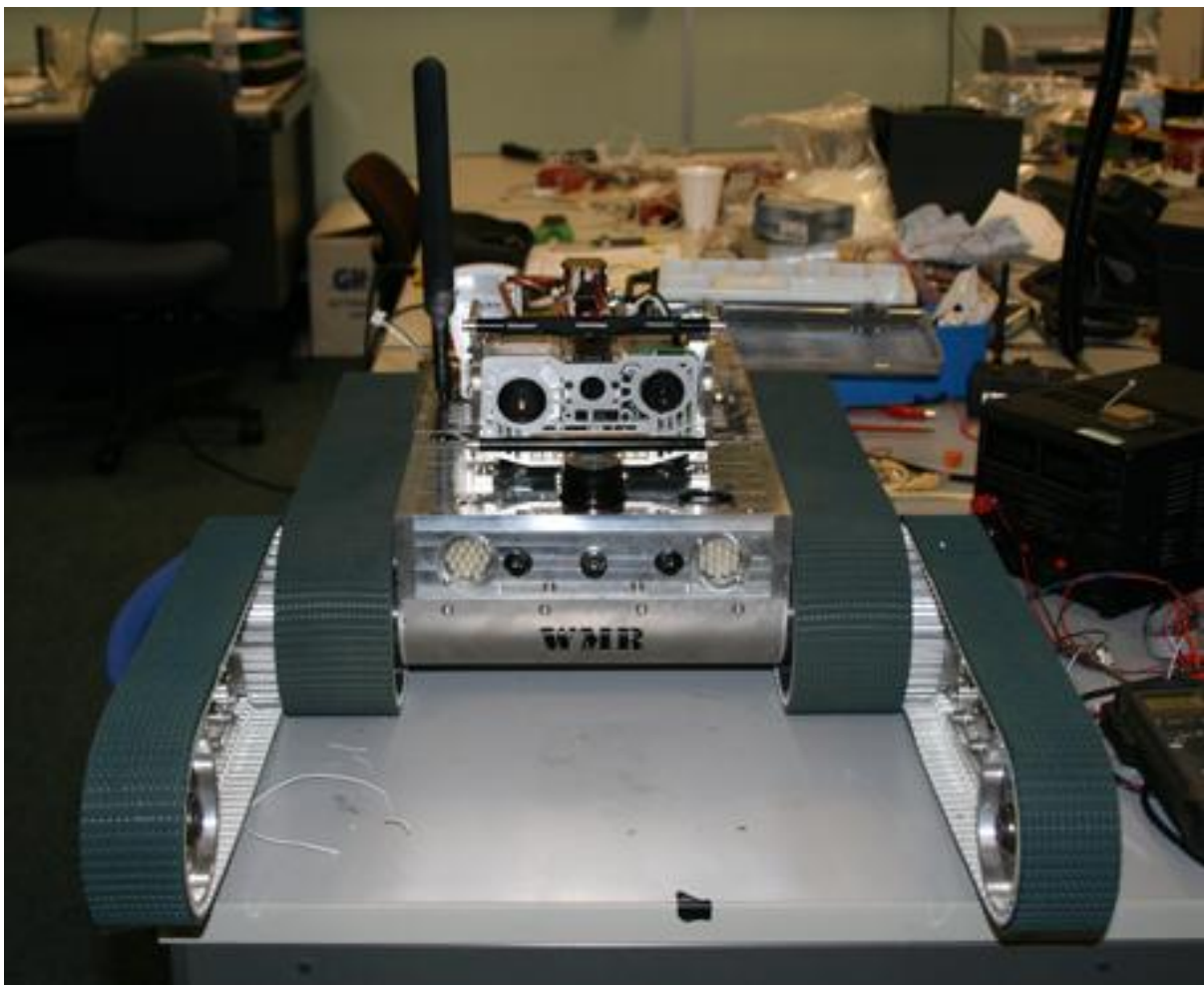


Figure 112 - Complete Robot Assembly

11.0 CONCLUSIONS

The chassis assembly process had very few problems due to the use of SolidWorks CAD software to test the fit of all components in the assembly before manufacture. Unfortunately the short time scales of the project allowed very little testing time for the chassis before entry to the competition which meant several problems regarding wiring and insufficient fuse ratings caused downtime at the competition venue. Fortunately most of the problems were found outside of the competition area. The main problem in the competition environment is the tendency for the onboard computer to crash under side impact loads, no hardware fault could be found at the competition thus the only remaining solution was to drive extremely carefully over rough terrain. One solution to this problem would be to mount the processing electronics in a spring loaded gimble to prevent shocks travelling to sensitive electronics.

Considering the original aim of competing in the European Rescue League within three years the project has been a huge success with a full working prototype produced in less than 7 months. There are many recommendations associated with the current design however, even in hindsight there are very few design changes the first prototype could have benefitted from given more time. By producing a working prototype it has given future teams a base platform for which to develop their new sensors, electronics and software systems. It has also given a huge insight to the mechanical problems associated with navigating such terrain such as ruggedness and traction.

12.0 RECOMMENDATIONS

A project with such scope inevitably has many recommendations associated at a midway stage such as this, in order to prioritise them they have been split into recommendations for the current chassis and for future redesigns of the entire concept.

12.1 GENERAL PROJECT RECOMMENDATIONS

- Investigate the use of PDM works, a data file management system from SolidWorks to allow versioning and checking in and out of CAD files between multiple designers.

12.2 ADDITIONAL FUNCTIONALITY WITH EXISTING CHASSIS

- Purchase a set of profiled belts, i.e. belts with a minimum of 10mm teeth on the outer edges to help traction over rough surfaces such as the step fields.
- Harden the gears to prevent excessive wear; manufacturers quote 67 – 72 Rockwell hardness.
- Add additional cameras or wider angle cameras to allow the operator to see the extremities of the robot and preferably all corners.
- Reduce the gear ratio further still, increase voltage to motors, purchase more powerful motors, perhaps the same case size with a different winding from Magmotor.
- Build a strong roll cage, perhaps as an integral part of the side plate to ensure the robot arm and sensor head cannot be damaged.
- Shift centre of mass forward to allow the robot to climb stairs more easily.
- Redesign the top plates to guard the fans more effectively.
- Add a docking port to the chassis with connectivity for Ethernet, Power, VGA and USB with the hope of reducing the need to disassemble the centre section when the PC is not available on the network.
- Increase the length of the machined shoulders on the flipper drive shaft to allow a stronger, wider belt. (15mm is easily achievable as opposed to 9mm)
- Fix the flipper motor control loops to prevent the overcorrecting between movements
- Implement the feedback loops integral to the rear speed controller.
- Move the flipper control loop into the computer software to remove the endless rotation limit set by the speed controller feedback capability to allow endless 360° rotation.
- Add carry handles to the chassis to allow easier transport
- REDUCE WEIGHT
- Add sensors to the bottom of the chassis at the front and rear to warn the operator as they approach the edge of steps, slops or cliffs.

12.3 ELECTRONICS RECOMMENDATIONS

Although the power control and microcontroller PCBs generally worked quite well, some possible improvements have been established for future project groups:

- There should be a main isolator switch on the robot to cut off power from the batteries. This would be better than the current setup, where power can only be cut by physically unplugging the batteries.
- The microcontroller PCB should be redesigned to properly incorporate the MOSFET switching.
- Investigate the size issues with the main power control PCB. Try and reduce the PCB area by sourcing smaller components or redesigning elements of the schematic.
- Re-connect the indicator LEDs for the switching status. Ensure that there is sufficient current to turn on these diodes.
- Introduce MOSFETS on all outputs of the power control PCB. This gives the option of power cycling any component that is connected to the board.

12.4 REDESIGN

- Build a stronger robot arm with only one joint at the rear of the robot with pan and tilt functionality at the head, this would allow a more rigid construction.
- Increase the ground clearance to prevent grounding on the step fields.
- Allow more space inside all areas of the chassis to allow the components more cooling space and the addition of the compass and IMU.
- Eliminate tools for battery changes and reduce the number of tools required for basic servicing, e.g. investigate the use of thumb screws etc.
- Add quicker connectors to the battery packs, preferably that connect when the pack is inserted into the chassis.
- REDUCE WEIGHT

13.0 GLOSSARY

Bearing Journal	- Bearing running surface
CAD	- Computer Aided Design
CoM	- Centre of Mass
FEA	- Finite Element Analysis
IP	- Internet Protocol
Off the Shelf	- Readily available, standard components
PIC	- Programmable Interface Controller
USB	- Universal Serial Bus
VGA	- Video Game Adaptor

14.0 BIBLIOGRAPHY AND REFERENCES

AEM. 2007. Aluminium vs. Plastic. [Online] Advanced Engine Management, Inc, 2007.
<http://www.aempower.com/ViewNews.aspx?NewsID=7>.

Atmel Corporation. 2004. *ATmega64-16AU Datasheet, p327*. 2004.

Axis. 2008. *207 IP Camera*. http://www.omegacubed.net/axis/axis_207/images/axis_207_large.jpg,
s.l. : 2008.

Gates Mectrol Limited. 2008. *T10V Tooth Section*.

Gramlich. 2005. Ansmann. *Ansmann Energy*. [Online] 27 12 2005.
<http://www.ansmann.de/cms/consumroot/batteries/rechargeable-batteries-nimh/mono-d/10000-mah.html>.

HSE. 2008. Manual Handling Assessment Chart. *Health and Safety Executive*. [Online] HSE, 2008.
<http://www.hse.gov.uk/msd/mac/index.htm>.

IGUS. [Online] <http://www.igus.com/iglide.asp>.

Imaging, Flir. 2008. *Photon Thermal Imaging Camera Core*. www.focus2k.co.uk/images/Photons.gif,
s.l. : 2008.

IRobot Corp. 2008. *IRobot Packbot 510*.

Jacobs University. Robotics at IUB. *Jacobs University*. [Online] [Cited: 04 26 2008.] <http://robotics.iu-bremen.de/labsrobots/rugbot.htm>.

Machine Design. Basics of Design Engineering: Bearings. *Machine Design*. [Online] [Cited: 08 04 2008.] http://machinedesign.com/BDE/mechanical/bdemech6/bdemech6_26.html.

MaxSonar. 2008. *MaxSonar EZ3*. MaxSonar, s.l. : 2008.

Mr Isidor Buchmann, CEO of Cadex Electronics Inc. Battery Info. *Battery University*. [Online]
<http://www.batteryuniversity.com/partone-3.htm>.

Novotechnik. 2008. *Siedle Group*.

OceanServer. 2008. *OS5000 Digital Compass*. <http://www.ocean-server.com/>, s.l. : 2008.

Parvalux. 2008. *DC Planetary Gearmotor*. Parvalux Ltd., s.l. : 2008.

Remotec Unmanned Vehicle Systems. 2008. *Wheelbarrow MK8*.

Ripmax. 2007. Ripmax, Pro Peak Power Supplies. *Ripmax*. [Online] Ripmax Ltd, 2007.
<http://www.ripmax.com/item.asp?itemid=O-IP2000&selectedtab=070&Category=070>.

Robbe. 2006. *Robbe Charger 2006*. Grebenhain : Robbe Modellsport, 06 11 2006. No. 8429.

Roboteq. AX3500 Product Folder. *Roboteq*. [Online] [Cited: 10 04 2008.]
<http://www.roboteq.com/ax3500-folder.html>.

RoboticsConnection. 2008. *Traxster Web2*.

Roy Mech. Circlips External. *Roy Mech*. [Online]
http://www.roytech.co.uk/Useful_Tables/Circlips/Circlips_External.html.

Sparkfun. 2007. *6 Dof Inertial Measurement Unit*.
http://www.sparkfun.com/commerce/product_info.php?products_id=8191, s.l. : 2007.

ToyoBearings. 2008. *Needle Roller Bearing*.

Unibrain. 2008. *FireI*. http://www.unibrain.com/products/visionimg/Fire_i_DC.htm, s.l. : 2008.

University of New South Wales. Rescue Robots. *CSE at UNSW*. [Online]
http://www.cse.unsw.edu.au/~claude/research/robotics/rescue_robots.html.

University of North Texas. Resquake Gallery. *Resquake Robotic Group*. [Online]
<http://saba.kntu.ac.ir/resquake/Gallery.htm>.

US motors. Bearing Types. *US motors*. [Online] [Cited: 08 04 2008.]

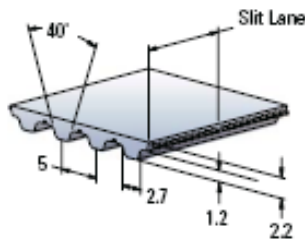
USSAutomotive. 2008. Steel vs Aluminium. [Online] USSAutomotive, 02 2008.
<http://www.ussautomotive.com/auto/>.

15.0 APPENDICES

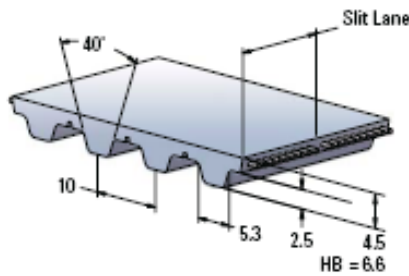
15.1 CD OF CAD MODELS

T Pitch Belts

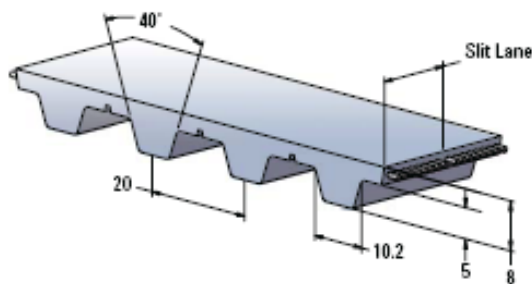
T5 5 mm Pitch



T10, T10-HF 10 mm Pitch
WT10 10 mm Pitch
from 150 to 450 mm wide



T20 20 mm Pitch



		T5	T10*, T10-HF*	T20
Min. Welded Belt Length	mm	440 (50 mm wide) 450 (100 mm wide)	450 (100 mm wide) 850 (150 mm wide)	1000
Standard Roll Lengths	meters	100	100	100
Standard Slitting Lanes	mm	25	25	25
Available Slitting Lanes	mm	10, 16	16, 32	N/A

All roll lengths are $\pm 1\%$.
*Heavy Back (HB) option available.

Available Widths

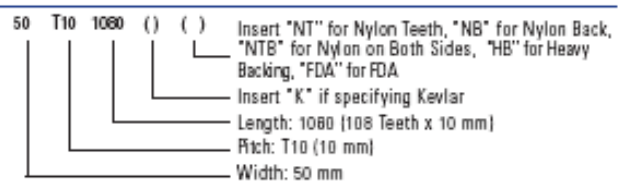
mm	T5	T10, T10-HF	T20
6	X		
10	X	X	
12	X	X	
16	X	X	
20	X	X	
25	X	X	X
32	X	X	X
50	X	X	X
75	X	X	X
100	X	X	X
150		X	X

All belts are available in any width between the minimum and maximum listed width.

Width Tolerances

Width	T5	T10, T10-HF	T20
Up to 50 mm	± 0.5 mm	± 0.5 mm	± 1.0 mm
> 50-100 mm	± 0.75 mm	± 0.75 mm	± 1.0 mm
> 100-150 mm	N/A	± 0.75 mm	± 1.0 mm

To Order T Pitch Belts



Application Characteristics

- Long length conveying or linear positioning where tracking is an issue
- Conveying applications where design considerations prevent the use of pulley flanges
- Reduce or eliminate any belt 'wander' by providing continuous guiding along conveyor length

Integral V-Guides

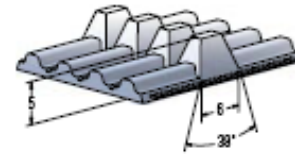
		T5V	T10VS	T10V	AT5V	ATL5V	AT10V	HV
Min. Welded Belt Length	inch							36
	mm	920	900	900	900	N/A	950	
Standard Roll Length	feet							200
	meters	100	100	100	100	100	100	
Standard Slitting Lanes	inch							1
	mm	25	25	25	25	25	25	

All roll lengths are ±1%.

Width Tolerances

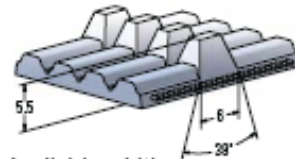
Width	T5V	T10VS	T10V	AT5V	ATL5V	AT10V	HV
Up to 50 mm Up to 2"	±0.5 mm	±0.5 mm	±0.5 mm	±0.5 mm	±0.5 mm	±0.75 mm	±0.020 in
>50 - 100 mm >2" - 4"	±0.75 mm	N/A	±0.75 mm	N/A	N/A	±1.0 mm	±0.030 in
>100 mm to 150 mm >4" - 6"	N/A	N/A	±0.75 mm	N/A	N/A	±1.0 mm	±0.030 in

T5V (K6 Section)



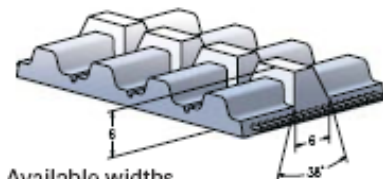
Available widths
– 16, 25, 32, 50, 75, 100 mm

AT5V, ATL5V (K6 Section)



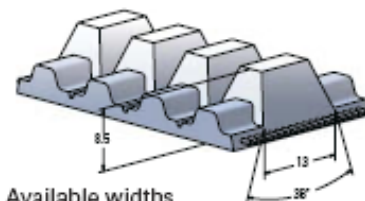
Available widths
– 16, 25, 32, 50 mm

T10VS (K6 Section)



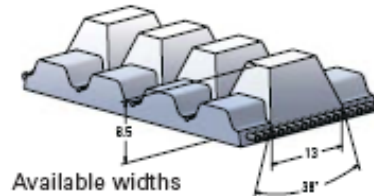
Available widths
– 16, 25, 32, 50 mm

T10V (K13 Section)



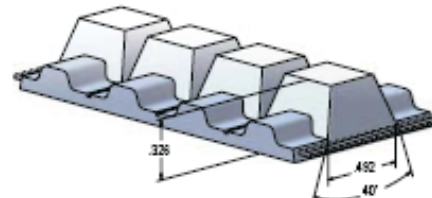
Available widths
– 32, 50, 75, 100, 150 mm

AT10V (K13 Section)



Available widths
– 25, 32, 50, 75 mm

HV (A Section)

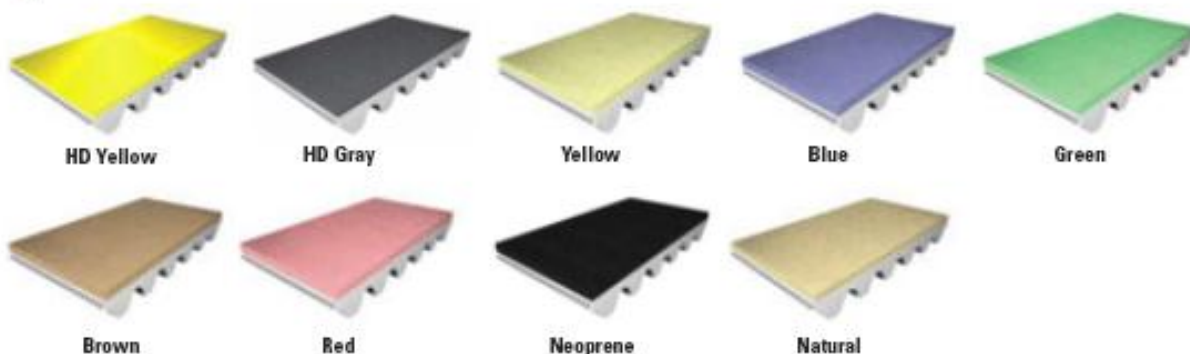


Available widths
– 1.5, 2, 3, 4, 6 inch

Backings

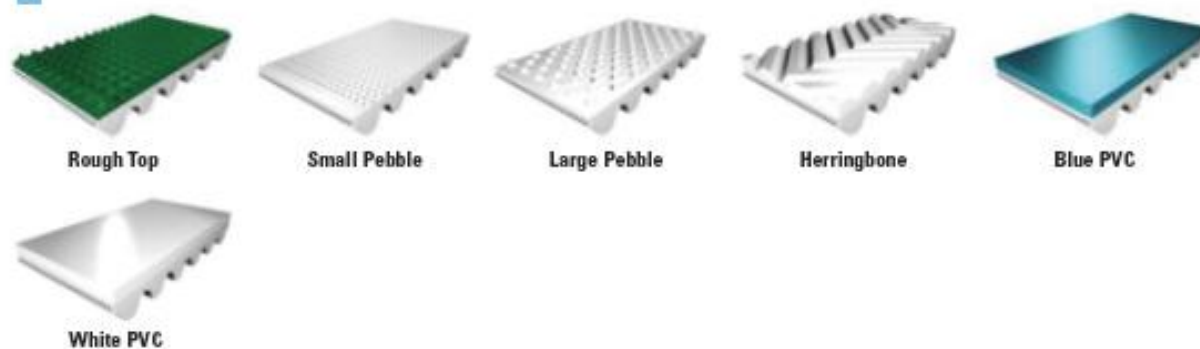
Foam

Many applications require a combination of friction and the ability to conform to unusual product shapes. Gates Mectrol foam backings are available in different densities for various compliance, cushioning and friction surfaces. Belts can be constructed with a foam layer for cushioning and a tougher high friction outer layer.



PVC

Available with unusual surface patterns and characteristics, PVC backings offer a well bonded, economical solution with very good wear properties.



Specialty Backings



Backings – Specifications

	Hardness Shore A / Density Kg/m ³	Material Thickness mm	Abrasion Resistance Rating ‡	Static Coefficient of Friction †	Kinetic Coefficient of Friction †	Max. Temp. Degrees C	Pulley Diameter Factor	Oil Resistance	Color
Polyurethane									
HB	92	2	10	0.5	0.5	80	30	E	Clear
U2*	85	2 or 3	9	0.6	0.5	80	30	E	Clear
U4†	80	1	8.5	1.0	0.8	80	30	E	Clear
U3*	75	2 or 3	8	0.6	0.6	70	30	E	Clear
G32	75	5	8	0.6	0.6	70	Ø100mm	E	Clear
G2†	85	3	9	0.6	0.5	80	Ø100mm	E	Clear
U5*	75	2 or 3	8	0.6	0.6	70	25	E	White
Rubber									
L**	35	1/16" to 1/2"	6	1.6	1.6	60	20	P	Red
LP**	38	1/16" to 3/16"	6	1.4	1.4	60	20	P	White
LT**	40	1/16" to 1/4"	6	1.5	1.5	60	20	P	Tan
LB**	60	1/16" to 1/4"	6.5	0.7	0.5	110	25	E	Black
RM*	57	2, 3, 6	7	2.1	1.4	105	25	G	Red
Foam									
FUY*	50	2 to 5	5.5	0.8	0.8	60	30	E	Yellow
FUG*	50	2 to 5	5.5	0.8	0.8	60	30	E	Gray
FY*	- / 160	6 to 12	3	1.0	1.0	60	15	E	Yellow
FB*	- / 220	6 to 12	3.5	0.8	0.8	60	15	E	Blue
FG*	20 / 300	6 to 12	4	1.0	1.0	60	15	E	Green
FN*	30 / 400	6 to 12	4	0.8	0.8	60	15	E	Brown
FR*	40 / 500	6 to 12	4.5	0.9	0.9	60	20	E	Red
LP**	- / 250	1/8" to 1/2"	3	0.9	0.9	60	15	A	Black
FC*	30 / 400	2 to 5	4	0.6	0.5	60	15	E	Natural
PVC									
RT	40	4.5	5.5	1.4	1.3	60	Ø 90mm	P	Blue-green
SPT	50	1.5	5.5	0.7	0.6	60	Ø 25mm	P	White
LPT	35	6	5.5	0.8	0.7	60	Ø 40mm	P	White
PH	40	4.5	5.5	0.6	0.3	60	Ø 90mm	P	White
PB	40	1 or 2	5	1.1	1.1	60	Ø 40mm	P	Blue-green
PW	75	2	5	1.1	1.1	60	Ø 40mm	P	White
Special									
ATB	92	N/A	7.5	0.3	0.3	80	N/A	E	Black

* Add thickness in mm to designator

** Add thickness in 1/16" to designator

‡ 10 = very high resistance

† Friction measured against aluminum

Oil resistance: E = Excellent G = Good P = Poor A = Acceptable

Minimum Pulley Diameter = (Pulley Diameter Factor) x (Material Thickness)
or above listed diameter

Note: Pulley diameter must be greater than or equal to the minimum pulley
required for a given belt type. See belt specifications.



50-100 oz-in Continuous Torque



Key Performance Features:

- High Energy Neodymium Magnets
- Peak Torque to 1000 oz-in
- Excellent Torque to Weight Ratio
- Encoder Ready
- 12-120 VDC Typical

S23 BRUSHED SERVO MOTOR SERIES

Motor Characteristics


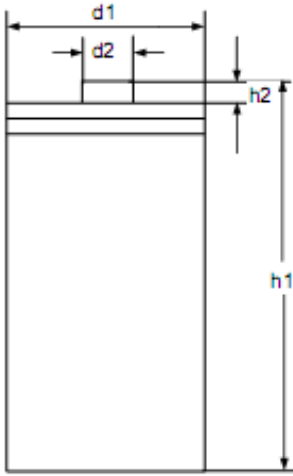
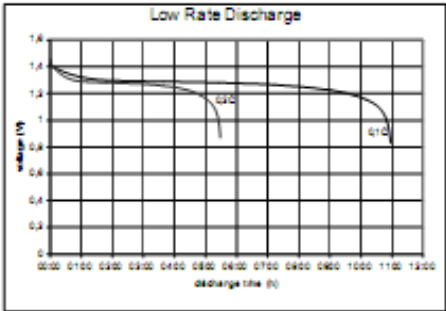
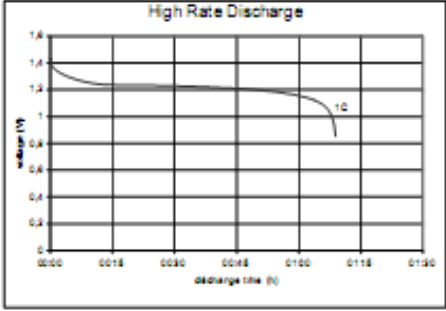

FRAME SIZE	STACK LENGTH	PEAK STALL TORQUE (T _s) OZ-IN	CONT. STALL TORQUE (T _c) OZ-IN	ROTOR INERTIA (J _r) OZ-IN-SEC ²	FRICTION TO RQUE (T _r) OZ-IN	THERMAL RESISTANCE (RM) °C/WATT	MAX RECOMMEND SPEED RPM	MAX WINDING TEMP. °C	POWER RANGE W	WEIGHT LB
S23	-- 100	500	50	0.006	5	4.5	4000	155	70	2
S23	-- 200	800	75	0.010	6	4.0	4000	155	100	2.6
S23	-- 285	1000	100	0.014	7	3.5	4000	155	130	3.2

Sample Windings CONSULT MAGMOTOR APPLICATION STAFF FOR OTHER AVAILABLE WINDINGS

	S23 -- 100				S23 -- 200				S23 -- 285			
	E	G	I	K	F	H	J	M	E	G	I	K
Torque Constant (Kt) oz-in/amp	5.1	8.0	13.0	20.1	12.8	19.3	30.4	60.8	14.4	22.7	36.2	56.3
Voltage Constant (Ke) Volts/Krpm	3.7	6.0	9.6	14.9	9.4	14.3	22.5	45.0	0.6	16.8	26.8	41.5
Term. Resistance (Rt) Ohms (cold)	0.5	0.7	1.45	3.15	0.65	1.35	2.86	10.32	0.5	1.9	2.5	5.5
Peak Current (A) Amps	75	48	24	15	75	48	24	15	75	48	24	15
Cont. Current (A) Amps	7.3	4.7	3.0	2.0	7.3	4.7	3.0	2.0	7.3	4.7	3.0	2.0

VALUES AS LISTED ARE TEST CONDITIONS, ACTUAL RESULTS MAY VARY

15.4 ANNSMAN BATTERY DATA SHEET

nominal voltage:	1,2V	conditions	
max. charge voltage:	1,5V	at standard charge (0,1C / 20°C)	
capacity			
nominal :	10000mAh	discharge at 0,2C	
	8300mAh	discharge at 1C	
minimum:	9300mAh	discharge at 0,2C 1,0V end discharge voltage ambient temperature 20°C	
max. continuous discharge current:	10A	ambient temperature 20...50°C	
charge		charge current	charge time
standard charge:	1000mA		16hrs
rapid charge:	2500mA		4,4hrs
fast charge:	5000mA		2,2hrs
recommended charge termination control parameters:	-dV: 0...5mV dT/dt: 0,8...1°C per min TCO: 45...50°C		
trickle charge current:	100...500mA	(recommended)	
continuous overcharge: (less than 1 year)	≤750mA	no conspicuous deformation, no leakage	
internal resistance:	≤15mOhms	at 1000Hz, battery fully charged	
life expectancy:	>500 cycles	IEC standard	
ambient temperature range:	0...45°C 10...40°C -20...60°C -20...35°C -20...45°C	standard charge fast charge discharge storage less than 6 months storage less than 1 month	
			
			
		mechanical specifications	
		cell dimensions (with sleeve)	
		diameter d1:	33,0 -1,0mm
		diameter d2:	8,0 ±1,0mm
		height h1:	61,5 -2,0mm
		height h2:	min. 1,5mm
		weight:	approx. 155g
		27	
	specifications for model/type:	D – NiMH 10000mAh	
	Ansmann drawing number / part number:	5030641	
	drawn by / date:	Gamlisch / 27.12.2005	

Manufacturer reserves the right to alter or amend the design, model and specification without prior notice

Aluminium Alloy 6082

Aluminium alloy 6082 is a medium strength alloy with excellent corrosion resistance. It has the highest strength of the 6000 series alloys. Alloy 6082 is known as a structural alloy. In plate form, 6082 is the alloy most commonly used for machining. As a relatively new alloy, the higher strength of 6082 has seen it replace 6061 in many applications. The addition of a large amount of manganese controls the grain structure which in turn results in a stronger alloy.

It is difficult to produce thin walled, complicated extrusion shapes in alloy 6082. The extruded surface finish is not as smooth as other similar strength alloys in the 6000 series.

In the T6 and T651 temper, alloy 6082 machines well and produces tight coils of swarf when chip breakers are used.

Applications

6082 is typically used in:

- ◆ High stress applications
- ◆ Trusses
- ◆ Bridges
- ◆ Cranes
- ◆ Transport applications
- ◆ Ore skips
- ◆ Beer barrels
- ◆ Milk churns

Chemical Composition

Element	% Present
Si	0.7 to 1.3%
Fe	0.5%
Cu	0.1%
Mn	0.4 to 1.0%
Mg	0.6 to 1.2%
Zn	0.2%
Ti	0.1%
Cr	0.25%
Al	Balance

Mechanical Properties

Temper	O	T4	T6/T651
Proof Stress 0.2% (MPa)	60	170	310
Tensile Strength (MPa)	130	260	340
Shear Strength (MPa)	85	170	210
Elongation A5 (%)	27	19	11
Hardness Vickers (HV)	35	75	100

Physical Properties

Property	Value
Density	2.70 g/cm ³
Melting Point	555°C
Modulus of Elasticity	70 GPa
Electrical Resistivity	0.038x10 ⁻⁶ Ω.m
Thermal Conductivity	180 W/m.K
Thermal Expansion	24x10 ⁻⁶ /K

Alloy Designations

Aluminium alloy 6082 also corresponds to the following standard designations and specifications:

AA6082	HE30
DIN 3.2315	EN AW-6082
ISO: Al Si1MgMn	A96082



Aalco is a registered trademark of Aalco Metals Ltd

© Copyright: Aalco Metals Ltd, The Hershams Centre, Hershams Green, Hershams, Surrey KT12 4HP

All Data is indicative only and must not be seen as a substitute for the full specification from which it is drawn. In particular, the mechanical property requirements vary widely with temper, product form and product dimensions. For more complete details please refer to the relevant specification – The BS EN Specifications for aluminium are listed on a separate Datasheet.

Welding

6082 has very good weldability but strength is lowered in the weld zone. When welded to itself, alloy 4043 wire is recommended. If welding 6082 to 7005, then the wire used should be alloy 5356.

Temper

The most common tempers for 6082 aluminium are:

- ◆ O - annealed wrought alloy
- ◆ T4 - Solution heat treated and naturally aged
- ◆ T6 - Solution heat treated and artificially aged
- ◆ T651 - Solution heat treated, stress relieved by stretching and then artificially aged

Fabrication

Process	Rating
Workability - Cold	Good
Machinability	Good
Weldability - Gas	Good
Weldability - Arc	Good
Weldability - Resistance	Good
Brazability	Good
Solderability	Good

Supplied Forms

6082 aluminium is available from Aalco in the following forms with a T6 temper:

- ◆ Square bar
- ◆ Square box section
- ◆ Rectangular box section
- ◆ Channel
- ◆ Tee section
- ◆ Equal angle
- ◆ Unequal angle
- ◆ Flat bar
- ◆ Tube
- ◆ Sheet

Rate and shate can also be supplied as 6082-T651.

This information is based on our present knowledge and is given in good faith. However, no liability will be accepted by the Company in respect of any action taken by any third party in reliance thereon. As the products detailed may be used for a wide variety of purposes and as the Company has no control over their use; the Company specifically excludes all conditions or warranties expressed or implied by statute or otherwise as to dimensions, properties and/or fitness for any particular purpose. Any advice given by the Company to any third party is given for that party's assistance only and without liability on the part of the Company. Any contract between the Company and a customer will be subject to the Company's Conditions of Sale. The extent of the Company's liabilities to any customer is clearly set out in those Conditions; a copy of which is available on request.

aalco[®] Aalco is a registered trademark of Aalco Metals Ltd

© Copyright: Aalco Metals Ltd, The Hershams Centre, Hershams Green, Hershams, Surrey KT12 4HP

All Data is indicative only and must not be seen as a substitute for the full specification from which it is drawn. In particular, the mechanical property requirements vary widely with temper, product form and product dimensions. For more complete details please refer to the relevant specification - The BS EN Specifications for aluminium are listed on a separate Datasheet.

15.6 NYLON 66 PHYSICAL PROPERTIES

PRODUCT DATA SHEET

www.quadrantplastics.com

ERTALON® 6 SA



This material offers an optimal combination of mechanical strength, stiffness, toughness, mechanical damping properties and wear resistance. These properties, together with a favourable electrical insulating ability and a good chemical resistance make ERTALON 6 SA a 'general purpose' grade for mechanical construction and maintenance.

Physical properties (indicative values*)

PROPERTIES	Test methods ISO/IEC	Units	VALUES
Colour	—	—	natural (white)/black
Density	1182	g/cm ³	1.16
Absorption:			
- after 24/60 h immersion in water @ 23°C (1)	52	mg	85/108
- at saturation in air at 23°C / 50% RH	52	%	1.18/1.50
- at saturation in water at 23°C	—	%	2.5
- at saturation in water at 100°C	—	%	9
Thermal Properties (2)			
Melting temperature	—	°C	260
Thermal conductivity at 23°C	—	W/(K·m)	0.24
Coefficient of linear thermal expansion:			
- average value between 22 and 50°C	—	m/(m·K)	60·10 ⁻⁶
- average value between 22 and 100°C	—	m/(m·K)	105·10 ⁻⁶
Temperature of deflection under load:			
- method A (3, 8 MPa)	+ 75	°C	70
Max. allowable service temperature at str:			
- for short periods (3)	—	°C	50
- continuously for 5,000/20,000 h (4)	—	°C	30/20
Min. service temperature (5)	—	°C	-40
Flammability (6):			
- "Oxygen Index"	45.8	%	23
- according to UL 94 (3/5 mm thickness)	—	—	10 V-0
Mechanical Properties at 23°C (7)			
Tension test (8):			
- tensile stress at yield (9)	+ 527	MPa	50
- tensile stress at break (9)	+ 527	MPa	50
- tensile strain at break (9)	+ 227	%	200
- tensile modulus of elasticity (10)	+ 237	GPa	2,250
- tensile modulus of elasticity (10)	+ 237	GPa	2,400
Compression test (11):			
- compressive stress at 1/2/5% nominal strain (10)	+ 504	MPa	26/45/80
Shear test: A tension (8):			
- stress to produce 1% strain in 1,000 h (9, 10)	+ 85	MPa	18
- stress to produce 1% strain in 1,000 h (9, 10)	+ 250	MPa	7
Barry impact strength - Unnotched (12)	+ 17	kJ/m ²	62/m ²
Barry impact strength - Notched	+ 16	kJ/m ²	5.5
Notch impact strength - Notched	+ 16	kJ/m ²	5.5
Notch impact strength - Notched	+ 16	kJ/m ²	15
Ball indentation hardness (13)	+ 103-1	N/mm ²	150
Rockwell hardness (13)	+ 120-2	—	R 80
Electrical Properties at 23°C			
Dielectric strength (14)	+ (50243)	kV/mm	25
Volume resistivity	+ (50243)	Ω·cm	18
Surface resistivity	+ (50093)	Ω·cm	> 10 ¹⁴
Surface resistivity	+ (50093)	Ω·cm	> 10 ¹²
Relative permittivity ε _r :			
- at 100 Hz	+ (50250)	—	2.9
- at 1 MHz	+ (50250)	—	2.6
- at 1 MHz	+ (50250)	—	2.3
- at 1 MHz	+ (50250)	—	2.8
Dielectric dissipation factor tan δ:			
- at 100 Hz	+ (50250)	—	0.019
- at 1 MHz	+ (50250)	—	0.13
- at 1 MHz	+ (50250)	—	0.021
- at 1 MHz	+ (50250)	—	0.06
Compassive tracking index (CTI)			
- at 100 Hz	+ (50112)	—	600
- at 100 Hz	+ (50112)	—	600

Notes: 1 g/cm³ = 1,000 kg/m³; 1 MPa = 1 N/mm²; 1 W/m = 1 KW/m

Availability

Round Rods: Ø 5-320 mm • Sheets/Plates: Thicknesses 0.5-100 mm • Tubes: O.D. 20-100 mm

All information supplied by or on behalf of Quadrant Engineering Plastic Products in relation to its products, whether in the nature of data, recommendations or otherwise, is supported by research and believed reliable, but Quadrant Engineering Plastic Products assumes no liability whatsoever in respect of application, processing or use of the above mentioned information or products, or any consequences thereof. The user undertakes full liability in respect of the application, processing or use of the above mentioned information or products, whose quality and other properties he shall verify, or any consequences thereof, his liability whatsoever shall attach to Quadrant Engineering Plastic Products for any infringement of the rights owned or controlled by third party in intellectual, industrial or other property by reason of the application, processing or use of the above mentioned information or products by the user.

Quadrant Engineering Plastic Products

global leader in engineering plastics for machining
www.quadrantplastics.com

Legend

- + : values determined experimentally
- : values determined by calculation in accordance with the standard atmosphere 23°C/50% RH (unless otherwise stated from literature)
- (1) According to method 10f of ISO 6272 - samples of size Ø 50 x 100 mm
- (2) The values given for stress and strain are for the most part derived from an internal supplier data and other publications.
- (3) Only for short time periods (in the hour) in applications where no mechanical load is applied to the material.
- (4) Temperature reduction over a period of 5,000/20,000 hours. In these periods of time, there is a decrease in tensile strength of about 50% as compared with the corresponding temperature values given here are thus based on the thermooxidative degradation which takes place. In all thermoplastics, the maximum allowable service temperature depends in many cases essentially on the material and the magnitude of the mechanical stresses to which the material is subjected.
- (5) Impact strength decreasing with decreasing temperature, the minimum allowable service temperature is precisely defined by the extent to which the material is subjected to impact. The value given here is based on unfavourable impact conditions and may consequently not be considered as being the absolute practical limit.
- (6) These estimated ratings, derived from raw material supplier data, are not intended to reflect hazards presented by the materials under actual fire conditions. There is no UL-yellow card available for ERTALON 6 SA stock shapes.
- (7) The figures given in the properties of dry material (+) are for the most part average values of tests run on test specimens machined out of rods Ø 40-50 mm.
- (8) Test specimens: Type 1 B.
- (9) Test speed: 20 mm/min.
- (10) Test speed: 1 mm/min.
- (11) Test specimens: cylinders Ø 12 x 30 mm.
- (12) Pendulum used: 10 J.
- (13) 10 mm thick test specimens.
- (14) Electrode configuration: 25/75 mm coaxial cylinders; in transformer oil according to IEC 60296; 5 mm thick natural coloured test specimens. It is important to know that the electric strength of black extruded material can be as low as 50% of the value for natural material.

* This table is a valuable help in the choice of material. The data listed here fall within the normal range of product properties. However, they are not guaranteed and they should not be used to establish material specification limits nor used alone as the basis of design.

ERMUM® is a registered trade mark of Quadrant AG. © 2003 Copyright Quadrant AG. - 10/03en January 2003

